الجمهورية الجزائرية الديمقراطية الشعبية

République Algérienne Démocratique et Populaire

Ministère de L'Enseignement Supérieur et de la Recherche Scientifique

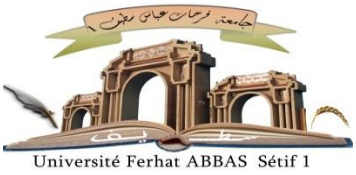

UNIVERSITÉ FERHAT ABBAS - SETIF 1

FACULTÉ DE TECHNOLOGIE

THESE

Présentée au Département d'Electronique

Pour l'obtention du diplôme de

DOCTORAT EN SCIENCES

Option : Electronique

Par

SAHLI Abdeslem

THÈME

Optimisation de la qualité d'énergie dans les Smart grids

Soutenue le 21/02/2021 devant le Jury :

ZEGADI Ameur	**Professeur**	**Univ. Sétif 1**	**Président**
KRIM Fateh	**Professeur**	**Univ. Sétif 1**	**Directeur de thèse**
SEMECHEDDINE Samia	**Professeur**	**Univ. Sétif 1**	**Examinateur**
REKIOUA Toufik	**Professeur**	**Univ. Bejaia**	**Examinateur**
HAMIDAT Abderrahmane	**Directeur de Recherche**	**CDER. Alger**	**Examinateur**
BOUZEKRI Hacene	**Professeur**	**Univ. Skikda**	**Examinateur**

Energy Quality Optimization in Smart Grids

By

SAHLI Abdeslem

A thesis
presented at the University of Ferhat Abbas -Sétif 1

for the degree of

Doctor in Sciences

in

Electronics

Abstract

Power quality and renewable energy integration are two potential promises for the smart grid expansion, including power quality improvement and capability to integrate more renewable energy resources.

In this thesis, a modified packed U-cell five-level inverter (MPUC5) with Model predictive control (MPC) strategy is proposed for a single-phase active power filter (APF) application, which is applied to eliminate harmonic current and compensate reactive power at the point of common coupling (PCC), caused by local non-linear loads connected to the grid. In this context, a new model predictive control (MPC) has been designed and implemented to ensure the voltage balancing for the DC-link capacitors, and generate five-level voltage at the output to ensure high power factor correction.

On the other hand, this study introduces the MPUC5 converter in transformer-less single-phase double stage grid-tied photovoltaic (PV) system. The proposed system operates as a single-phase APF able to compensate reactive power generated by non-linear loads connected to grid, feeds the non-linear load by the generated PV power, and injects the extra power into the grid, where the proposed FCS-MPC algorithm is designed to ensure a high grid current quality, taking into consideration the issue of the capacitor voltages balancing and the switching frequency minimization. Furthermore, this topology shows a great enhancement in safety and protection of the PV system with an elimination of the common mode leakage current in non-isolated system.

To show the performance improvement of the proposed systems, completed simulation models have been developed using MATLAB/Simulink™ environment and confirmed through real-time hardware in the loop (HIL) system. The obtained results indicated the excellent performance of the proposed control schemes.

Dedication

To my family.

Acknowledgements

*In the name of **ALLAH**, the Most Gracious and the Most Merciful. Thanks to **ALLAH** who is the source of all the knowledge in this world, for the strengths and guidance in completing this thesis.*

*I express my deep sense of gratitude and heart-felt thanks to my supervisor, Prof. **KRIM Fateh**, for his invaluable guidance, patience, kindness and consistent encouragement throughout the course of this work.*

*I would like to express my appreciation to my thesis committee members: Prof. **ZEGADI Ameur**, Prof. **SEMECHEDDINE Samia**, Prof. **REKIOUA Toufik**, Dr. **HAMIDAT Abderrahmane** and Prof. **BOUZEKRI Hacene** for their discussions, suggestions, and feedbacks to improve my thesis.*

*I cannot forget to mention all my friends **LEPCI** group, **TALBI Billel**, **LAIB Abdelbaset**, **ARABI Abderrazak**, **BELAOUT Abdesslam**, **FEROURA Hamza**, **BOUYAHIA Semcheddine**, **BEY Habib** and **KIHEL Abbes**, for their great friendship, help and support.*

*A Special thanks to my friends Dr. **BENHAMADOUCHE Abdelouahab** and Mr. **RABHI Abdelbaki**, for their friendship and support in all these years.*

SAHLI Abdeslem

Table of Contents

List of Figures

List of Tables

List of Acronyms and symbols

AC	Alternative current
DSO	Distributed system operators
PV	Photovoltaic
HIL	Hardware in the loop
DC	Direct current
APF	Active power filter
SAPF	Shunt active power filter
DSTATCOM	Distribution static compensators
DVR	Dynamic voltage restorers
SSSC	Series static synchronous compensators
UPQC	Unified power-quality conditioners
ASD	Adjustable-speed drive
HVDC	High voltage direct current
PPF	Passive power filter
DSP	Digital signal processor
CSI	Current source inverter
VSI	Voltage source inverter
HB	Half-bridge
FB	Full-bridge
THD	Total of harmonic distortion
MLI	Multi-level inverter
CHB	Cascade h-bridge
NPCC	Neutral point clamped converter
FCC	Flying capacitor converter
MMC	Modular multilevel converter
PUC	Packed unit cell
MPUC	Modified packed unit cell
PCC	Point of common coupling
MPC	Model predictive control
FCS-MPC	Finite control set MPC
CCS-MPC	Continuous control set
DG	Distributed generation

L_f	Filter inductance
Vdc	DC-link voltage
C_{dc}	DC-link capacitor
if _ref	Filter reference current
if	Filter current
Vin	Inverter output voltage
v_s	Grid voltage
g	Cost function
R_l	Rectifier side load resistor
L_l	Rectifier side load inductor
f_s	Grid frequency
fsw	Inverter switching frequency
Ps	Grid active power
Qs	Grid reactive power
is	Grid current
iL	Load current
$S_{a,b,c}$,	Switching signals of the inverter.
P_g	Active power
Q_g	Reactive power
C_p	Virtual parasitic capacitor
Vpv	Photovoltaic voltage
Ppv	Photovoltaic power
Isc	Short circuit current
Voc	Open circuit voltage
Imp	Current at MPP
Vmp	Voltage at MPP
Pmp	Power peak
fsw	Switching frequency
SWC	Number of IGBT commutations
Vs	Grid voltage
Ts	MPC sampling time
G	Solar Irradiance

PI	Proportional integral
CPU	Control processing unit
RMS	Root mean square
GW	Gigawatt
RES	Renewable energy system
DER	Distributed energy resources
IGBT	Insulated gate bipolar transistor
PWM	Pulse width modulation
PLL	Phase-locked loop
PD	Phase detector
PI-LF	PI based loop filter
VCO	Voltage-controlled oscillator
FLC	Fuzzy logic control (controller)
GA	Genetic algorithm
NFIS	Neuro-fuzzy networks
AI	Artificial intelligence
INC	Incremental conductance
P&O	Perturb and observe
KCL	Kirchhoff’s current law
MPP	Maximum power point
MPPT	Maximum power point tracking
V-MPPT	Voltage based MPPT
VO-MPPT	Voltage oriented MPPT

General Introduction

1. INTRODUCTION TO SMART GRID

The electric power system has witnessed many new developments that not only revived interest in research and development but also resulted in significant socio-economic benefits to the community. The increased awareness of the environmental impact and the carbon footprint of all energy sources, including electric power production, have given motivation to go further to adopt renewable energy sources as alternative energy. The deregulation of the power utility is a second important factor that shaped the direction of electric power technology. The rise of the new power utility "smart grid" is a great advantage not only for the society but to the entire electric power industry.

Actually, the electric power distribution system is almost entirely a mechanical system, with only modest use of sensors, minimal electronic communication and almost no electronic control. In the last decades, all industries in the developed countries have renewed their power grid infrastructures with the use of high-tech devices such as sensors, communications and computational capability toward smart electric grid. Consequently, there has been massive enhancements in term of production, efficiency and quality of the energy with better environmental performance.

In brief, a smart grid is the use of sensors, communications, computational capability and control to improve the overall functionality of the electric power system. A conventional electrical system becomes smarter by using those modern devices in term of control and ability to continual adjustments of the system. Furthermore, this infrastructure improvement permits numerous functions which allow optimization in distribution, transmission and distributed resources which ensure consistency and optimize the use of energy, mitigate environmental impact and contain cost.

2. BACKGROUND OF SMART GRID

The smart grid is the dominating topic in today's energy domain. However, many definitions of smart grid exist all around the world, and depending on them the smart grid is defined as state, transition process or target infrastructure. The basic content of each definition is influenced by many different factors, for example different generation structures caused by natural resources and regulation and different consumption structures caused by energy prices, using habits as well as urban population density.

The following definitions highlight the influence of the above-mentioned factors:

" The term 'Smart Grid' refers to a modernization of the electricity delivery system so it monitors, protects and automatically optimizes the operation of its interconnected elements – from the central and distributed generator through the high-voltage network and distribution system, to industrial users and building automation systems, to energy storage installations and to end-use consumers and their thermostats, electric vehicles, appliances and other household devices. "

" A Smart Grid is an electricity network that can intelligently integrate the actions of all users connected to it - generators, consumers and those that do both - in order to efficiently deliver sustainable, economic and secure electricity supplies."

"A Smart Grid is an electricity network that can cost-efficiently integrate the behavior and actions of all users connected to it generators, consumers and those that do both in order to ensure economically efficient, sustainable power system with low losses and high levels of quality and security of supply and safety"

The first definition [1] was published by the US National Institute of Standards and Technology (NIST) and defines the smart grid as a transition process from the existing power system to the future, Information and Communication Technologies (ICT) based power system. The second definition [2] was published by the European Technology Platform (ETP) Smart Grids and defines the smart grid as a target architecture. The third definition [3] was published by Publications Office of the European Union, where power quality and renewable energy integration in the grid take great intention in the development of the future mixed grid.

Based on these definitions, smart grid system could be described as a microgrid that has some special features that would improve the overall effectiveness of the power system to make

it environment friendly, integrate more renewable energy sources, improve power quality to correspond to new demands, become more reliable, resilient, flexible and sustainable.

However, all definitions have some requirements, recommendations and ideas in common for the new mixed grid:

- Accommodates and facilitates all renewable energy sources, distributed generation, residential micro generation, and storage options, thus reducing the environmental impact of the whole electricity sector. It will provide simplified interconnection similar to ‘plug-and-play’.
- Assures and improves reliability and the security of supply by being resilient to disturbances, anticipating and responding to system disturbances (predictive maintenance and self-healing), and strengthening the security of supply through enhanced transfer capabilities.
- Maintains the power quality of the electricity supply to cater for sensitive equipment that increases with the digital economy.

In Smart Grid projects today, these technologies are being applied to electric grid applications, involving devices at the consumer level through the transmission level, to make our electric system more responsive and more flexible. In addition to economic motivations, smart grid employments respond to the rate of advances in emerging technologies, such as power electronic devices, computing power and renewable generation.

The main characteristics of smart grids with comparison to conventional grids are shown in Table 1 [4].

In this thesis we focus on two potential promises of the smart grid which includes improved consistency and power quality and capability to integrate more renewable energy resources, and where power quality plays a central role that should be maintained, especially, with the ability to accommodate more renewables into the system, which make the grid more vulnerable to power quality issues.

3. RENEWABLE ENERGY SYSTEMS AND THE SMART GRID

Distributed power generation is becoming an important part of the developing plans for most countries to meet the energy demand in the future [5]. The idea of distributed power generation is particularly attractive when different kinds of renewable energy sources are available. Distributed power generation of these renewable energy systems allows for the

integration of renewable and nontraditional energy sources. With distributed energy generation and storage, the power and energy engineering will definitely face a new situation in which small-distributed power generators and distributed energy storage devices have to be integrated into a single grid commonly known as the Smart Grid. In this way, it will reduce cost, save energy, and increase reliability with more transparency [6]. Demand for electricity is set to increase further as a result of rising household incomes, with the electrification of transport and heat, and growing demand for digital connected devices and air conditioning with an anticipated growth of 2.1% per year to 2040 [5]. Therefore, the efficient utilization of electricity, its production and distribution are important in order to optimize the overall energy consumption. The Smart Grid is considered to be one of the key technologies to play an important role in solving parts of those current and future challenges.

Table 1 Comparison between conventional grid and smart grid.

Characteristic	Conventional grid	Smart grid
Enables active participation by consumers	Consumers are uniformed and non-participative with power system	Informed, involved and active consumers, demand response and distributed energy resources
Accommodates all renewables	Dominated by central generation, many obstacles for distributed energy resources	Many distributed energy resources, focus on renewable
Enables new products, services and markets	Limited wholesale markets, not well integrated, limited opportunities for consumers	Mature, well-integrated wholesale markets,
Provides power quality for the digital economy	Focus on outages, slow response to power quality issues	Power quality is a priority, rapid resolution of issues
Anticipates and responds to system disturbances	Focus on protecting assets following faults	Automatically detects and responds to problems
Operates resiliently against attack and nature disasters	Vulnerable to natural disasters	Resilient to attack and natural disasters with rapid restoration capabilities

Figure 1 shows the worldwide energy demand in the last two years and also the estimated energy demand until 2040. As it can be observed, due to the continuous increase in gross domestic product, the overall energy demand rises by 1.3% a year to 2040 [5]. To achieve this primary goal, renewable energy will be an important part in the expectable future energy production (hydro, renewable and biomass, etc.).

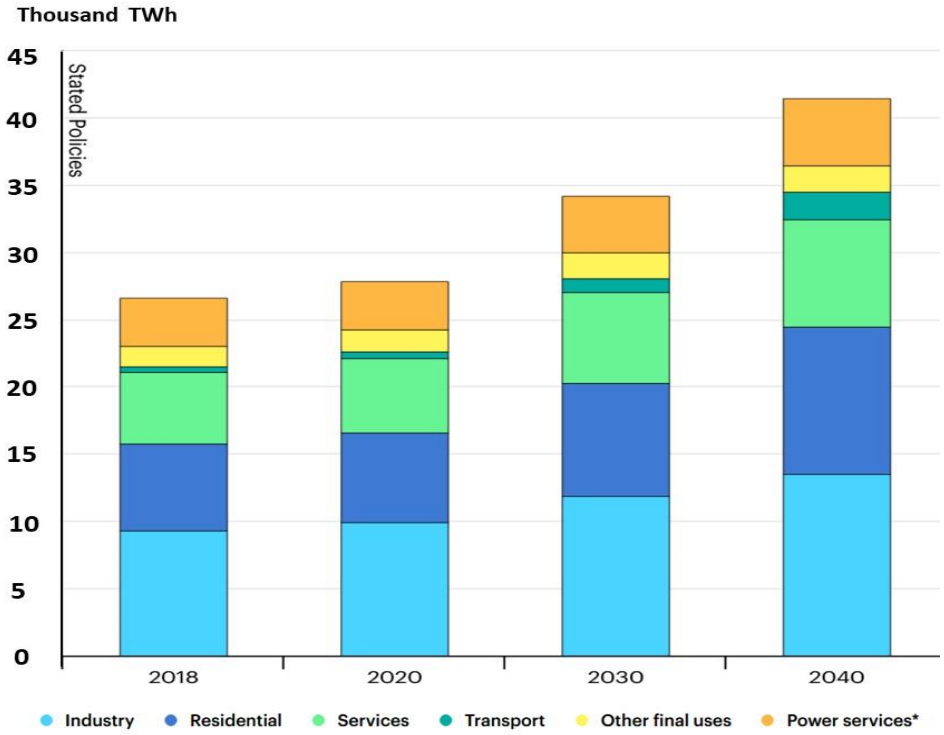

Figure 1: Worldwide energy demand by sector since 2018 and the estimated until 2040 [5].

Worldwide research, development, and major implementation efforts are focused on renewable energies. In recent years, renewable sources, such as wind (onshore and offshore), solar (photovoltaics [PV] and concentrated solar power [CSP]), geothermal, bioenergy (solid biomass, biogas), and marine energy, are gained more attention with a considerable percentage of the installed capacity as shown in Figure 2.

Among the renewable energy resources presented in Figure 2, the electricity produced from photovoltaic installation, in 2025, can rise to 1200 GWh, according to [5]. The PV industry is experiencing rapid growth and solar energy is highly promoted. Nevertheless, the high penetration level of PV systems especially imposes new challenges for the Distributed System Operators (DSO) and the end-consumers [7–8]. It may introduce significant impacts on the availability, quality and reliability of the electrical grid, since it makes the distributed networks more decentralized, uncontrollable and heterogeneous [9], leading to further research and discussion about the appropriate implementation of PV power systems. Consequently, grid guidelines are continuously updated in order to enhance the PV hosting capacity in distributed grids [8]. On the other hand, it calls for an emerging development of advanced control strategies accordingly [10].

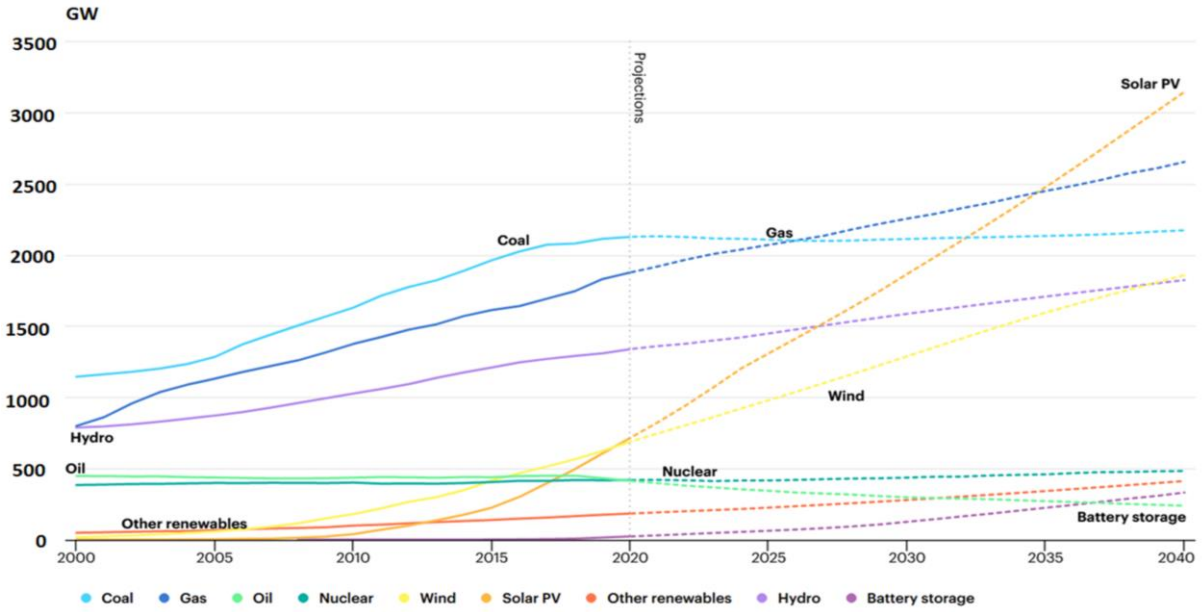

Figure 2: Annual evolution (2000-2020) of the worldwide energy generation capacity and the estimated until 2040 [5].

Amid the technologies that reinforced the growth of renewable energy, power electronics has been representing a major technology enabler. The power electronics converters have made it possible to connect renewable energy generators to the power systems, as illustrated in Figure 3, improving the efficiency of energy harvesting through dedicated controls. Furthermore, power electronic devices are widely used on the consumer side and have been considered as a core technology for the new smart grid.

The demands and new requirements are growing continuously with related standards newly updated and proposed for single phase grid connected PV systems. There are many demands on advanced functions in grid-connected power electronics facilities to improve power quality and reliability issues [10]. Therefore, it is essential to explore the functions that inverter-based power generating system can contribute to grid safety operation and assess the grid fault effects on the control of grid-connected PV systems, and also to develop advanced control strategies to further enable an increase of the penetration degree of PV systems with cost-effective solutions. In addition, the basic requirements, related to active and reactive power output, frequency and voltage control, power quality and voltage stability, should also be fulfilled by every generating system. Since PV systems have a high penetration in residential applications with much lower power ratings (several kW) compared to wind turbine power systems, single-phase topologies are still widely-used solutions for PV applications at present [11].

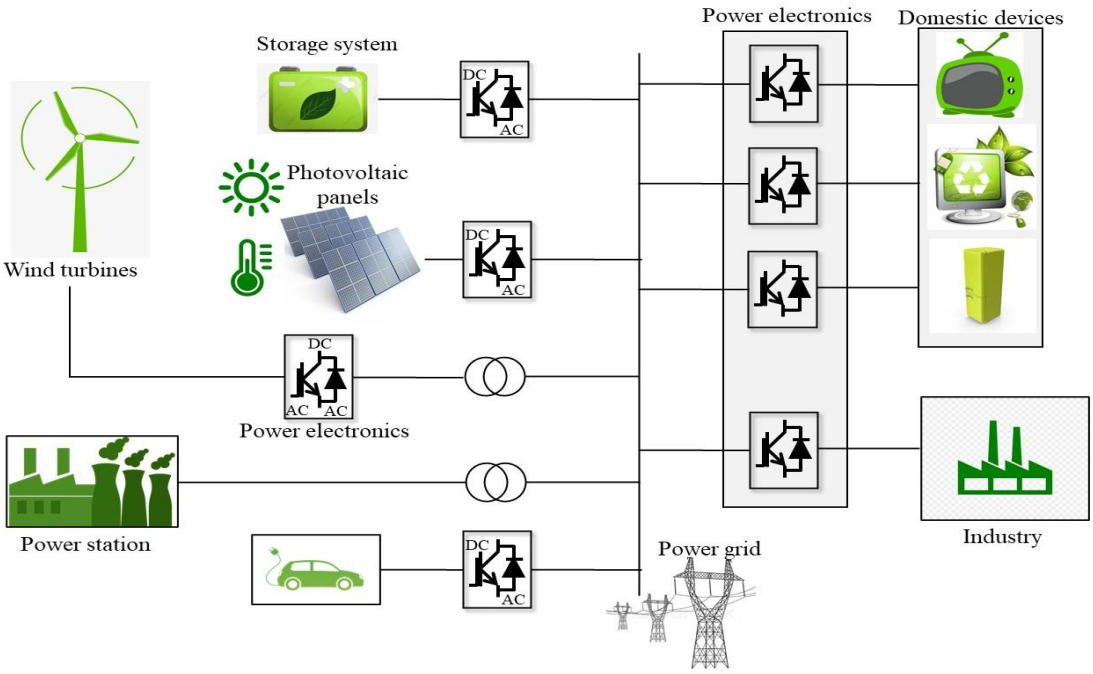

Figure 3: Modern power system representation incorporating renewables, energy storage and consumers.

In order to meet the grid code requirements, the future PV systems are expected to provide multiple functionalities similar to those of conventional power plants by means of offering supplementary services, such as reactive power support, peak power shaving, load leveling, frequency control through active power control, low voltage ride through during grid faults. The power electronics interface of the PV systems enables an appropriate reactive power exchange with the grid, thus providing reactive power support and keeping the bus voltages within operating limits. The control of voltages, reactive power and line flows represent one of the most important activities in the operation of modern electric utility system. This control is known as the “Voltage/Reactive Power” or “Voltage/Var” control. The main objective of this control can be generally regarded as an attempt to achieve an overall improvement of the system security, service quality and economy. The dynamic control on output reactive power of distributed generator is suggested and recommended in updated new standards, such as California Rule 21 [12] and IEEE 1547a Standard [13].

Power quality and reliability are attracting much attention in such systems. In order to meet the grid code requirements and maximize the value of inverter system, advanced inverter systems are expected to provide more functionality including ancillary services such as dynamic reactive power support. The power electronics interface of the PV systems enables them to exchange reactive power with the utility grid.

4. AIM AND SCOPE OF THE THESIS

Taking into account the new demands and challenges mentioned above mainly for single-phase grid-connected PV systems, several issues will be addressed in this thesis with proposed solutions and strategies. One objective of this thesis is to improve the power quality of future mixed grid and taking on consideration PV system integration performance of single-phase grid-connected PV system, the main idea is to replace the conventional two-level inverters by a multi-level inverter in order to increase the performance of the system. Consequently, advanced control strategies are proposed to further increase the penetration level of PV systems. The objectives and contributions of this thesis are listed as follows

i. A new single-phase active power filter based modified packed unit-cell inverter (MPUC5) is proposed for power quality mitigation and for harmonic elimination in the future mixed residential power grid.

ii. A new multifunctional single-phase grid-connected MPUC5 inverter interfaced with PV system configuration is proposed.

iii. A novel MPC algorithm is deployed for MPUC5 inverter to work properly, where, the proposed algorithm does not introduce any additional complexity.

5. LAYOUT

The research work presented in this thesis is organized into four chapters. The content of the work carried out in each chapter is summarized as follows:

Chapter-1: gives a review on power quality enhancement in single phase AC grid. Power quality issues, solutions to harmonic elimination and reactive power compensation are presented. Different single-phase multi-level inverters are discussed, among which, MPUC5 inverter is found to be the most suitable topology for APF applications. Then, we present an overview on classical control strategies for multi-level inverters, in which we propose the predictive control strategy as the most effective control strategy that can be used in such application.

Chapter-2: a single phase APF system is developed using multilevel MPUC5 inverter controlled by a new MPC algorithm in order to compensate a contaminating load with small power factor, to enhance reactive power in the grid and to eliminate harmonic currents at the PCC. The proposed MPC algorithm is employed to reduce the

computational burden and provides high power factor correction, in addition to ensure the balance of the DC-link capacitor voltages. **S**imulations and real-time hardware in the loop (HIL) implementations are provided to confirm the performance improvement of the proposed control scheme.

Chapter-3: gives a review on how photovoltaic energy integration in electrical grid has been introduced. An overview on the commonly converters based on advanced power electronics are used in single-phase grid-tied PV systems in residential applications. General control schemes in single phase system are also addressed with respect to power quality requirement and to better integration of this kind of renewable energy in future smart grid.

Chapter-4: Herein, a transformer-less single-phase grid-tied PV system is developed using multi-level MPUC5 inverter controlled by a novel MPC strategy with the objective to compensate a contaminating load with poor power factor, enhance reactive power in the grid, eliminate harmonic currents at the PCC and inject the produced PV power into the grid under various levels of solar irradiation. The proposed system provides better control of the leakage current where the safety and protection of PV installation is always ensured.

Simulations and real-time hardware in the loop (HIL) implementations are provided also in order to confirm the good performance of the proposed system.

Finaly, thesis general conclusion and the author's contributions are summarized. Possible extensions to the research presented in this thesis are suggested.

REFERENCES

[1] U.S. Department of Energy, Smart Grid System Report, July 2009 https://www.energy.gov/sites/prod/files/2019/02/f59/Smart%20Grid%20System%20Report%20November%202018_1.pdf (accessed September 01, 2019).

[2] European Commission (2006) European Smart Grids Technology Platform:Vision and Strategy for Europe's Electricity, http://ec.europa.eu/research/energy/pdf/smartgrids _en.pdf.

[3] E. C. D.-G. f. Employment and I. D. A., Employment and Social Developments in Europe: Publications Office of the European Union, 2011.

[4] DOE 2009a The smart grid: An introduction. Technical report, The U.S. Department of Energy.http://energy.gov/sites/prod/files/oeprod/DocumentsandMedia/DOE_SG_Book_Single_Pages.pdf.

[5] International Energy Agency (IEA), World energy outlook 2019 https://www.iea.org/news/world-energy-outlook-2019-highlights-deep-disparities-in-the-global-energy-system, (Published 13 November 2019)

[6] Guerrero, J.M., Vasquez, J.C., Matas, J. et al. (2011) Hierarchical control of droop-controlled DC and AC microgrids – a general approach towards standardization. IEEE Transactions on Industrial Electronics, 58 (01), 158–172.

[7] A. Izadian, N. Girrens, and P. Khayyer, "Renewable Energy Policies: A Brief Review of the Latest U.S. and E.U. Policies," IEEE Industrial Electronics Magazine, vol. 7, pp. 21-34, 2013.

[8] F. Blaabjerg, C. Zhe, and S. B. Kjaer, "Power electronics as efficient interface in dispersed power generation systems," IEEE Transactions on Power Electronics, vol. 19, pp. 1184-1194, 2004.

[9] G. Petrone, G. Spagnuolo, R. Teodorescu, M. Veerachary, and M. Vitelli, "Reliability Issues in Photovoltaic Power Processing Systems," IEEE Transactions on Industrial Electronics, vol. 55, pp. 2569-2580, 2008.

[10] S. Kouro, J. I. Leon, D. Vinnikov, and L. G. Franquelo, "Grid-Connected Photovoltaic Systems: An Overview of Recent Research and Emerging PV Converter Technology," IEEE Industrial Electronics Magazine, vol. 9, pp. 47-61, 2015.

[11] W. Li, Y. Gu, H. Luo, W. Cui, X. He, and C. Xia, "Topology Review and Derivation Methodology of Single-Phase Transformerless Photovoltaic Inverters for Leakage Current Suppression," IEEE Transactions on Industrial Electronics, vol. 62, pp. 4537-4551, 2015.

[12] "IEEE Standards Coordinating Committee 21, http://grouper.ieee.org/ groups/ scc21/ index. html."

[13] "IEEE 1547 Series of Standards, http://grouper.ieee.org/groups/scc21/dr_shared/."

Chapter 1

Power Quality: Problems Overview and Mitigation Technologies

1. INTRODUCTION

Smart grids generally refer to grids equipped with smart sensors/meters, real-time data collection and processing and fast communications. Smart grid technologies will lead to a stronger economy, reliability, power quality, and eventually better energy efficiency and environmental impact. The focal points of this chapter are on power quality issues and the most effective solutions used to enhance the energy quality within future smart grids.

The chapter gives a review on single-phase active power filtering processes with a detailed presentation of multi-level inverters. These are very promising topologies being used in power quality issues. Of these topologies, single phase packed unit cell converter (PUC) arises as best suited in single phase systems. Finally, a review on power converter control techniques is presented, in which the predictive control technique is discussed.

2. OVERVIEW ON POWER QUALITY ISSUES

The power quality problems have been present since the inception of electric power. There have been several conventional techniques for mitigating the power quality problems and in many cases even the equipment's are designed and developed to operate satisfactorily under some of the power quality problems. Nevertheless, recently the awareness of the customers toward the power quality problems has extensively increased because of the following reasons [1]:

• The customer's equipment's have become very sensitive to power quality problems because of the extensive use of digital control and power electronic converters, which are highly sensitive to the supply and other disturbances. Moreover, the industries have also become more conscious for loss of production.

• The increased use of power semiconductor devices in a number of equipment in order to decrease power losses, increase overall effectiveness, and reducing the cost of power production leads to an increase in harmonic levels, distortion, notches, and other power quality problems.

• Direct and indirect penalties enforced on customer's, which are caused by interruptions, loss of production, equipment failure, are other raisons of the increased awareness for power quality problems.

• Disturbances to other important equipment such as domestic devices, telecommunication network, and protection systems have enforced power end-users to reduce or remove power quality problems or dispense the use of contaminating devices and equipment.

• Power systems deregulation is another important factor of power quality awareness, due to the fact that power quality is considered as performance indicator, and it has become difficult to preserve good power quality in power networks.

• Distributed generation systems using renewables energy and their integration to the power systems have increased power quality problems, due to the need of using power conversion systems based-on semi-conductor devices in such applications.

• The pollution of power networks has become an environmental issue with other consequences in addition to financial issues.

• Several standards and guidelines are developed and enforced on the customers, manufacturers, and utilities to prevent such quality problems.

A considerable development is observed in developing new equipments with enhanced power quality. Beginning with conventional techniques used for mitigating power quality problems in the utilities, distribution systems, and end-user's equipment, a significant literature has appeared in research publications, patents, and manufacturers' manuals for new techniques of mitigating power quality problems. A substantial research on power filters of numerous types such as passive, active, with series or shunt configurations, or a mixture of all these configurations for single-phase, three-phase three-wire, and three-phase four-wire systems has appeared for mitigating problems of harmonics, reactive power, and balancing of the linear and

nonlinear loads. Similar progress has been noticed in custom power devices such as distribution static compensators (DSTATCOM) for power factor correction, voltage regulation, compensation of neutral current harmonics, and load balancing [2, 3]; dynamic voltage restorers (DVR) [4, 5] and series static synchronous compensators (SSSC) for voltage quality problems mitigating in both transient and steady-state conditions [6, 7]; and unified power-quality conditioners (UPQC) for current and voltage quality problems mitigation in various applications [8, 9]. These mitigation techniques for power quality problems are considered for retrofitting existing equipment in electric power utility. An exponential evolution is also observed in several converter circuit configurations providing inherent power quality enhancements in equipment from fraction of watts to MW ratings. The use of various AC/DC and AC/AC converters of buck, boost, buck–boost, multilevel, and multi-pulse types with unidirectional and bidirectional power flow capability in the input stage of these equipment and providing suitable circuits for specific applications has changed the scenario of power quality improvement techniques and the features of these systems [10].

3. POWER QUALITY PROBLEMS CLASSIFICATION

Power quality problems may be classified into three categories according to [10], problems based on events such as transient and steady state, quantity such as current, voltage, and frequency, or load and supply systems.

The transient categories of power quality problems include most of the phenomena occurring in transient nature (impulsive or oscillatory in nature), such as sag (dip), power frequency variations, short-duration voltage variations, and voltage fluctuations. On another hand, the steady-state categories comprise long-duration voltage variations, waveform distortions, unbalanced voltages, notches, DC offset, flicker, poor power factor, unbalanced load currents, load harmonic currents, and excessive neutral current.

The second classification is based on quantity such as voltage, current, and frequency. For the voltage, these include voltage distortions, flicker, notches, noise, sag, swell, unbalance, undervoltage, and overvoltage; similarly, for the current, these include reactive power component of current, harmonic currents, unbalanced currents, and excessive neutral current.

The third classification of power quality problems is based on the load or the supply system. Where, power quality problems due to load nature are reactive power component of current, load current consisting of harmonics, unbalanced load currents, and DC offset. The power quality problems caused by the supply system include voltage and frequency related

issues such as voltage distortion, voltage unbalance, sag, swell, flicker, and noise. The frequency related problems are frequency variation above or below the desired frequency value. These affect the performance of loads and other equipment in the distribution system such as transformers.

4. CAUSES OF POWER QUALITY PROBLEMS

The main reasons of power quality problems can be classified into natural and man-made in terms of current, voltage, frequency, and so on. The natural causes of poor power quality include regulator dysfunction, lightening, weather conditions such as storms, equipment failure. However, Man-made causes (due to human activities on the power network) include switching operations or starting of large motors, power system faults (short circuit), power swings, sudden load changes, generating stations coming on/offline, unplanned heavy loads and indiscriminate integration of distributed generation [11].

The natural causes result in power quality problems that are generally transient in nature, such as voltage sag (dip), voltage distortion, and swell.

However, one of the important power quality problems is the presence of harmonics, because of several loads that behave in a nonlinear manner, such as transformers, electrical machines, and furnaces and new ones such as power converters, adjustable-speed drive (ASD), cyclo-converters, AC voltage controllers, high voltage direct current (HVDC) transmission, and renewable energy systems.

5. POWER QUALITY STANDARDS

Customers or power end-users are very affected by power quality problems in many ways, beginning with economic penalty in terms of power loss, equipment failure due to poor power factor, and loss of production. In view of these facts, various standards have been developed by many organizations and institutes such as IEC, IEEE, American National Standards Institute (ANSI), British Standards (BS), European Norms (EN), Computer Business Equipment Manufacturers Association (CBEMA), and Information Technology Industry Council (ITIC) to quantify power quality problems in terms of different performance indicators. These standards are applied to the customers, manufacturers, and utilities to preserve an acceptable level of power quality.

Nowadays, all developed standards are based on all power quality aspects, include deviations permissible level, mitigation, and monitoring. Some of them are given here;

however, standards are continuously being updated, with modifications in the existing ones on various aspects such as limits, monitoring, and mitigation devices.

IEEE 519-1992, IEC 61000 standards are the most used ones in different countries, where, there development is based on the permissible limits in deviations levels and distortions in various electrical quantities such as voltage, current, and power factor [12]. Table 1.1 quotes some currently available standards on various aspects of power quality.

Tables 1.2–1.3 presents some important limits on voltages and currents in these standards.

Table 1.1. Most used standards on power quality issues.

Standards	Description
IEEE Standard 519-1992	Recommended Practices and Requirements for Harmonic Control in Electrical Power Systems
IEEE Standard 1159-1995	Recommended Practice for Monitoring Electric Power Quality
IEEE Standard 1100-1999	Recommended Practice for Powering and Grounding Sensitive Electronic Equipment
IEEE Standard 1250-1995	Guide for Service to Equipment Sensitive to Momentary Voltage Disturbances
IEEE Standard 1366-2012	Electric Power Distribution Reliability Indices
IEC 61000-2-2	Compatibility Levels for low-frequency Conducted Disturbances and Signaling in Public Supply Systems
IEC 61000-2-4	Compatibility Levels in Industrial Plants for Low-Frequency Conducted Disturbances
IEC 61000-3-2	Limits for Harmonic Current Emission
EN 50160	Voltage Characteristics of Public Distribution Systems

Table 1.2. Std IEC 61000-3-2: Maximum permissible current (equipment current less than or equal to 16A per phase), (input power P< 600W).

Harmonic order, h	Maximum permissible harmonic current per watt (mA/W)	Maximum permissible harmonic current (A)
3	3.4	2.30
5	1.9	1.14
7	1.0	0.77
9	0.5	0.40
11	0.35	0.33
13<h<39 (odd harmonics)	3.85/h	0.15-0.15/h

Table 1.3. Standard IEEE 519-1992 voltage distortion limits.

PCC Bus voltage	Individual voltage distortion (%)	Total voltage distortion (%)
69kV and below	3.0	5.0
69.001-161 kV	1.5	2.5
Up to 161.001 kV	1.0	1.5

6. OVERVIEW ON POWER QUALITY SOLUTIONS

6.1 Single phase passive power filter

Usually, passive power filters (PPFs) are used to reduce harmonics, where, capacitors are generally employed to improve the power factor of AC loads [13]. There are many categories of passive filters such as series, shunt, hybrid, single or double tuned, damped, band-pass, and high-pass.

In medium and low power distribution systems, passive filters are widely used because of their low cost and simplicity.

6.1.1 Classification of Passive Filters

Single phase passive filters can be classified based on topology and connection. The topology can be series, shunt or hybrid and additionally subclassified as tuned or damped to perform as low-pass or high-pass for shunt filters or as low-block and high-block for series filters. Passive filters may be connected in a combination of shunt/series filters for compensating different types of nonlinear loads.

6.1.1.1 Shunt Filters

Passive shunt filters are connected in parallel to harmonic-producing loads, where, a low-impedance path is provided for harmonic currents, as result of that, these harmonic currents do not enter supply systems and are confined to flow in the passive circuits consisting of passive elements (inductors (*L*) and capacitors (*C*)) to reduce losses in the filter system as shown in Figure 1.1.

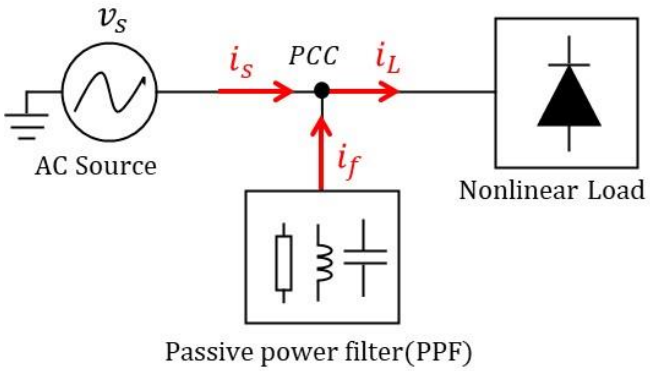

Figure 1.1: Shunt power passive filter.

Shunt filter can be a single filter tuned at one particular frequency. It is a simple series *RLC* circuit, in which *R* is the resistance of the inductor. The size of the filter is defined by the

value of the capacitor, where, the value of the capacitor is decided by the loads reactive power requirements and the inductor value is decided by the tuned frequency as shown in Figure 2 (a) & (b).

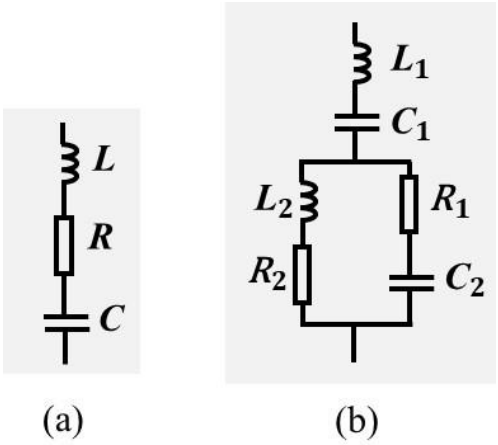

Figure 1.2: Shunt passive tuned filter: (a) single tuned; (b) double tuned.

Others types of passive filters, shown in Figure 1.3 (a) & (b), are known as high-pass filters also known as damped filters. These types of filters absorb all higher order harmonics and provide damping due to the presence of a resistor in the circuit.

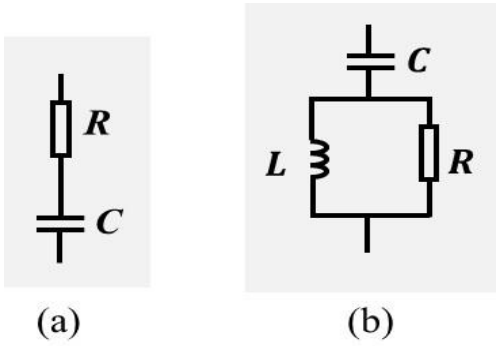

Figure 1.3: Shunt passive damped or high-pass filters: (a) first order; (b) second order.

6.1.1.2 Series Filters

Passive series filters are connected in series with polluted loads in order to provide high impedance for blocking harmonic currents to not enter supply systems and remain confined to flow in the local passive circuits consisting of parallel connected passive elements (inductors and capacitors) to reduce losses in the filter system. The passive series filter is a simple parallel *LC* circuit, as shown in Figures 1.4 and 1.5. Series filters are used to block single harmonic current such as third harmonic current.

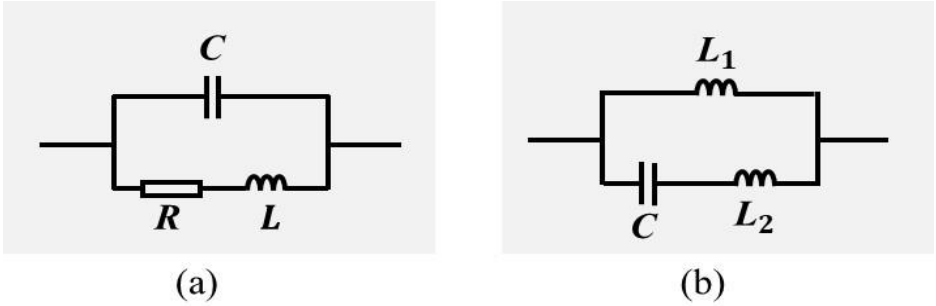

Figure 1.4: Series passive tuned or band-block filters: (a) single tuned; (b) double tuned.

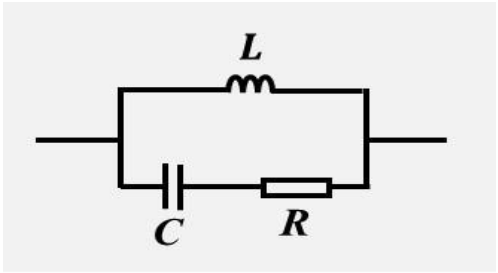

Figure 1.5: A series passive damped or high-block filter.

In order to blocking multiple harmonic currents, multiple passive filters need to be connected in series. These may also have a high-block filter with a parallel *LC* circuit and a resistance in series with the capacitor. Such a configuration of multiple series connected filters has significant series voltage drop and losses at fundamental frequency.

6.1.1.3 Hybrid Filters

The use of passive shunt and passive series filters independently has some drawbacks. In order to alleviate these drawbacks hybrid filters, based on a combination of both series and shunt passive filters as shown in Figures 1.6–1.7 are developed.

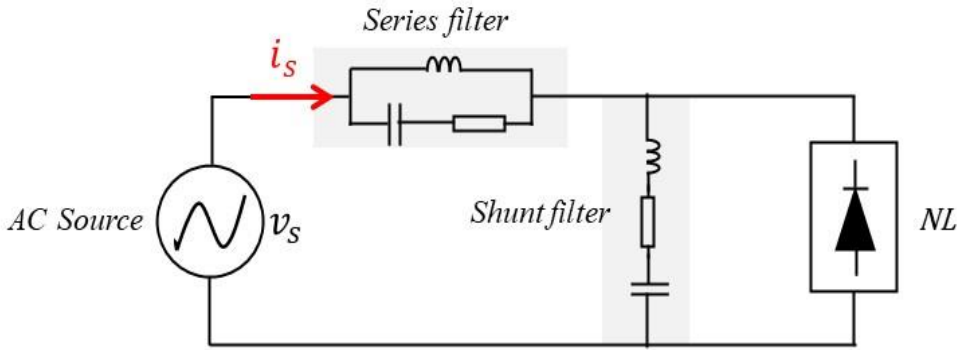

Figure 1.6: A hybrid filter as a combination of passive series (PFs) and passive shunt (PFsh) filters.

However, passive hybrid filter consisting of a single tuned passive series filter with a single tuned passive shunt filter and a high-pass passive shunt filter offers very good filtering characteristics. Furthermore, hybrid passive filters offer high filtering characteristics under loads change, with a low cost, that's why these filters are widely used in many industrial applications.

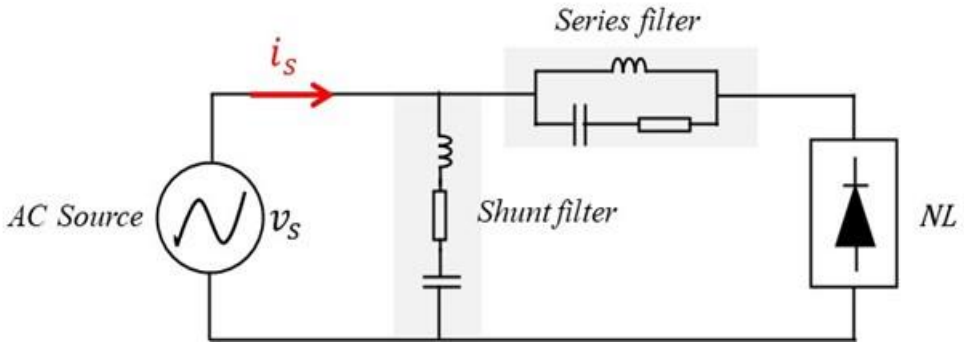

Figure 1.7: A hybrid filter as a combination of passive shunt (PFsh) and passive series (PFs) filters.

6.2 Active Power Filters

Conventionally, passive filters have been used to minimize harmonics in power supply utility, where, power capacitors have also been employed to improve power factor of the AC loads. However, passive filters have some drawbacks such as fixed compensation where, passive filters usually are designed to eliminate a specific harmonic, large size, and resonance.

The increased severity of harmonic pollution in power networks has attracted attention of power electronics and power system engineers to develop dynamic and adjustable solutions to the power quality problems. Such equipment generally known as active power filters (APFs) [14–16], which are able to deal with the most power quality problems in the power network, such as harmonic currents and voltages issues, reactive power compensation, regulate terminal voltage and suppress flicker.

One of the major factors in advancing the APF technology is the advent of fast, self-commutating solid-state devices. In the initial stages, thyristors, bipolar junction transistors (BJTs), and power MOSFETs (metal–oxide–semiconductor field-effect transistors) have been used to develop APFs [17]; later, SITs and GTOs have been employed to develop APFs [18]. With the introduction of insulated gate bipolar transistors (IGBTs), the APF technology has got a real boost and at present it is considered as an ideal solid-state device for APFs [19, 20]. The improved sensor technology has also contributed to the enhanced performance of the APF. The

availability of Hall effect sensors and isolation amplifiers at reasonable cost and with adequate ratings has improved the APF performance.

The next breakthrough in the APF development has resulted from the microelectronics revolution. Starting from the use of discrete analog and digital electronics components, the progression has been to microprocessors, microcontrollers, and DSPs. Now it is possible to implement complex algorithms online for the control of APF at a reasonable cost [21]. This development in APF has made it possible to use different control algorithms such as PI (proportional–integral) control, variable structure control, fuzzy logic control, and neural network-based control algorithms for improving the dynamic and steady-state performance of APFs. With these improvements, APFs becomes more able to provide fast corrective action even with changing nonlinear loads. Moreover, these APFs are found to compensate higher order harmonics (typically up to 25th harmonics).

APF can be classified according to: (1) the ways it is connected to the power system (series or shunt), (2) power rating (low-power, medium-power or high-power), (3) types of power converter employed (current-source or voltage-source converters), (4) circuit topology of the power converter employed (such as inverter, switch-capacitor, or hybrid-topology), (5) power system characteristic (two-wire for single-phase system, three-wire or four-wire for three-phase system), and (6) the targeted mitigation variables (such as current/voltage harmonics, reactive power, power factor, balancing of three-phase system, or combinations between them).

As it can be concluded from the literature [14], shunt active power filters (SAPFs) are the most suitable topology for active power filtering application, for their advantages such as their ability to compensate many harmonic orders in the same time; eliminate the risk of resonance phenomena between the power utility and the filter, and adapts automatically to changes in the network and load fluctuations.

6.2.1 Classification of single-phase shunt active power filters

In the last two decades, many studies have appeared on harmonics, reactive power, load balancing, and neutral current compensation associated with linear and nonlinear loads, where, shunt active power filters are used studied extensively and classified on the basis of converter used such as current source inverter (CSI), voltage source inverter (VSI), and on topology used such as half-bridge (HB) converters and full-bridge (FB) converters.

a) Converter-Based Classification

Two types of converters are used to develop SAPFs. Figure 1.8 (a) shows a SAPF using a voltage-fed PWM inverter or voltage source inverter (VSI). It has a self-supporting DC-link voltage with a large DC capacitor. SAPF based VSI are widely used to compensate current harmonics, reactive power, and load current unbalanced of critical nonlinear loads. It can also be used as a static var generator in power system networks and improving voltage profile. It is lighter, cheaper, and expandable to multilevel versions to enhance the performance with lower switching frequencies. It is more popular in UPS-based applications because in the presence of AC mains, the same voltage source converter can be used in SAPF to eliminate harmonics of critical nonlinear loads.

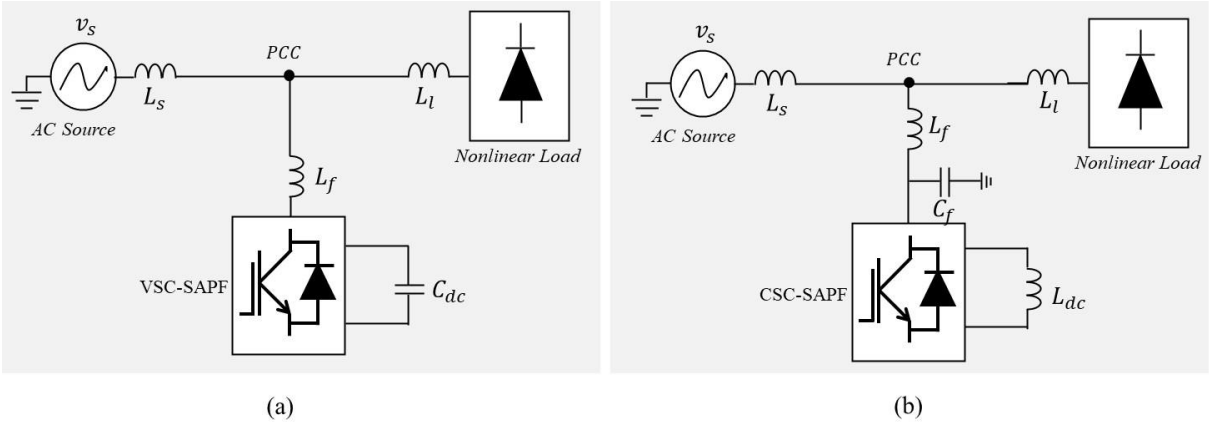

Figure 1.8: (a) VSI-based SAPF; (b) CSI-based SAPF.

The other converter used in SAPF is a current fed PWM (pulse-width modulation) inverter or a CSI bridge shown in Figure 1.8 (b). It behaves as a non-sinusoidal current source to encounter the harmonic current requirement of the nonlinear loads. A diode is used in series with the self-commutating device (IGBT) for reverse voltage blocking. However, GTO-based circuit configurations do not need the series diode, but they have restricted frequency of switching. These CSI-based SAPFs are considered sufficiently reliable, but have higher losses and require higher values of parallel AC power capacitors. Moreover, they cannot be used in multilevel modes to improve the performance of SAPFs in higher ratings.

b) Topology-Based Classification

SAPFs can also be classified based on topology, namely, half-bridge (HB) topology, full-bridge (FB) topology for SAPF based on VSI converter, and H-bridge topology for SAPF based on CSI converter. Figures 1.9–1.11 show these topologies of SAPFs.

Single-phase two-wire SAPFs are used in both converter configurations; PWM CSI bridge with inductive energy storage element and PWM VSI bridge with capacitive DC-link energy storage element.

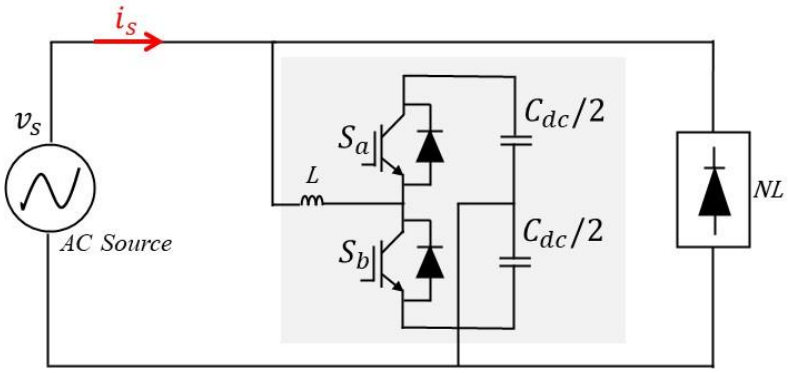

Figure 1.9: Half-bridge topology of the VSC-based single-phase shunt active power filter.

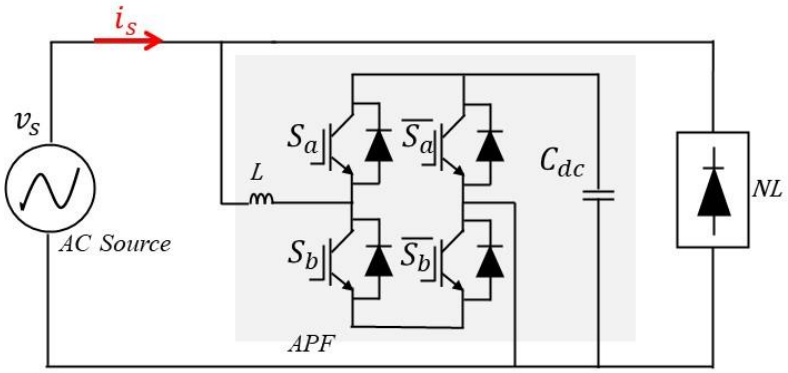

Figure 1.10: Full-bridge topology of the VSI-based single-phase shunt active power filter.

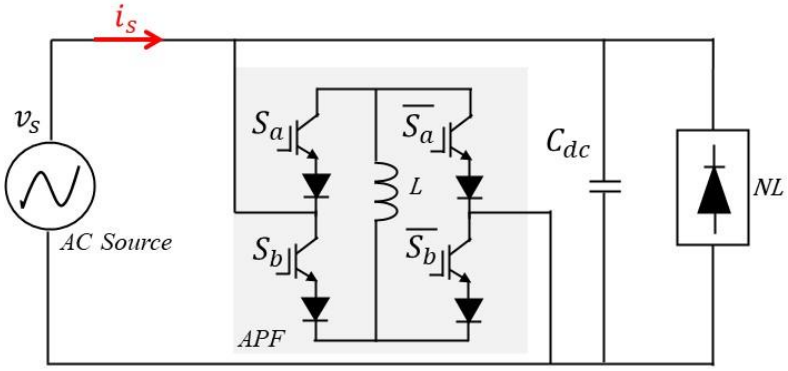

Figure 1.11: A single phase SAPF with a current source inverter (CSI).

Generally, the two-level VSIs are widely used in SAPF systems [22–26]. However, they have several disadvantages, such as voltage output rich in harmonics (High THD) with non-sinusoidal form and high switching losses, corona discharge and over-voltage [27]. Therefore, the multi-level topologies have become the most suitable topologies to be considered in such application [28–31].

7. OVERVIEW ON COMMONLY USED MULTILEVEL INVERTERS

The major weakness of conventional single phase 2-level converters is their limited power rating, high harmonic pollution and high switching frequency which prevents their usage in medium and low renewable energy conversion system and APF applications. The conventional 2-level inverter voltage output is limited to +Vdc or −Vdc from one DC capacitor with voltage magnitude Vdc which make the voltage harmonic elimination more complicated. Moreover, because of the limited voltage output, the two-level inverter switches have to suffer high amount of voltage and current especially in active filtering applications, PV or Wind farm energy conversion systems. Furthermore, high frequency operation of two-level inverter is limited only for high power applications due to increased power losses. Moreover, it is required to use high voltage switches which are limited by the existing technologies.

One solution to overcome that limitation is using Multilevel Inverters (MLIs) to produce various voltage levels by combination of switches and DC sources which is being used in medium-voltage high-power applications. Those switches are turned on and off according to a switching pattern to produce the desired combination of DC voltages at the output, whereas the switches are blocking just a part of the DC-link voltage, because, they are not able to see the whole DC-link voltage. As result, output voltage waveform becomes more smoother with less harmonic voltage which lead to reduces the filter size and power losses, while operating always at lower switching frequency.

The MLI technology has been started by the concept of multilevel step wave in cascade H-Bridge converters in the late 1960s [32]. In 1970, the Diode Clamped Converter was introduced in low power applications [33]. For medium-voltage applications, the Neutral Point Clamped (NPC) and then the Cascade H-Bridge (CHB) have been introduced in 1980s [24–35]. In addition to these two types, the Flying Capacitor (FC) inverter, which was introduced in 1960 for low power applications, and has been modified to be employed in medium-voltage and high-power industries in 1990 [36].

MLI consists of several semiconductor switches and DC supplies sources, where various voltage levels at the output are produced by a combination of switching actions and DC supplies voltages. Figure 1.12 illustrates the general concept of an MLI operation mode. It shows the DC-link and one leg of inverter in two-level, three-level and n-level configuration. Figure 1.12 (a) shows a conventional inverter which can produce +Vdc or −Vdc at the output point of 'a' with respect to the grounded neutral point, while the three-level inverter in Figure 1.12 (b)

produces +Vdc, 0 and −Vdc at the output and finally the n-level inverter in Figure 1.12 (c) generates multilevel voltages of 0, ±Vdc, ±2Vdc, …±nVdc. In MLI operation mode, the voltage value applied to the switches is only Vdc or less, however the output voltage can be more than Vdc.

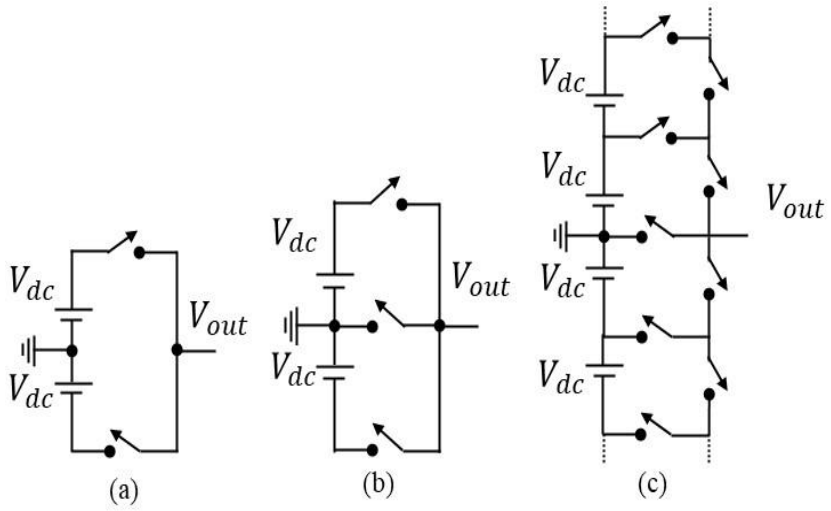

Figure 1.12: One leg of (a) 2-level, (b) 3-level and (c) n-levels inverter.

This feature of MLI allows to reach high power ratings using medium-voltage equipment in the industries and renewably energy conversion systems. The most attractive single-DC-source topologies used to produce multi-levels voltage at the output are the flying capacitors converter (FCC), Neutral-Point Clamped (NPC), T3 and Modular Multilevel Converter (MMC).

7.1 Flying Capacitors Converter

Recently, FC converters (FCC) have taken attention of the researchers and industrials due to their advantages such as natural voltage balancing feature, transformer-less operation (without transformer in grid connected mode), and the stress amid power semiconductor switches is equally distributed. Figure 1.13 shows single phase FCC converter scheme, comprised of switching power cells connected in series to form the converter phase leg. In FC converter, each pair of semiconductor devices with a flaying capacitor forms a power cell [37–38]. This implies that using these series-connected switching power cell, it is possible to achieve higher voltage/ power ranges (multilevel output voltage). To avoid the short-circuit of the voltage source, the switches S1 and S4, or S2 and S3 must be controlled in a complementary manner.

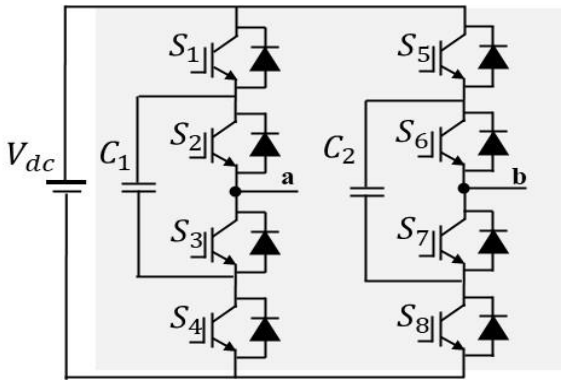

Figure 1.13: Single-phase FCC converter.

7.2 Neutral-Point Clamped (NPC)

One of the mostly used single-DC-Source MLI topologies is the 3-level NPC (Figure 1.14 (a)) [39] and the modified NPC configuration (T3) shown in Figure 1.14 (b) [40]. In T3 configuration the clamping diodes of the NPC are replaced by bidirectional switches. Those configurations can generate 3-level voltage waveform at the output. The multilevel NPC and T3 inverters are widely used in grid connected renewable energy conversion system and active filtering applications. This is owing to their good performance compared to the 2-level converter structure, where the operating voltage and power rating can be doubled. However, one of the major drawbacks is the voltage balancing and low-frequency ripple at higher modulation indices. The voltage potential of the neutral-point might have large ripples. To resolve these problems, several solutions are proposed such as the use of linear/nonlinear controllers, carrier based PWM schemes or the implementation of an external circuit devoted to the capacitor voltages balancing. However, these solutions become more complex and add supplementary costs to the converter.

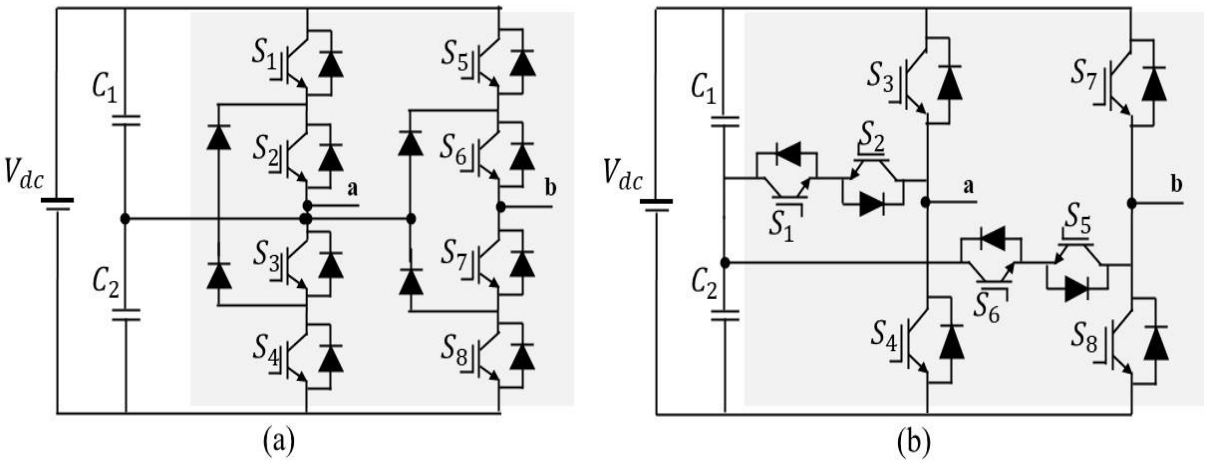

Figure 1.14: NPC based topologies: (a) standard NPC; (b) T3 converter.

7.3 Modular Multilevel Converter

The MMC is a very promising and attractive converter used especially in high-voltage direct current (HVDC) transmission system applications [41]. Recently, the MMC became the center of interest for many researches, where many configurations and control methods have been developed. Single-phase and three-phase topologies are both used [42, 43]. Figure 1.15 (a) shows a single phase 3-level MMC circuit, where $SM_{i\{1-4\}}$ denotes the cascaded connection of multiple sub-modules. The MMC configuration consists of an upper arm and a lower arm connected in series through two identical inductors *L*, which are formed by a series connection of many half-bridge cells.

7.4 Multi DC Source Cascade H-Bridge (CHB)

Multiple-DC-source topologies have at least one more supply than a single-DC-source one, which means undesired additional size and cost. The most popular MLI with multiple-DC-source is the CHB as depicted in Figure 1.15 (b). The main advantages of CHB are the modularity and identical voltage rating of switches due to using equal DC sources [54]. The major issue with this type of MLI is the power sharing among feeders.

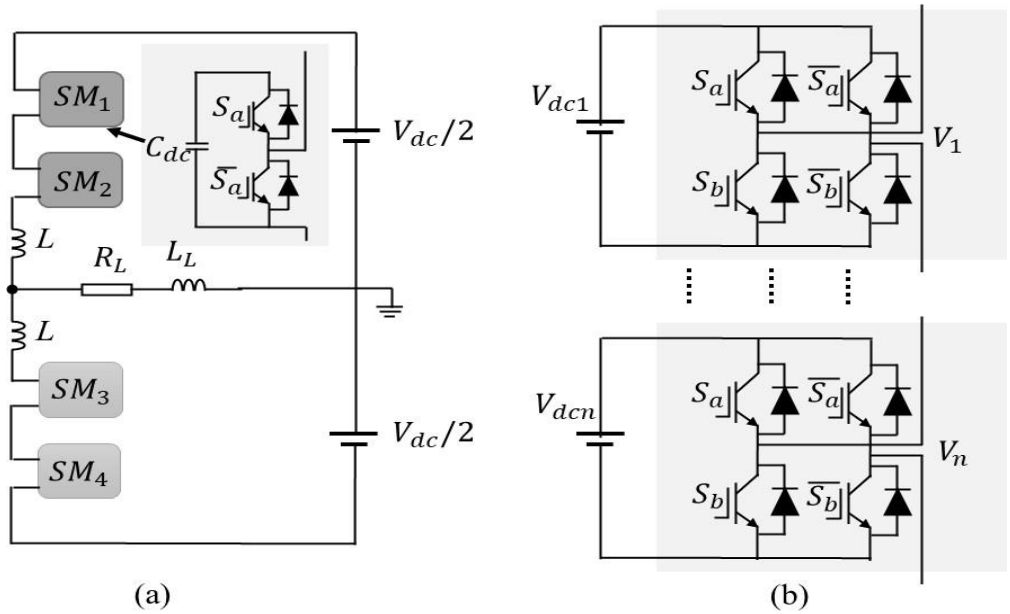

Figure 1.15: Schematic of: (a) 3-level MMC; (b) Multi DC source CHB converter.

7.5 Techniques of Capacitor Voltage Balancing

The topologies presented above are the most preferred ones in industrial applications because of their auxiliary capacitors which can be controlled through switching states without adding additional linear/nonlinear regulators and more complexity to the system. Such

topologies can be installed in all power system applications where 2-level converters are already operating. Thus, the DC side input and AC side output of the MLIs do not require to be modified. Moreover, the controller remains the same since only a single DC-link should be regulated and the error signal goes into the reference current. However, the modulation block should be replaced by a multilevel switching technique with integrated voltage balancing using redundant switching states which is considered as the most convenient technique to balance the capacitors voltages. Therefore, many research works have proposed new voltage balancing techniques such as Phase Disposition Pulse Width Modulation (PD-PWM) strategy [44] for FCC inverter. Authors in [45] used the same balancing techniques but this time with 7-level MMC inverter. Another work proposed an optimal switching-based voltage balancing method for the same converter [46]. Model Predictive Control (MPC) with its different forms has been also extensively used as an alternative to control FCCs and MMCs due to its fast-dynamic response and ability to include constraints in the cost function [47–50]. MPC control technic will be further explained in the last section of this chapter.

7.6 Modified packed unit cell multi-level inverter (MPUC)

Many topologies have been developed for single phase multilevel inverters that combine a large number of isolated DC sources and switches to reach high number of voltage levels [51]. However, in active filtering application since no isolated DC source is used, all DC-links should be replaced by capacitors and their voltages should be balanced consequently [52–57]. Such fact distinguishes the best multilevel converter topologies that can work in both modes of inverters and rectifiers.

Most of the researchers have been working on different controllers applied on STATCOM to inject reactive power to the grid with robust dynamic performance [58, 59]; however, there are a few works dedicated on the topology of the APFs like employing multilevel converters or combining different type of filters [60–62]. On the other hand, multilevel configurations have not been widely studied for reactive power compensation due to the main issue of voltage balancing for numerous DC-links existing in their structures inherently.

The initial configuration of MPUC topology has been derived from the PUC topology developed in [63] as shown in Figure 1.16. It first application was about inverter operation in grid connected mode which two isolated DC sources were used to generate a multilevel AC voltage waveform at the output [62]. However, due to requiring two isolated DC sources, it has never found a chance for further development. On the other hand, the rectifier operation of MPUC topology received more attention. It has been first proposed in [64] as a cell in modular

multilevel converters (MMC), but no more analysis have been performed to confirm the capacitor voltage balancing, power sharing and feasibility for such application. The next use of the MPUC structure is about as an active buck rectifier with dual output DC terminals [65]. Since the multilevel voltage waveform peak is the sum of two output DC terminals amplitudes, the grid will see a higher voltage and the converter operates as a boost mode in which a single inductor is used to link the converter to the grid at Point of common coupling (PCC). The voltage balancing technique and power sharing issue has been analyzed to prove the feasibility of the converter topology in such application. Furthermore, power sharing analysis revealed that the MPUC rectifier could work with two identical loads at those DC terminals. Therefore, it has been concluded that the MPUC rectifier can also work at no load condition properly which is the case of APF. In this application, equal power is consumed at DC terminals to keep the capacitors voltages fixed identically at the reference level using redundant switching states integrated into the switching pattern. Consequently, five level MPUC converter topology has been proposed as an APF application in this thesis for power quality enhancement in single phase grid.

From Figure 1.16, it is clear that 2 switches and second capacitor have been reversed in MPUC5 configuration. As a result, the output voltage of MPUC5 would be the summation of two DC-links voltage and it operates as a voltage booster. On the other hand, the main advantage of MPUC5 structure is the split DC outputs. Since the PCC sees the output voltage waveform peak equals to the sum of the two DC-links voltages, each individual DC outputs voltage amplitudes could be lesser than the PCC voltage in order to have a boost operation of the converter and inject the harmonic compensating current into the grid.

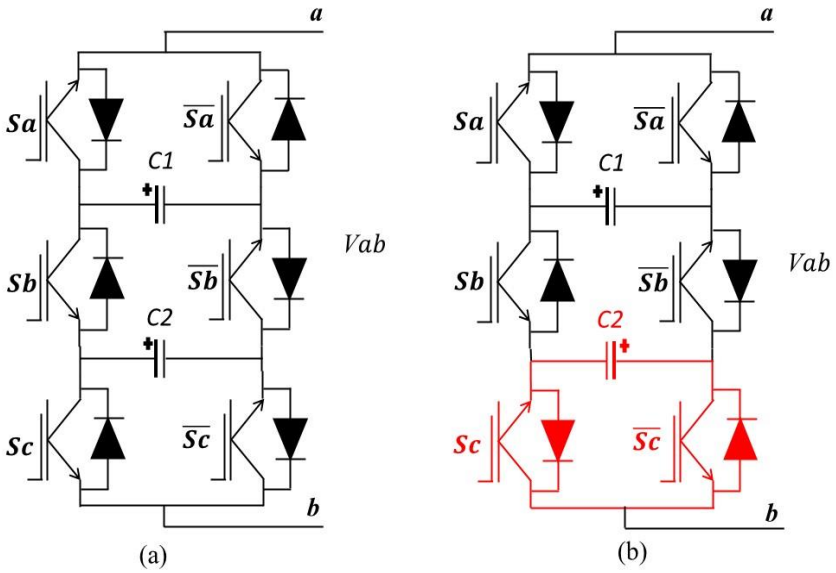

Figure 1.16: Configuration of a) PUC b) MPUC.

However, the main issue is the design of voltage balancing technique using the redundant switching states of 2, 3, 6 and 7 as listed in Table 1.4. Such redundancy helps changing the current path without changing the output voltage level.

The first task in designing the voltage balancing technique is to analyze the effect of switching states on the capacitor's voltages [66, 67]. The result of this analysis has been shown in Table 1.5.

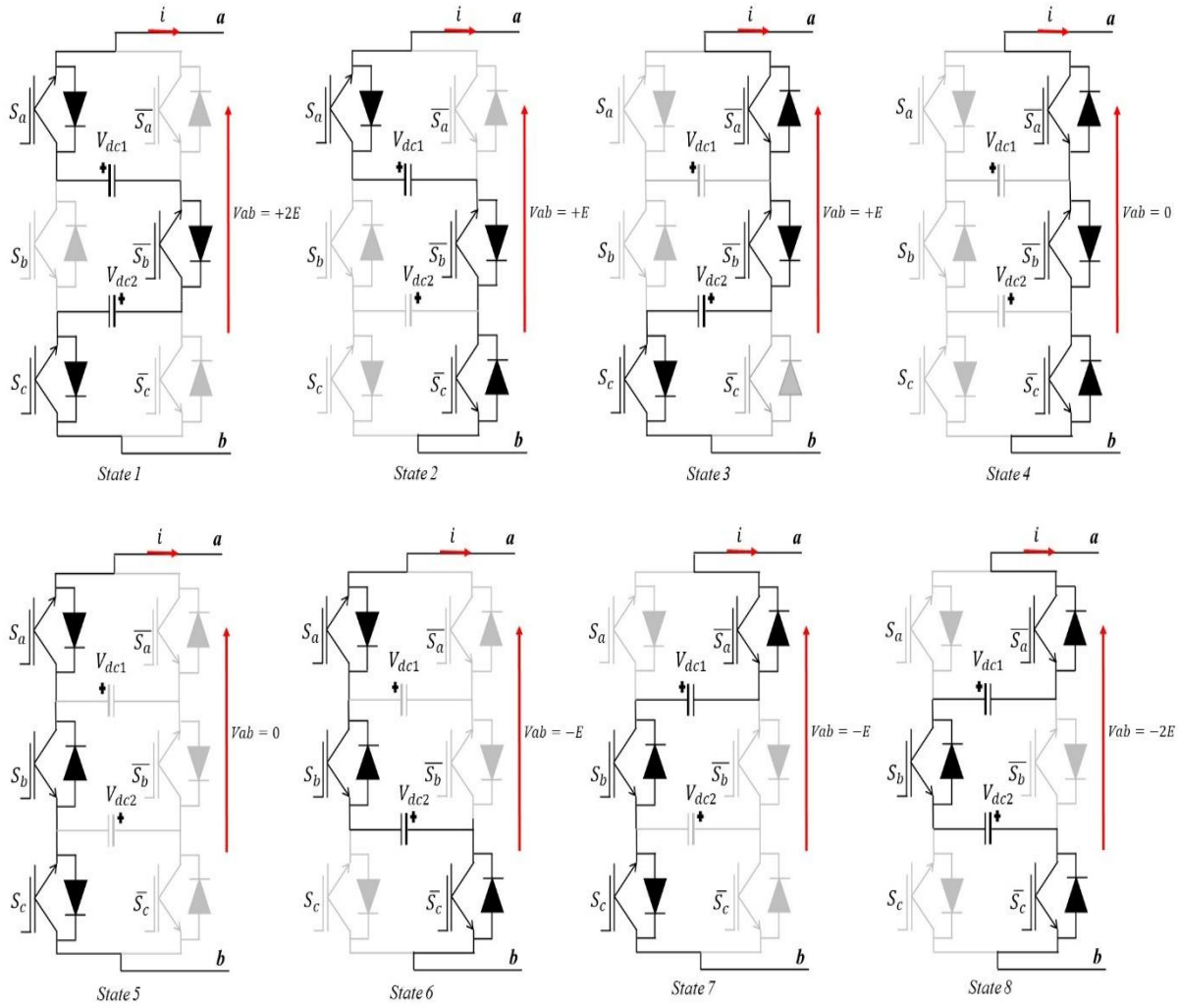

Figure 1.17. MPUC5 switching states configuration and conducting paths.

In order to design the voltage balancing technique, the redundant states 2, 3, 6, and 7 are taken into consideration, to their effects on the capacitor's voltages. Those switching states can be changed according to the capacitor instantaneous voltage. For example, if state 2 is active, then Vdc1 voltage would be increased while Vdc2 voltage would be decreased. Reciprocally, state 7 can charge up the C1 and discharge the C2. Consequently, switching between such states can keep the capacitors voltages balanced. As presented in Table 1.4, states

2, 3, 6 and 7 are used in MPUC5 inverter in order to balance the capacitor voltage at the desired level. Those configurations are shown in Figure 1.17.

Table 1.4. Switching states of the 5-level MPUC converter.

Switching states	S_a	S_b	S_c	$\overline{S_a}$	$\overline{S_b}$	$\overline{S_c}$	Voltage levels generated by MPUC5 (*Vab)*
State 1	1	0	1	0	1	0	*Vab= Vdc1+Vdc2*
State 2	1	0	0	0	1	1	*Vab= Vdc1*
State 3	0	0	1	1	1	0	*Vab= Vdc2=+E*
State 4	0	0	0	1	1	1	*Vab= 0*
State 5	1	1	1	0	0	0	*Vab= 0*
State 6	1	1	0	0	0	1	*Vab= -Vdc2*
State 7	0	1	1	1	0	0	*Vab=-Vdc1*
State 8	0	1	0	1	0	1	*Vin= -Vdc1-Vdc2*

Table 1.5. Switching effects on DC-link capacitors.

Switching states	Effect on C1	*Effect on C2*
State 1	*Charging*	*Charging*
State 2	*Charging*	*Discharging*
State 3	*Discharging*	*Charging*
State 4	*Discharging*	*Discharging*
State 5	*Discharging*	*Discharging*
State 6	*Discharging*	*Charging*
State 7	*Charging*	*Discharging*
State 8	*Charging*	*Charging*

7.7 Comparison between MPUC5 and Other MLIs topologies

To evaluate the quality of MPUC5 topology, some comparisons should be done. The selected topologies include the most popular in literature, and manufactured by industries such as Full-Bridge (FB), CHB, NPC, T3, and FC [68]. The comparison summary has been listed in Table 1.6.

The comparison table can be analyzed by each column. By noticing the number of levels, one can see that FB, NPC and MMC may be excluded, because, the higher number of voltage levels produced, the lower is the harmonic content (lower THD), the smaller size of filter and manufactured product. The second column is the number of DC terminals used in the APF, so the MMC topology is eliminated. Considering the next two columns, MPUC5 has

lower number of components among the other topologies. From these comparisons, one can conclude that, the MPUC5 topology generates more voltage levels while using less components.

Table 1.6. Comparaison between MPUC and most popular topologies.

Topology	Levels	Capacitor	Switch	Diode	Voltage balancing
FB	2	1	4	0	No need
CHB	5	2	8	0	External Regulator
NPC	3	2	8	4	External Regulator
T3	5	2	8	0	External Regulator
FC	5	2	8	0	Redundant States
MMC	3	4	8	0	External Regulator
MPUC	5	2	6	0	Redundant States

8. CLASSICAL CONTROL TECHNIQUES FOR POWER CONVERTERS

Several control methods have been proposed for the control of inverters, the most frequently used ones being shown in Figure 1.18.

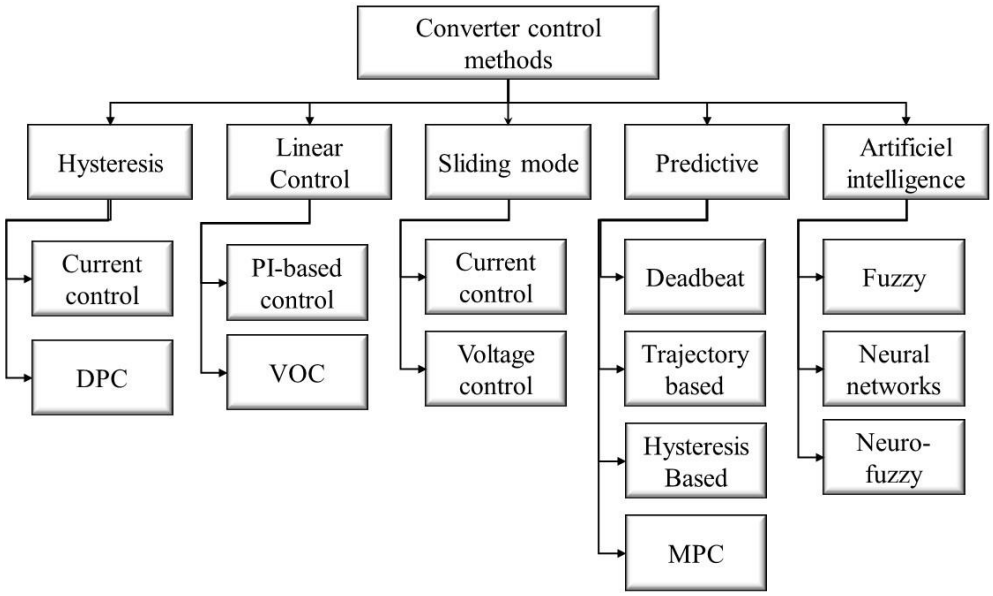

Figure 1.18: Different types of converter control schemes for power converters.

From these, hysteresis control and linear control with pulse width modulation are the most established in the literature [69–71].

8.1 Hysteresis Current Control

The basic idea of hysteresis current control is to keep the current inside the hysteresis band by changing the switching state of the converter each time the current reaches the boundary. Figure 1.19 shows the hysteresis control scheme for a single-phase inverter. Here, the current error is used as the input of the comparator and if the current error is higher than the

upper limit $\delta/2$, the power switches T1, T4 are turned on and T2, T3 are turned off. The opposite switching states are generated if the error is lower than $-\delta/2$.

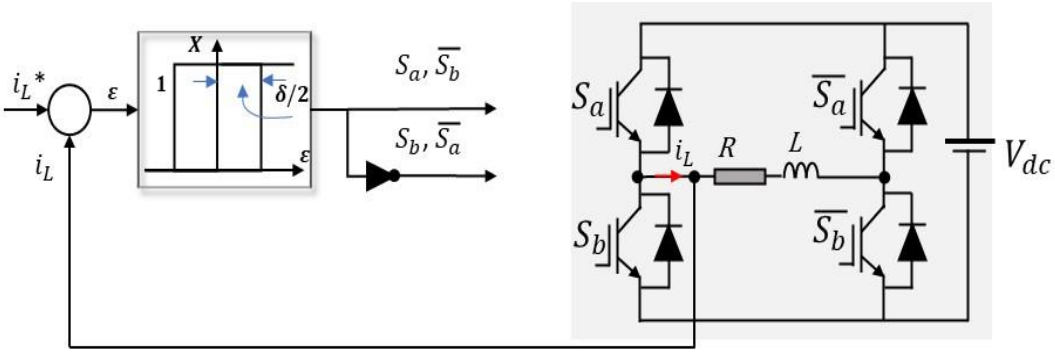

Figure 1.19: Hysteresis current control for a single-phase inverter.

8.2 Pulse Width Modulation PWM

In a pulse width modulator (PWM), the reference voltage is compared to a triangular carrier signal and the output of the comparator is used to drive the inverter switches. The application of a pulse width modulator in a single-phase inverter is shown in Figure 1.20. A sinusoidal reference voltage is compared to the triangular carrier signal generating a pulsed voltage waveform at the output of the inverter. The fundamental component of this voltage is proportional to the reference voltage.

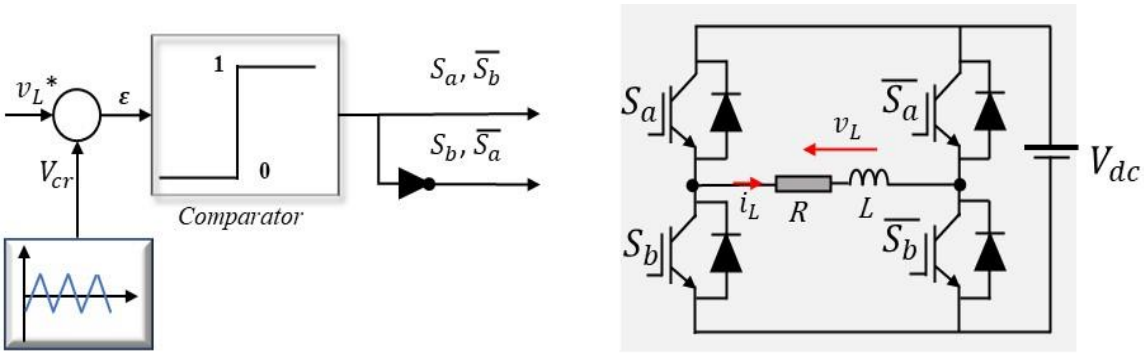

Figure 1.20: Pulse width modulator for a single-phase inverter.

8.3 Model predictive Control (MPC)

With the development of faster and more powerful microprocessors, implementation of new and more complex control schemes is possible. Some of these new control schemes for power converters include fuzzy logic, sliding mode control, and predictive control. Predictive control has appeared as an attractive solution for the control of power converters due to its fast-dynamic response and increased control accuracy [72–74].

The main approach is based on the computation of the future system dynamics to calculate optimal actuation variables. Therefore, this technique requires a high number of

calculations, compared with classic control schemes; fortunately, parallel computational capable microprocessors are available in the current market to make possible the implementation of predictive control [75].

Furthermore, predictive control brings considerable benefits to power electronics systems. First of all, concepts are intuitive and easy to understand and implement, it allows for nonlinearities and constraints to be incorporated into the control law in a straightforward manner, a multivariable case can be considered, and the resulting controller is easy to implement [76, 77].

8.3.1 Theory of Predictive Control

Predictive control uses a discrete-time model of the system to predict the future behavior of the controlled parameters during a certain time window called a receding horizon. A basic block diagram of this control technique is given in Figure 1.21.

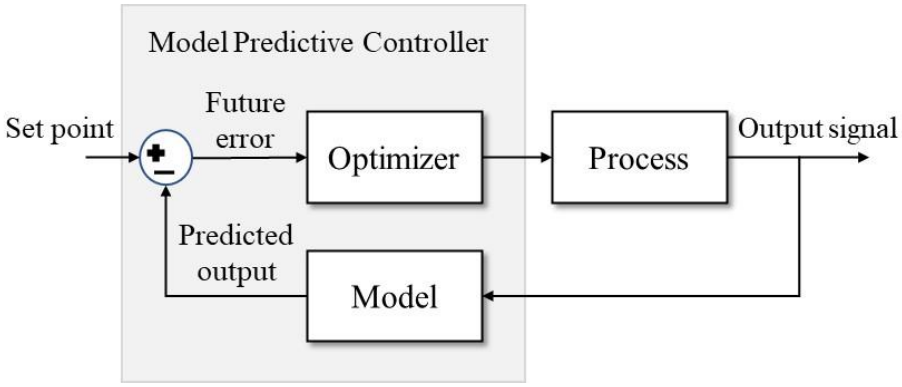

Figure 1.21: Block diagram of predictive control.

It can be observed that predictive control consists of two main blocks: model and optimizer. To predict behavior of the system at the next sampling time, the system discrete time model is used. Then, the future error between predicted output and the reference value is minimized by using predefined cost function in the optimizer. So, the basic idea of MPC can be summarized as follows:

• In order to predict system output at the next sampling instant, a discrete-time model of the system should be established.

• A cost function that represent the desired behavior of the system is used in the optimizer block.

• Finally, the optimal actuation is obtained by minimizing the cost function.

The model used for prediction is a discrete-time model which can be expressed as a state space model as follows:

$$x(k+1) = Ax(k) + Bu(k) \tag{1}$$

$$y(k+1) = Cx(k) + Du(k) \tag{2}$$

where *x(k+1)*, *u(k)*, and *y(k)* are the state variable vector, the input vector, and the output vector, respectively. Furthermore, A is the system matrix, B is the control matrix, C is the output matrix, and D is the feedthrough matrix. The prediction model can be obtained by combining *N* equations at *k+1th* through *k+Nth* instants as follows [78]:

$$\begin{bmatrix} x(k+1) \\ x(k+2) \\ \cdot \\ \cdot \\ x(k+N) \end{bmatrix} = \begin{bmatrix} A \\ A^2 \\ \cdot \\ \cdot \\ A^N \end{bmatrix} x(k) + \begin{bmatrix} B & 0 & 0 & 0 \\ AB & B & 0 & 0 \\ \cdot & \cdot & \cdot & \cdot \\ \cdot & \cdot & \cdot & \cdot \\ A^{N-1}B & A^{N-2}B & . & B \end{bmatrix} \begin{bmatrix} u(k) \\ u(k+1) \\ \cdot \\ \cdot \\ u(k+N-1) \end{bmatrix} \tag{3}$$

This prediction model can be expressed as

$$\begin{gathered} x(k+1:k+N) = \hat{A}x(k) + \hat{B}u(k:k+N-1) \\ x(:) = \hat{A}x(k) + \hat{B}u(:) \end{gathered} \tag{4}$$

A cost function (g) is needed to be determined to select an optimal actuation in the next sampling time. Since the objective of the controller is to guide the system state toward zero from any given initial conditions, the cost function can be defined as follows:

$$g = \|x(:)\|^2 + \lambda\|u(:)\|^2 = \left\|\hat{A}x(k) + \hat{B}u(:)\right\|^2 + \lambda\|u(:)\|^2 \tag{5}$$

where λ is a weighting factor.

Figure 1.22 illustrates the working principle of predictive control. The future values of the system states are predicted until a predefined horizon in time *k+N* using the system model and the available measured data until time *k*. The sequence of the optimal actuation is calculated by minimizing the cost function. This process is repeated taking into account the new measured data for each sampling time [78].

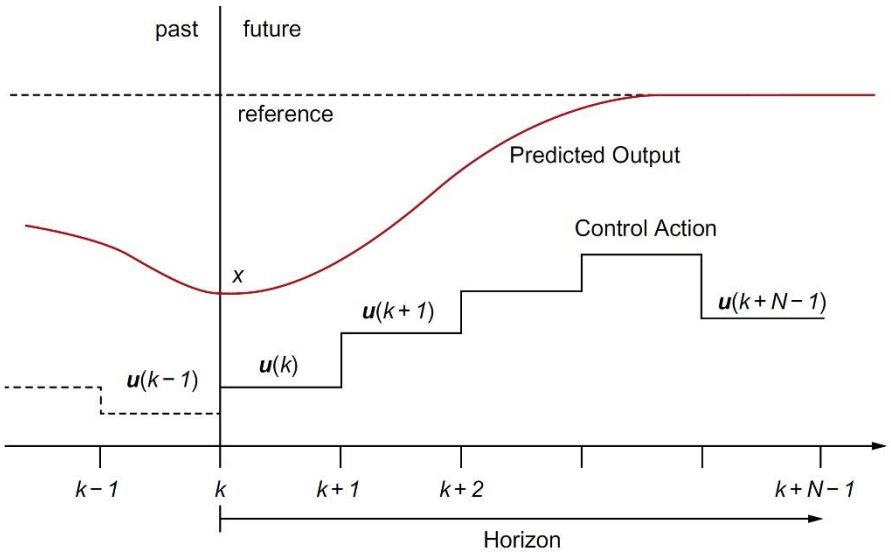

Figure 1.22: Working principle of predictive control.

8.3.2 Predictive Control classification

As illustrated previously in Figure 1.18, predictive control can be classified into four main categories. Figure 1.23 summarizes the four categories of predictive control and their specifications.

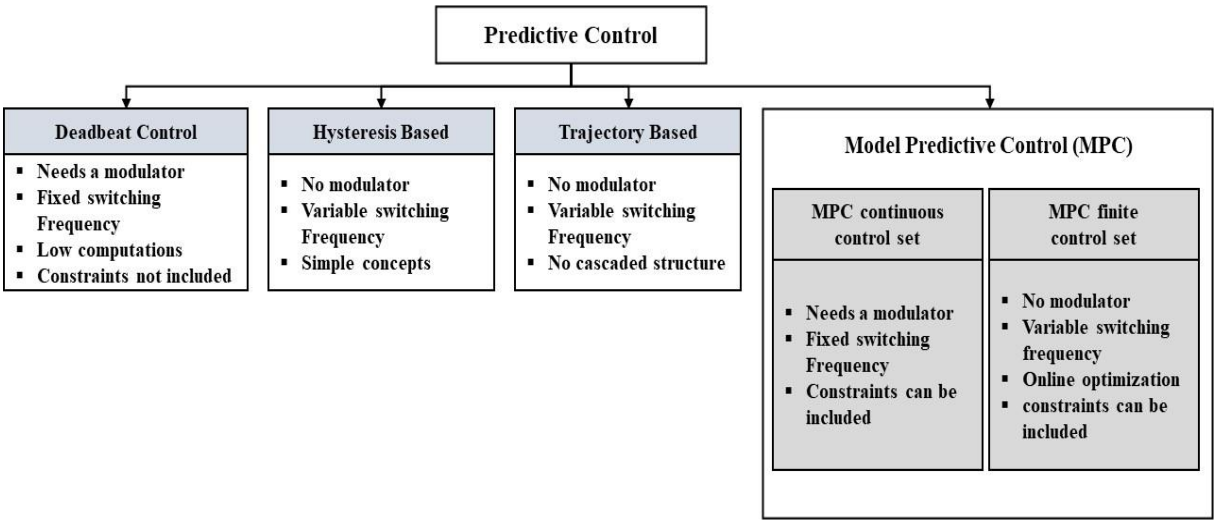

Figure 1.23: Classification of predictive control.

Model predictive control (MPC), which is the most significant predictive control technique for power electronic converters among the others, can be classified in two categories: continuous control set MPC (CCS-MPC) and finite control set MPC (FCS-MPC). CCS-MPC requires a modulator to generate the switching states, while in FCS-MPC, the switching state can be generated without modulator stage. In FCS-MPC approach, to solve the optimization problem, a finite number of switching states is used. To achieve that, a discrete-time model of

the system is employed to predict the future behavior of the system. Then, an optimal control actuation is selected by the predefined cost function as detailed in flowchart presented in Figure 1.24. Although FCS-MPC can generate switching signals without a modulator, which means that the switching frequency is variable.

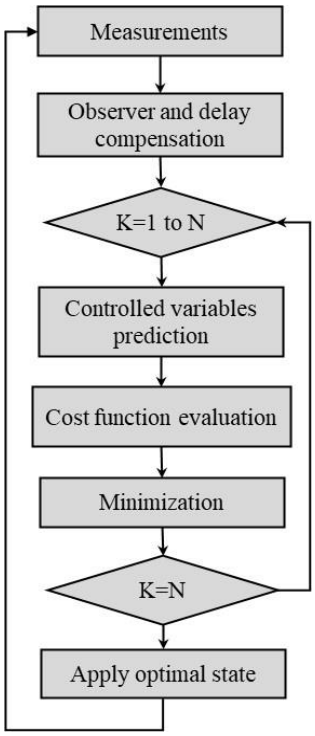

Figure 1.24: Flowchart of FCS-MPC.

Simplicity and easy implementation concept are the most important advantages of predictive control. Using predictive control technique also allows avoiding the cascaded control structure, which results in fast dynamic response in control. Furthermore, some constraints can be included in the control in order to improve the system performance.

8.3.3 Model predictive control for power converters

One of the main advantages of the predictive method is that the control algorithm is always the same. Other components such as the model, the cost function and the switching states may change depending on the load, the control objectives and the converter topology, respectively. As shown in Figure 1.24, the algorithm starts with the measurements of voltages and currents. Later, in a loop the next sample time variable for each switching state is predicted using the discrete model, and the cost function is evaluated and minimized [79, 80]. Finally, the optimal switching state is selected and applied to the converter as illustrated in Figure 1.25.

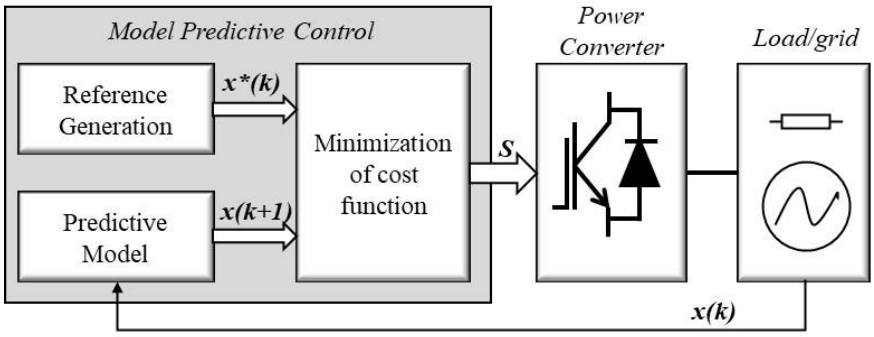

Figure 1.25: Model predictive control scheme for power converters.

9. SUMMARY

In this chapter, an overview on power quality enhancement in single phase AC grid has been presented. Harmonics' causes and distortion have been discussed. As a result, many solutions to eliminate harmonics and compensate reactive power have been proposed, such as shunt active power filter.

Single phase packed unit cell multi-level inverters are considered to be the most suitable topology for APF applications using MLI as compared to other popular ones. In order to get better performances in power quality enhancement model predictive control has been proposed as the most effective control strategy that can be used in such application owing to several advantages in contrast to classical control techniques.

REFERENCES

[1] Masand, D., Jain, S., & Agnihotri, G. (2008). Control strategies for distribution static compensator for power quality improvement. IETE Journal of research, 54(6), 421-428.

[2] Kumar, Alladi Pranay, Ganjikunta Siva Kumar, and Dharmavarapu Sreenivasarao. "Model predictive control with constant switching frequency for four-leg DSTATCOM using three-dimensional space vector modulation." IET Generation, Transmission & Distribution 14.17 (2020): 3571-3581.

[3] Singh, Bhim, P. Jayaprakash, and D. P. Kothari. "A T-connected transformer and three-leg VSC based DSTATCOM for power quality improvement." IEEE transactions on power electronics 23.6 (2008): 2710-2718.

[4] Kandil, Tarek, and Mohamed Adel Ahmed. "Control and Operation of Dynamic Voltage Restorer With Online Regulated DC-Link Capacitor in Microgrid System." Canadian Journal of Electrical and Computer Engineering 43.4 (2020): 331-341.

[5] Elkady, Z., Abdel-Rahim, N., Mansour, A. A., & Bendary, F. M. (2020). Enhanced DVR Control System Based on the Harris Hawks Optimization Algorithm. IEEE Access, 8, 177721-177733.

[6] Mihalic, R., & Gabrijel, U. (2004). A structure-preserving energy function for a static series synchronous compensator. IEEE Transactions on Power Systems, 19(3), 1501-1507.

[7] Lee, S. J., Kim, H., Sul, S. K., & Blaabjerg, F. (2004). A novel control algorithm for static series compensators by use of PQR instantaneous power theory. IEEE Transactions on Power Electronics, 19(3), 814-827.

[8] Khadkikar, V., & Chandra, A. (2011). UPQC-S: A novel concept of simultaneous voltage sag/swell and load reactive power compensations utilizing series inverter of UPQC. IEEE transactions on power electronics, 26(9), 2414-2425.

[9] Ambati, B. B., & Khadkikar, V. (2014). Optimal sizing of UPQC considering VA loading and maximum utilization of power-electronic converters. IEEE transactions on power delivery, 29(3), 1490-1498.

[10] Singh, B., Chandra, A., & Al-Haddad, K. (2014). Power quality: problems and mitigation techniques. John Wiley & Sons.

[11] Ipinnimo, O., Chowdhury, S., Chowdhury, S. P., & Mitra, J. (2013). A review of voltage dip mitigation techniques with distributed generation in electricity networks. Electric Power Systems Research, 103, 28-36.

[12] IEEE Standard 519. IEEE recommended practice and requirement for harmonic control in electric powersystems. InIEEE Std 519-2014 (Revision of IEEE Std 519-1992); IEEE: Piscataway, NJ, USA, 2014; pp. 1–29.

[13] Das, J.C. Passive filters—Potentialities and limitations.IEEE Trans. Ind. Appl.2004,40, 232–24.

[14] Akagi, H. Active harmonic filters. Proc. IEEE2005,93, 2128–2141.

[15] El-Habrouk, M.; Darwish, M.K.; Mehta, P. Active power filters: A review.IEEE Proc. Electr. Power Appl.2000,147, 403–413.

[16] Singh, B.; Al-Haddad, K.; Chandra, A. A review of active filters for power quality improvement. IEEE Trans.Ind. Electron.1999,46, 960–971.

[17] L. Gyugyi, E. C. Strycula, "Active AC Power Filters ", Conference IAS Annual Meeting, 1976, pp. 529-535.

[18] H. Akagi, H. Fujita, "New Power Line Conditioner for Harmonic Compensation in Power Systems ", IEEE Trans. on Power Delivery, vol. 10, no. 3, pp. 1570-1575, Jul. 1995.

[19] Akagi, A. Nabae, S. Atoh, "Control Strategy of Active Power Filters using Multiple Voltage-Source PWM Converters ", IEEE Trans. on Industry Applications, vol. IA-22, no. 3, pp. 460-465, May/Jun. 1986.

[20] F. Z. Peng, H. Akagi, A. Nabae, "A Study of Active Power Filters Using Quad-Series Voltage-Source PWM Converters for Harmonic Compensation ", IEEE Trans. On Power Electronics, vol. 5, no. 1, pp. 983-990, Nov./Dec. 1990.

[21] H. Akagi, "Control Strategy and Site Selection of a Shunt Active Filter for Damping of Harmonic Propagation in Power Distribution Systems ", IEEE Trans. on Power Delivery, vol. 12, no. 1, pp. 354-363, Jan. 1997.

[22] A. Sakthivel, P. Vijayakumar, A. Senthilkumar, L. Lakshminarasimman, S. Paramasivam, Experimental investigations on ant colony optimized PI control algorithm for shunt active power filter to improve power quality, Control Eng. Pract. 42 (2015) 153–169.

[23] P. Karuppanan, K.K. Mahapatra, PI and fuzzy logic controllers for shunt active power filter—A report, ISA Trans. 51 (2012) 163–169.

[24] V.F. Corasaniti, M.B. Barbieri, P.L. Arnera, M.I. Valla, Hybrid power filter to enhance power quality in a medium-voltage distribution network, IEEE Trans. Ind. Electron. 56 (2009) 2885–2893.

[25] A.S. Ray, A. Bhattacharya, Improved tracking of shunt active power filter by sliding mode control, Int. J. Electr. Power Energy Syst. 78 (2016) 916–925.

[26] A. Chaoui, J.-P. Gaubert, F. Krim, Power quality improvement using DPC controlled three-phase shunt active filter, Electr. Power Syst. Res. 80 (2010) 657–666.

[27] M.E. Ortúzar, R.E. Carmi, J.W. Dixon, L. Morán, Voltage-source active power filter based on multilevel converter and ultracapacitor DC link, IEEE Trans. Ind. Electron. 53 (2006) 477–485.

[28] M. Sharifzadeh, H. Vahedi, R. Portillo, M. Khenar, A. Sheikholeslami, L.G. Franquelo, K. Al-Haddad, Hybrid SHM-SHE pulse-amplitude modulation for high-power four-leg inverter, IEEE Trans. Ind. Electron. 63 (2016) 7234–7242.

[29] A. Draou, M. Benghanen, A. Tahri, Multilevel converters and VAR compensation, Power

Electron. Handb. (2001) 615–622.

[30] H. Zhang, S.J. Finney, A. Massoud, B.W. Williams, An SVM algorithm to balance the capacitor voltages of the three-level NPC active power filter, IEEE Trans. Power Electron. 23 (2008) 2694–2702.

[31] S. Du, J. Liu, J. Lin, Hybrid cascaded H-bridge converter for harmonic current compensation, IEEE Trans. Power Electron. 28 (2013) 2170–2179.

[32] W. McMurray, "Fast response stepped-wave switching power converter circuit," US Patent 3581212, 1971.

[33] R. H. Baker, "High-voltage converter circuit," US Patent 4203151, 1980.

[34] R. H. Baker, "Bridge converter circuit," 4270163, 1981.

[35] A. Nabae, I. Takahashi, and H. Akagi, "A new neutral-point-clamped PWM inverter," IEEE Trans. Ind. Applications, no. 5, pp. 518–523, 1981.

[36] T. Meynard and H. Foch, "Dispositif électronique de conversion d'énergie électrique," France Patent, 1991.

[37] M. Khazraei, H. Sepahvand, K. A. Corzine, M. Ferdowsi,. Active capacitor voltage balancing in single-phase flying-capacitor multilevel power converters. IEEE Transactions on Industrial Electronics, 59(2), 769-778, 2011.

[38] Teixeira, C. A., Holmes, D. G., & McGrath, B. P. Single-phase semi-bridge five-level flying-capacitor rectifier. IEEE Transactions on Industry Applications, 49(5), 2158-2166, 2013.

[39] P. Acuna, L. Morán, M. Rivera, R. Aguilera, R. Burgos, V. G. Agelidis. A single-objective predictive control method for a multivariable single-phase three-level NPC converter-based active power filter. IEEE Transactions on Industrial Electronics, 62(7), 4598-4607, 2015.

[40] M. Schweizer and J. W. Kolar, "Design and implementation of a highly efficient three-level T-type converter for low-voltage applications," IEEE Trans. Power Electron., vol. 28, no. 2, pp. 899–907, 2013.

[41] A. Nami, J. Liang, F. Dijkhuizen, and G. D. Demetriades, "Modular multilevel converters for HVDC applications: Review on converter cells and functionalities," IEEE Trans. Power Electron., vol. 30, no. 1, pp. 18–36, 2015.

[42] H. Nademi, A. Das, R. Burgos, and L. E. Norum, "A new circuit performance of modular multilevel inverter suitable for photovoltaic conversion plants," IEEE Journal Emerg. and Select. Topics in Power Electron., vol. 4, no. 2, pp. 393–404, 2016.

[43] I. Gowaid, G. Adam, A. Massoud, S. Ahmed, and B. Williams, "Hybrid and Modular Multilevel Converter Designs for Isolated HVDC-DC Converters," IEEE Journal Emerg. And Select. Topics in Power Electron., vol. PP, no. 99, p. 1, 2017.

[44] A. M. Ghias, J. Pou, V. G. Agelidis, and M. Ciobotaru, "Voltage balancing method for a flying capacitor multilevel converter using phase disposition PWM," IEEE Trans. Ind. Electron., vol. 61, no. 12, pp. 6538–6546, 2014.

[45] A. M. Ghias, J. Pou, and V. G. Agelidis, “Voltage-balancing method for stacked multicell converters using phase-disposition PWM,” IEEE Trans. Ind. Electron., vol. 62, no. 7, pp. 4001–4010, 2015.

[46] T. Premkoumar, M. Rashmi, A. Suresh, and D. R. Warrier, “Optimal voltage balancing method for reduced switching power losses in stacked multicell converters,” in International Conference on Information Communication and Embedded Systems (ICICES), 2017, pp. 1–5.

[47] S. Kouro, P. Cortés, R. Vargas, U. Ammann, and J. Rodríguez, “Model predictive control—A simple and powerful method to control power converters,” IEEE Trans. Ind. Electron., vol. 56, no. 6, pp. 1826–1838, 2009.

[48] V. Monteiro, J. C. Ferreira, A. A. N. Melendez, and J. L. Afonso, “Model Predictive Control Applied to an Improved Five-Level Bidirectional Converter,” IEEE Trans. Ind. Electron., vol. PP, no. 99, pp. 1–1, 2016.

[49] S. Vazquez, R. Aguilera, P. Acuna, J. Pou, J. Leon, L. Franquelo, et al., “Model Predictive Control for Single-Phase NPC Converters Based on Optimal Switching Sequences,” IEEE Trans. Ind. Electron., vol. PP, no. 99, pp. 1–1, 2016.

[50] M. Ghanes, M. Trabelsi, H. Abu-Rub, and L. Ben-Brahim, “Robust adaptive observer-based model predictive control for multilevel flying capacitors inverter,” IEEE Trans. Ind. Electron., vol. 63, no. 12, pp. 7876–7886, 2016.

[51] K. K. Gupta and S. Jain, "A novel multilevel inverter based on switched DC sources," IEEE Trans. Ind. Electron., vol. 61, no. 7, pp. 3269-3278, 2014.

[52] M. Narimani, B. Wu, and N. Zargari, "A Novel Five-Level Voltage Source Inverter with Sinusoidal Pulse Width Modulator for Medium-Voltage Applications," IEEE Trans. Power Electron., 2015.

[53] H. Vahedi, P. Labbe, and K. Al-Haddad, "Sensor-Less Five-Level Packed U-Cell (PUC5) Inverter Operating in Stand-Alone and Grid-Connected Modes," IEEE Trans. Ind. Informat., vol. 12, no. 1, pp. 361-370, 2016.

[54] H. Vahedi and K. Al-Haddad, "Single-DC-source five-level CHB inverter with sensor-less voltage balancing," in IECON 2015-41st Annual Conference of the IEEE Industrial Electronics Society, Japan, 2015, pp. 4494-4499.

[55] H. Vahedi and K. Al-Haddad, "Real-Time Implementation of a Seven- Level Packed U-Cell Inverter with a Low-Switching-Frequency Voltage Regulator," IEEE Trans. Power Electron., vol. 31, no. 8, pp. 5967-5973, 2016.

[56] M. Sharifzadeh, H. Vahedi, R. Portillo, M. Khenar, A. Sheikholeslami, L. G. Franquelo, et al., "Hybrid SHM-SHE Pulse Amplitude Modulation for High Power Four-Leg Inverter," IEEE Trans. Ind.Electron., vol. 63, no. 11, pp. 7234-7242, 2016.

[57] H. Geng, S. Li, C. Zhang, G. Yang, L. Dong, and B. Nahid-Mobarakeh, "Hybrid Communication Topology and Protocol for Distributed-Controlled Cascaded H-Bridge Multilevel STATCOM," IEEE Trans.Ind. Applications, vol. 53, no. 1, pp. 576-584, 2017.

[58] H. Hafezi, E. Akpinar, and A. Balikci, "Cascade PI controller for single-phase STATCOM," in 16th International Power Electronics and Motion Control Conference and Exposition (PEMC), 2014, pp. 88-93.

[59] H. Vahedi, A. Dehghanzadeh, K. Al-Haddad, "Static VAr compensator using packed U-cell based multilevel converter". In 2018 IEEE 12th International Conference on Compatibility, Power Electronics and Power Engineering (CPE-POWERENG 2018) (pp. 1-5). IEEE.

[60] S. Du, J. Liu, and J. Lin, "Hybrid cascaded H-bridge converter for harmonic current compensation," IEEE Trans. Power Electron., vol. 28, no. 5, pp. 2170-2179, 2013

[61] M. Sharifzadeh, H. Vahedi, R. Portillo, M. Khenar, A. Sheikholeslami, L. G. Franquelo, et al., "Hybrid SHM-SHE Pulse Amplitude Modulation for High Power Four-Leg Inverter," IEEE Trans. Ind. Electron., vol. 63, no. 11, pp. 7234-7242, 2016.

[62] M. F. Kangarlu, E. Babaei, and M. Sabahi, "Cascaded cross-switched multilevel inverter in symmetric and asymmetric conditions," IET Power Electron., vol. 6, no. 6, pp. 1041-1050, 2013.

[63] H. Vahedi and K. Al-Haddad, "METHOD AND SYSTEM FOR OPERATING A MULTILEVEL INVERTER," US Patent 20160126862, 2015.

[64] A. Nami, J. Liang, F. Dijkhuizen, and G. D. Demetriades, "Modular multilevel converters for HVDC applications: Review on converter cells and functionalities," IEEE Trans. Power Electron., vol. 30, no. 1, pp. 18-36, 2015.

[65] H. Vahedi and K. Al-Haddad, "A Novel Multilevel Multi-Output Bidirectional Active Buck PFC Rectifier," IEEE Trans. Ind. Electron., vol. 63, no. 9, pp. 5442 - 5450, 2016.

[66] H. Vahedi, H. Y. Kanaan, and K. Al-Haddad, "PUC converter review: Topology, control and applications," in IECON 2015-41st Annual Conference of the IEEE Industrial Electronics Society, Japan, 2015, pp. 4334-4339.

[67] L. Tan, B. Wu, M. Narimani, D. Xu, and G. Joos, "Multicarrier-Based PWM Strategies with Complete Voltage Balance Control for NNPC Inverters," IEEE Trans. Ind. Electron., vol. PP, no. 99, p. 1, 2017.

[68] L. G. Franquelo, J. Rodriguez, J. I. Leon, S. Kouro, R. Portillo, and M. A. M. Prats, “The age of multilevel converters arrives,” IEEE Ind. Electron. Mag., vol. 2, no. 2, pp. 28–39, 2008.

[69] M. P. Kazmierkowski, R. Krishnan, and F. Blaabjerg, Control in power electronics. Academic Press, 2002.

[70] Rodriguez, J., & Cortes, P. (2012). Predictive control of power converters and electrical drives (Vol. 40). John Wiley & Sons.

[71] Blaabjerg, F. (Ed.). (2018). Control of Power Electronic Converters and Systems: Volume 2 (Vol. 2). Academic Press.

[72] W. Liuping, C. Shan, Y. Dae, G. Lu, N. Ki, PID and Predictive Control of Electrical Drives and Power Converters Using Matlab/Simulink, Wiley & IEEE Press, 2015. ISBN 97811118339442.

[73] M. Trabelsi, S. Bayhan, S.S. Refaat, H. Abu-Rub, L. Ben- Brahim, Multi-objective model

predictive control for grid-tied 15-level packed U cells inverter, in: 18th European Conference on Power Electronics and Applications (EPE'16 ECCE Europe), Karlsruhe, Germany, 2016, pp. 1–7.

[74] S. Bayhan, H. Abu-Rub, Model predictive sensorless control of standalone doubly fed induction generator, in: 40th Annual Conference of the IEEE Industrial Electronics Society, IECON 2014, 2014, pp. 2166–2172.

[75] M. Trabelsi, S.Bayhan, H.Abu-Rub, L.Ben-Brahim, P.Zanchetta, Finite control setmodel predictive control for Grid-TieQuasi-Z-source based multilevel inverter, in: IEEE International Conference on Industrial Technology, ICIT 2016, Taipei, Taiwan, 14–17 March, 2016.

[76] J. Rodriguez, M. Kazmierkowski, J.R. Espinoza, P. Zanchetta, H. Abu-Rub, H.A. Young, C.A. Rojas, State of the art of finite control set model predictive control in power electronics, IEEE Trans. Ind. Inform. 9 (2) (2013) 1003–1016.

[77] P. Cortes, M.P. Kazmierkowski, R.M. Kennel, D.E. Quevedo, J. Rodriguez, Predictive control in power electronics and drives, IEEE Trans. Ind. Electron. 55 (12) (2008) 4312–4324.

[78] S. Bayhan, M. Mosa, H. Abu-Rub, Model Predictive Control of Impedance Source Inverter, John Wiley & Sons Ltd, 2016. pp. 329–361.

[79] Bayhan, S., & Abu-Rub, H. (2018). Predictive Control of Power Electronic Converters. In Power Electronics Handbook (pp. 1325-1338). Butterworth-Heinemann.

[80] Rodriguez, J., & Cortes, P. (2012). Predictive control of power converters and electrical drives (Vol. 40). John Wiley & Sons.

Chapter 2

Power quality Enhancement in Single-Phase Power Grid using Multilevel Inverters

1. INTRODUCTION

Power electronics technology plays an important role in distributed generation (DG) systems. It is extensively being used and rapidly expanding, becoming more integrated in grid-based systems to address power quality issues and to improve the grid power quality by eliminating current harmonics and compensating the reactive power sent to the grid at the point of common coupling (PCC), which are caused by the proliferation of power electronics-based devices in residential and industrial applications such as personal computers, air conditioning systems, pumps and blowers[1, 2]. These devices increase the share of nonlinear loads compared with that of linear loads and affect the power quality of the grid, which changes in a sinusoidal shape of the grid current through accumulation of harmonic distortions. Increased harmonic pollution in power networks has led to the development of new dynamic and suitable solutions to solve power quality problems. These equipment's are, in general, known as active power filters [3, 4].

Shunt active power filters (APF) based on voltage source inverter (VSI) are progressively involved in reducing the effect of harmonic currents and reactive power, where different topologies are used and many works have contributed to the development of such a solution [5–7].

Active filters inject a current into the PCC point in a way that the sum of the compensation and load currents gives a current of sinusoidal waveform seen from the source as depicted in Figure 2.1. The important issue of active filters is how to generate the suitable

compensation current. In order to generate this filter current, a balance between instantaneous power supplied by the source, active filter power and load power should be achieved. Active filters are also programmed to achieve power factor correction as well as harmonics elimination. Those topologies can offer good quality of compensation for reactive power, as well as voltage and current with low distortion.

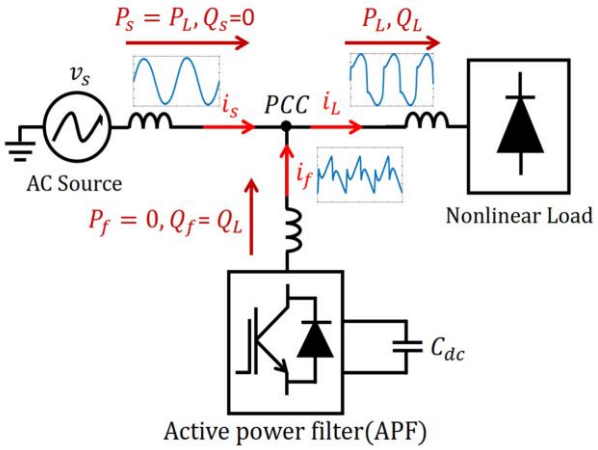

Figure 2.1: Shunt Active power filter topology.

Generally, the two-level VSIs are widely used in APF systems [8–12]. However, they have several disadvantages, such as voltage output rich in harmonics (High THD) with non-sinusoidal form and high switching losses, corona discharge and overvoltage [13]. Therefore, the multi-level topologies have become the most suitable topologies to be considered [14–17].

Several research works have been dedicated to develop various multilevel inverter topologies for different applications [18, 19]. The conventional topologies of multi-level inverters such as neutral point clamped (NPC) [16] and cascaded H-Bridge (CHB) [17] have been used as the most popular configurations in APF systems. They produce various and symmetrical voltage levels, which led to provide a high grid current quality with low value of filter-side inductor and less stress on semiconductor switches. However, they possess a high number of power electronic components (IGBT switching, diodes, capacitors). Numerous recent works have been devoted to develop some new multilevel inverter topologies with a smaller number of power electronics components [20–24]; one of these topologies is the modified packed U-cell five-level inverter (MPUC5) [22] which is under consideration in this chapter for APF systems.

The first configuration of MPUC inverter has been derived from the PUC topology presented in [21, 23], which is developed by authors of [22]. MPUC topology is mainly

composed of six semiconductor switches and two capacitors, it operates with two isolated DC capacitors and the DC voltage is used to generate a multi-level AC voltage at the output. However, the major problems of the MPUC inverter are the unbalancing capacitor potentials of DC-link voltage and the complexity of control design.

Several works based on PUC and MPUC topologies, proposed new control techniques in order to overcome the unbalancing capacitor voltages issue for grid connected and APF applications by using a self-voltage-balancing using some redundant switching states integrated in the multicarrier pulse width modulation (PWM) [20–22].

The authors of [22] proposed a new control scheme for single phase APF application using modified PUC inverter, where two PI controllers are employed with a self-voltage balancing technique integrated through PWM modulator. However, this control scheme based on cascade PI controllers and four multicarrier PWM, makes the system response very slow in dynamic state and has a few limitations on balancing capacitor voltages when a change in system parameters occurs. Furthermore, the complexity of PWM modulator including self-voltage balancing technique makes the control system hard to be implemented.

Model Predictive Control (MPC) technique is a simple and effective strategy based on the model of the controlled system to predict its future behavior and select the most appropriate control action based on an optimality criterion. In the last decades, it has been extensively explored in power converters control, due to the rapid growth of modern microcontrollers and digital signal processors (DSPs) with high computational capabilities, which makes the implementation for the MPC control schemes much easier [25–27]. MPC strategy takes advantage of the inherent discrete nature of power converters and the finite number of switching states to solve optimization problem by the prediction of the system behavior only for those possible switching states. Then, each prediction is used to evaluate a cost function, and consequently, the state with minimum cost is selected and generated [28–31]. Furthermore, it has some interesting characteristics such as design simplicity, a fast-dynamic response and ability to include nonlinearities and constraints in the design of the controller. On other hand, MPC strategy is employed in order to reduce the need for PI controllers and eliminates the need of PWM modulation stage. Moreover, it is easy to include the DC-link capacitor voltages balancing constraint in the objective control.

In this chapter, a single phase APF system is developed using multilevel MPUC5 inverter controlled by a new MPC algorithm in order to compensate a contaminating load with

small power factor, to enhance reactive power in the grid and to eliminate harmonic currents at the PCC. The proposed MPC algorithm is employed to reduce the computational burden and provides high power factor correction, in addition to ensure the balance of the DC-link capacitor voltages. To confirm the performance of the proposed configuration, complete simulations are carried out using Matlab/Simulink™ environment and then, a real-time hardware in the loop (HIL) tests are performed using dSPACE 1104 control board [32, 33].

This chapter is organized as follows: after an introduction, the proposed MPUC5 topology configuration is presented in section 2. Section 3 describes the MPC technique for the MPUC5 inverter in APF application. Section 4 demonstrates the simulation results. Experimental results with hardware in the loop (HIL) implementation using Matlab/Simulink™ and dSPACE 1104 control board are illustrated and discussed in section 5 to validate the dynamic performance of the proposed system.

2. PROPOSED MPUC5 INVERTER TOPOLOGY FOR APF APPLICATION

The proposed structure of APF with the control strategy is shown in Figure 2.2. It consists of an AC source, a nonlinear load connected in series and the MPUC5 inverter connected to the grid in parallel through a line inductor *(L_f)* at the PCC.

The main goals of this configuration are to compensate the reactive power and eliminate the harmonic components in the grid current caused by nonlinear loads at the PCC. The MPUC5 inverter injects a harmonic current into the grid in order to compensate the harmonic current requested by the nonlinear load from the grid.

The MPUC5 inverter topology as shown in Figure 2.2, has 6 active switches and two DC-link capacitors. The different states of this configuration are illustrated in Table 2.1. The main advantage of MPUC5 structure is that the two DC-side voltages of the converter provide voltages V_{dc1} and V_{dc2} separately; each voltage should be smaller than the PCC voltage. As a result, the voltage peak seen by the PCC is equal to the sum of the two DC outputs [21, 22], and in addition $V_{dc1} = V_{dc2}$ to ensure the voltage capacitors balancing of the MPUC5, in order to guarantee boost operation of the inverter and to inject the compensation current into the grid. By assuming ($V_{dc1} = V_{dc2} = E$), the switching states ($\boldsymbol{X}$) and voltage levels generated by the MPUC5 inverter (V_{in}) can be denoted as in Table 2.1.

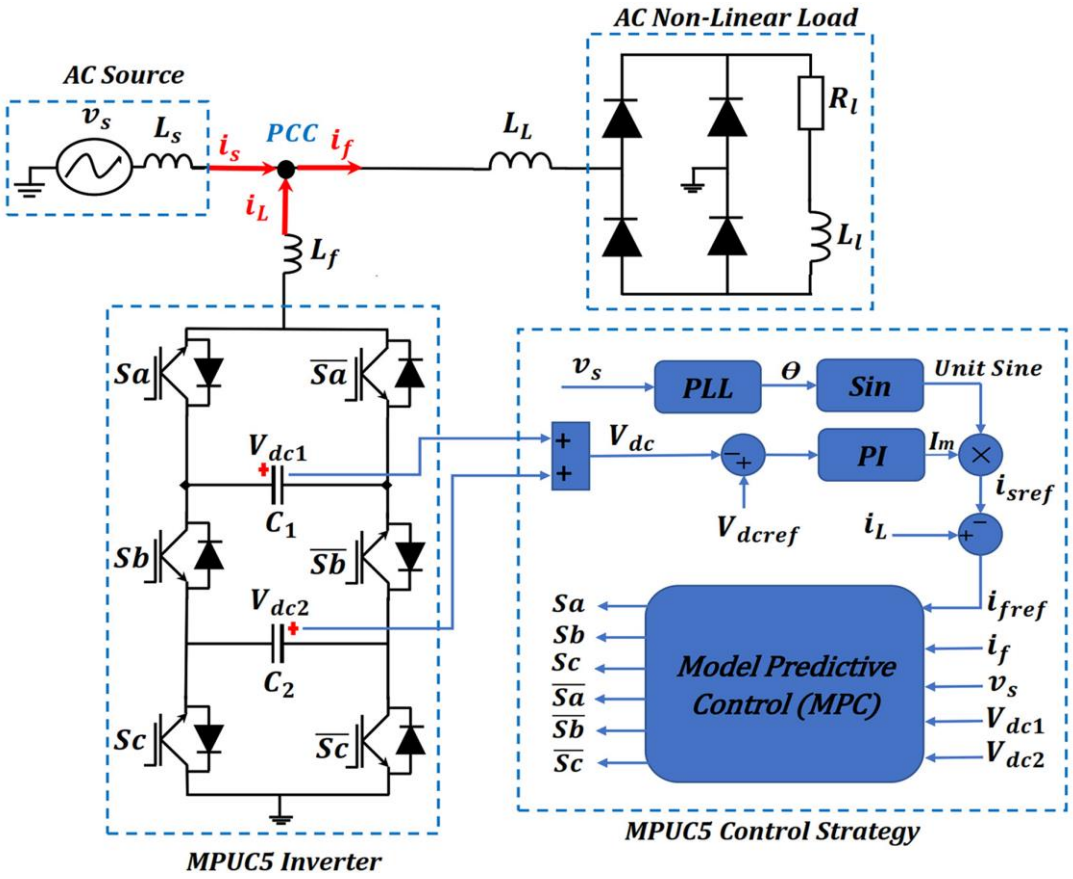

Figure 2.2: Five-level MPUC inverter for APF application.

Table 2.1. Switching states and voltage levels of the MPUC5 Inverter.

Switching State (*X*)	S_a	S_b	S_c	$\overline{S_a}$	$\overline{S_b}$	$\overline{S_c}$	Voltage levels generated by MPUC5 (V_{in})
State 1	0	1	0	1	0	1	V_{in} = -2E
State 2	1	0	1	0	1	0	V_{in} = +2E
State 3	1	1	1	0	0	0	V_{in} = 0
State 4	0	0	0	1	1	1	V_{in} = 0
State 5	0	1	1	1	0	0	V_{in} = -E
State 6	1	1	0	0	0	1	V_{in} = -E
State 7	0	0	1	1	1	0	V_{in} = +E
State 8	1	0	0	0	1	1	V_{in} = +E

3. MODEL PREDICTIVE CONTROL (MPC)

In general, MPC is an advanced and effective strategy to control the power converters. it is based on the mathematical model of the studied system in order to predict the future behavior of the controlled variables [25, 27]. Then, to form these predictions, a cost function is defined and evaluated in order to select the optimal control action [28–31].

Figure 2.3 shows the flowchart of the proposed MPC applied to MPUC5 inverter. From the measured values of the filter current i_f, the grid voltage i_s, the filter reference current i_{f_ref} estimated from the PI controller, and the capacitor voltages *(V_{dc1}, V_{dc2})*, the predicted value of filter current $i_f(k+1)$ is calculated for all switching states cases; the predicted capacitor voltages are also calculated only for the switching states which has an effect on capacitor voltages (one of the capacitors is discharged and the other one is kept constant *(V_{in}=+E or -E)*). Otherwise, the predicted capacitor voltages remain the same ($V_{dc1}(k+1) = V_{dc1}(k)$ & $V_{dc2}(k+1) = V_{dc2}(k)$*)* in the other states. After that, a cost function is evaluated in order to compute the optimal value. The optimal switch state chosen is applied during the next sampling time to the MPUC5 inverter through the switching pulses, which are produced according to the appropriate switching state chosen by the MPC from the switching table (Table 2.1).

The mathematical model of single phase APF using MPUC5 is given below:

$$\frac{di_s(t)}{dt} = \frac{1}{L}(V_{in} - v_s - Ri_s) \tag{1}$$

$$\begin{cases} \dfrac{dV_{cx}(t)}{dt} = \dfrac{1}{C_x} i_f \\ x = 1,2. \end{cases} \tag{2}$$

where i_s and v_s are the measured filter current and grid voltage respectively, V_{cx} is the DC-link capacitor voltages, i_f is the filter current and V_{in} is the output voltage of the MPUC inverter.

The variables that have to be controlled are the future filter current i_f and the capacitor voltages: V_{dc1}, V_{dc2}.

A PI controller is used to estimate the filter reference current by using Kirchoff current law

$$i_s + i_f = i_L \tag{3}$$

Therefore, the filter reference current can be expressed as follows

$$i_{f\_ref} = i_L - i_{s\_ref} \tag{4}$$

where, i_{f_ref} is the grid reference current generated by the PI controller and i_L is the measured load current at the PCC.

From Eq. (1) and by using the Euler Forward approximation, the future behavior of filter current can be expressed as

$$i_f(k+1) = (1 - R \cdot T_s/L_f) \cdot i_f(k) + (T_s/L_f) \cdot (V_{in} - v_s) \quad (5)$$

where, V_{in} is the voltage vector generated by the 5-level MPUC inverter, R is the internal resistor of the filter inductance, L_f the filter inductance, T_s the sampling period and v_s the AC source voltage.

In order to reduce the computation burden, two variables S_1 and S_2 are introduced to simplify the use of switching states S_a, S_b and S_c. They are calculated by using Eqs. (6) and (7).

$$S_1 = S_a - S_b \quad (6)$$

$$S_2 = S_c - S_b \quad (7)$$

The voltage vector generated by the 5-level MPUC inverter can be calculated as follows

$$V_{in} = S_1 \cdot V_{dc1} + S_2 \cdot V_{dc2} \quad (8)$$

Using again Euler approximation and Eq. (2), the two capacitor voltages for the next sampling time $V_{dc1}(k+1)$ and $V_{dc2}(k+1)$ can be predicted to ensure the balancing voltage of the two DC-link capacitors by activating the appropriate switches

$$V_{dc1}(k+1) = V_{dc1}(k) - ((T_s \cdot S_1)/C) \cdot i_f(k) \quad (9)$$

$$V_{dc2}(k+1) = V_{dc2}(k) - ((T_s \cdot S_2)/C) \cdot i_f(k) \quad (10)$$

where C_1, C_2 and C ($C_1 = C_2 = C$) are the DC-link capacitors.

Finally, the cost function g is derived as Eq. (11),

$$g = abs(i_{f\_ref}(k) - i_f(k+1) + \lambda \cdot abs(V_{dc1}(k+1) - V_{dc2}(k+1)) \quad (11)$$

where λ is the weighting factor, $i_{f\_ref}(k)$, $i_f(k+1)$ are the reference and future behavior of filter current respectively, $V_{dc1}(k+1)$, $V_{dc2}(k+1)$ are the future behavior of DC-link capacitor voltages.

The cost function g is calculated for the 8 possible switching states, according to the predefined switching table (Table 2.1).

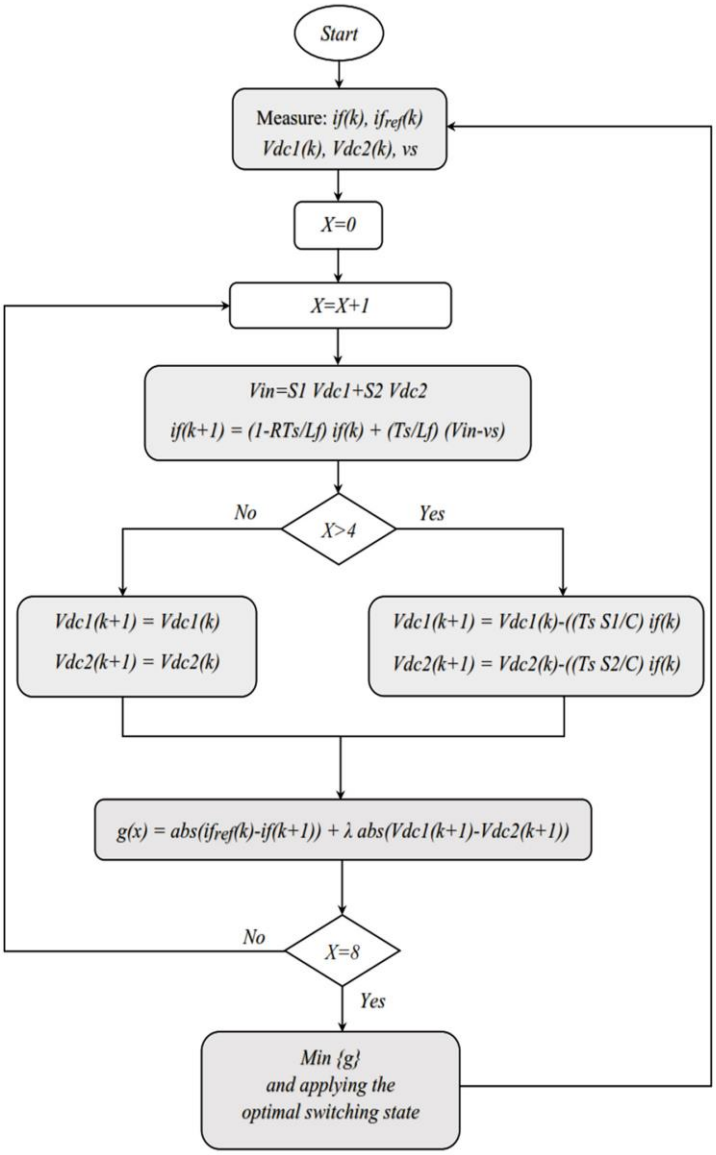

Figure 2.3: Flowchart of the proposed MPC.

4. ANALYTICAL STUDIES AND DISCUSSION

Several numerical simulations using Matlab/Simulink™ and SimPower systems packages of the proposed system have been carried out. The entire single-phase active filter was composed of an AC source, a nonlinear load (Rectifier & R_l, L_l), a 5-level MPUC inverter and MPC controller. The simulation parameters are presented in Table 2.2.

Figure 2.4 shows the simulation results of the APF system before and after filtering. The filter was switched on at $t = 0.15s$, the filter started to inject a filter current as shown in Figure

2.4(b). As a result, the grid current became sinusoidal and the nonlinear load continued to consume a distorted current as depicted in Figure 2.4(a) and Figure 2.4(c), respectively.

Table 2.2. Test parameters.

Parameters	**Values**
Grid Voltage (v_s)	120 *V*
Grid Frequency (*fs*)	50 *Hz*
Grid Side Inductor (*Ls*)	0.566 *mH*
Grid side resistor (*Rs*)	0.1 *Ω*
Filter Side Inductor (*Lf*)	2 *mH*
Rectifier AC Side Inductor (L_L)	0.566 *mH*
DC Capacitors (*C1&C2*)	1100 *μF*
Load DC Side Resistor (R_l)	6 *Ω*
Load DC Side Inductor (L_l)	20 *mH*
DC Voltage Reference (*Vdc_ref*)	200 *V*
Sampling frequency *fs*	20 kHz

The DC-link voltage V_{dc} reached the steady state within few cycles (ripple voltage less than 5%), with a perfect balancing of the two capacitor voltages (V_{dc1}& V_{dc2}) as depicted in Figure 2.4(d). In the same time, the active power reached the nominal value, and the reactive power became null when the filter was switched on as shown in Figure 2.4(e). Due to the perfect voltage balancing of the capacitors (C_1&C_2), the 5-level output voltage V_{in} of the inverter has been obtained easily as illustrated in Figure 2.4(f).

Figure 2.5 shows the steady state of the grid voltage v_s and grid current i_s with a perfect synchronization, which proves the power factor unity with low grid current THD (%) as presented in Table 2.3.

Figure 2.6 illustrates the dynamic state of grid current i_s and voltage v_s corresponding to 50% change in resistor R_l of the nonlinear load (from 6Ω to 3Ω). It can be seen that the grid current i_s has always a sinusoidal waveform with a lower value of THD (%) (Table 2.3), and in phase with grid voltage v_s, which demonstrates the good performance of the proposed control strategy.

Furthermore, to show the good performance of the proposed MPC algorithm, the average device switching frequency f_{sw} is calculated for all APF operating cases. The proposed

MPC maintains the THDi% below 5% and increases the reliability of the semiconductor switches, where the switching frequency f_{sw} is sustained below 10 kHz as indicated in Table 2.3.

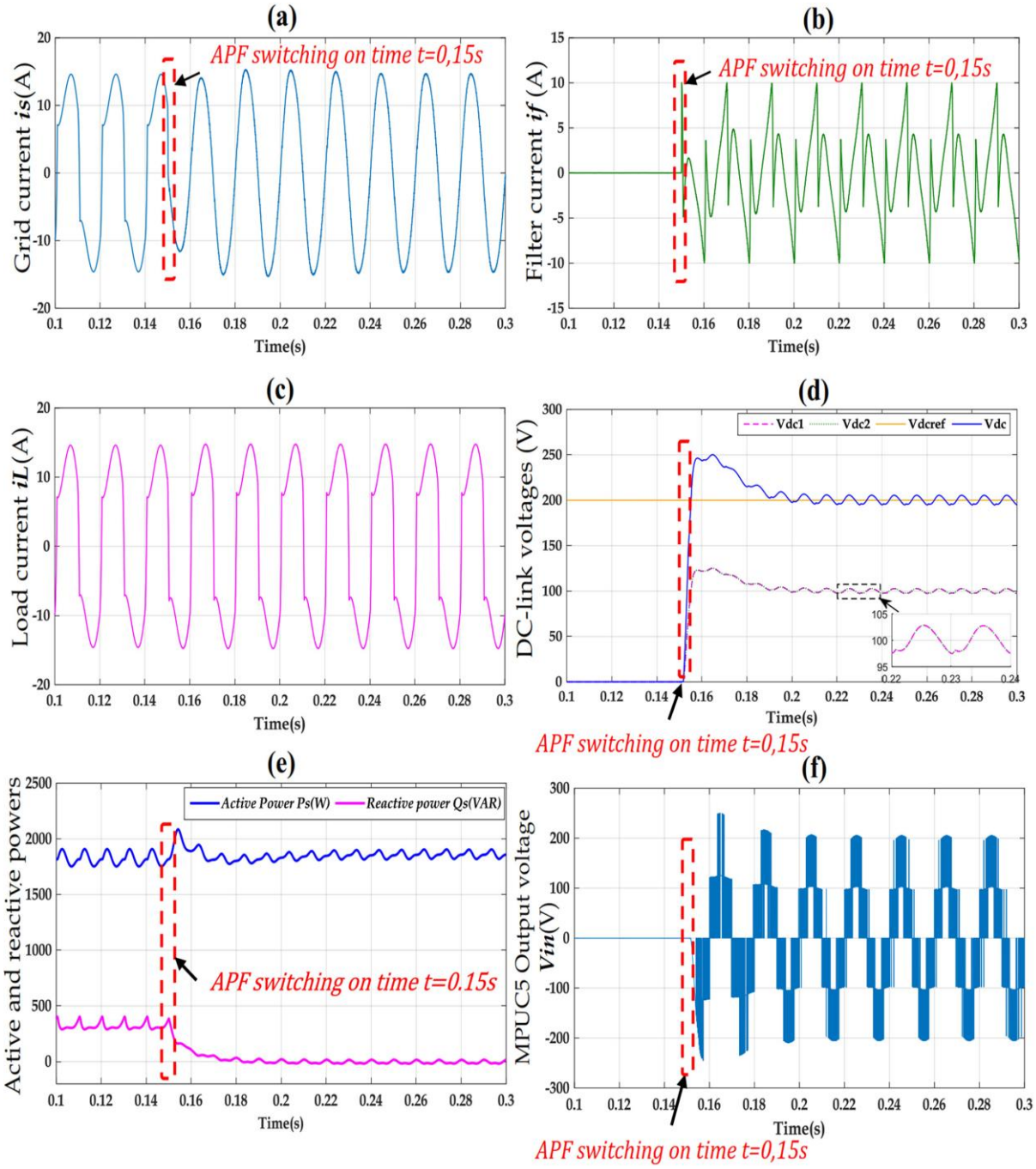

Figure 2.4: Simulation results of the APF system. Filter switched on at t=0.15 s.

Meanwhile, the APF continues to feed the grid with a compensation current to cover the need to the load for reactive power as depicted in Figure 2.7(a). Furthermore, the load current amplitude increases while keeping up the same waveform and the nonlinear load continues to absorb the distorted current as shown in Figure 2.7(b).

The responses of the DC-link voltage and the two capacitor voltages during load change at $t = 0.5s$ are illustrated in Figure 2.7(c). It is worth mentioning that the two capacitor voltages get balanced instantaneously and identically due to the dynamic performance of the proposed MPC.

Figure 2.7(d) shows the output voltage V_{in} of the inverter during load change, one can notice that the inverter output voltage is not affected during this change by keeping the same 5-level output voltage.

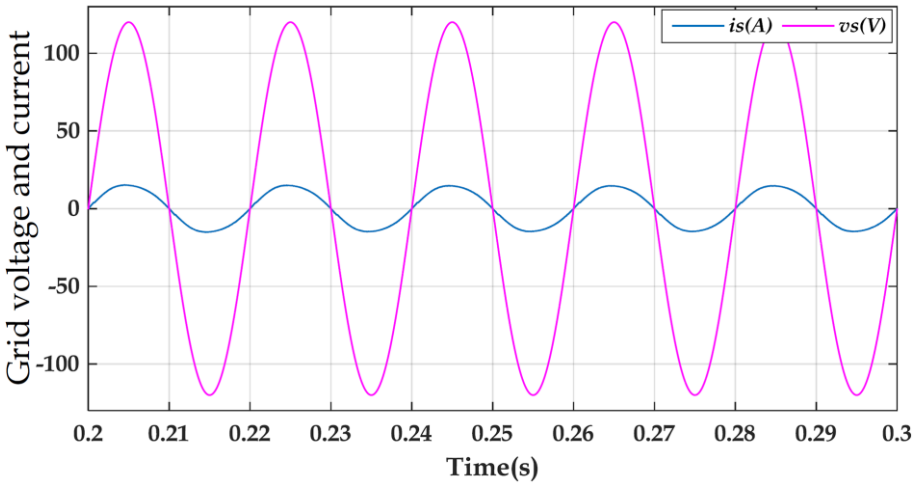

Figure 2.5: Waveforms in steady state for grid voltage (v_s) and current (i_s).

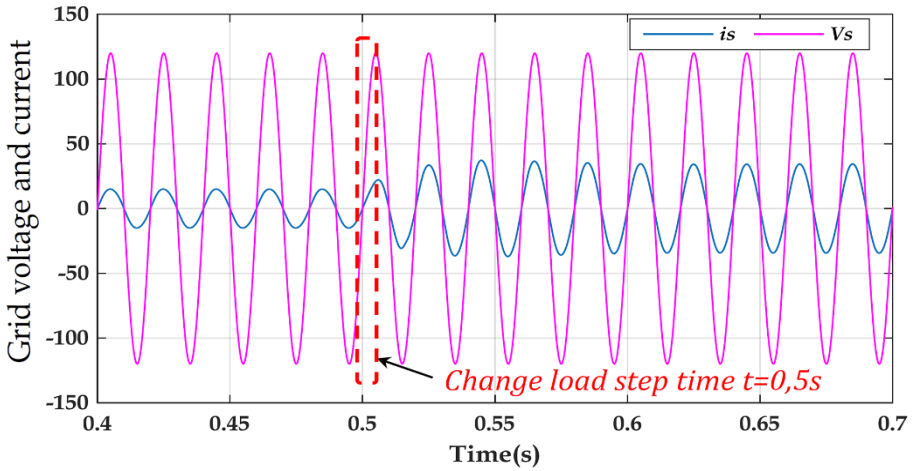

Figure 2.6: Waveforms in dynamic state for grid voltage ($\boldsymbol{v_s}$) and current ($\boldsymbol{i_s}$). Load change at $\boldsymbol{t = 0.5s}$.

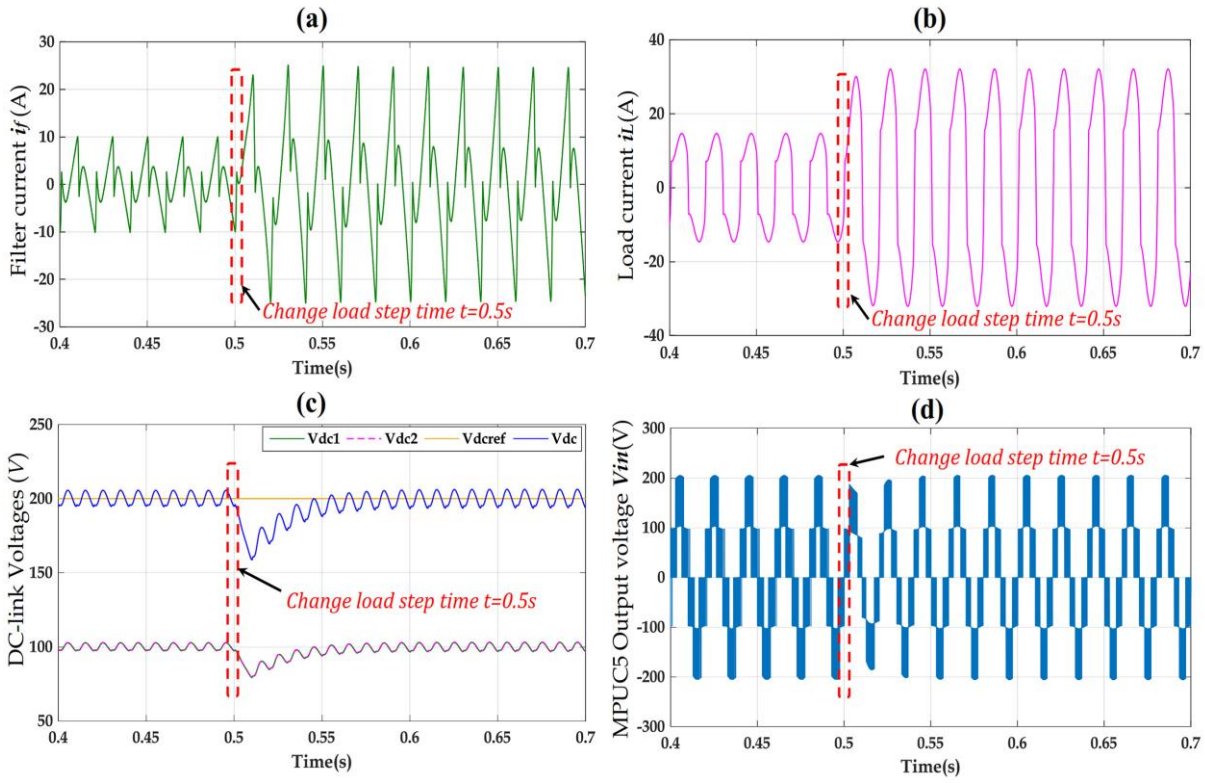

Figure 2.7: Waveforms in dynamic state for filter current, load current, DC-link capacitors voltages and inverter output voltage ($\boldsymbol{V_{in}}$). Load change at $\boldsymbol{t = 0.5s}$.

Table 2.3. Analysis of grid current THD and the average switching frequency $\boldsymbol{f_{sw}}$.

Case	Before filtering	After filtering	Load change
THDi(%)	*27,58%*	*1.89%*	*1.49%*
f_{sw} *(KHz)*	*0*	*4.2561*	*3.3616*

5. EXPERIMENTAL RESULTS

The proposed control technique shown in Figure 2.2 has been tested and implemented in the laboratory LEPCI Sétif using dSPACE DS1104 controller board for HIL system. The DS1104 controller Board is a cost-effective entry-level system with I/O interfaces and a real-time processor on a single board that can be plugged directly into a PC for rapid control prototyping which suitable for controller's development in power converters field. HIL system based on DS1104 controller board consists of an independent control processing unit (CPU) based on DS1104 controller board to build the control algorithms, a real-time simulator interface provides Matlab/ Simulink^{TM} blocks for graphical I/O configuration in order to simulate the plant model and a communication channel between the simulator and the DS1104 controller board. For each sample time, the DS1104 controller board obtains the state variables

from the real-time simulator through the communication channel. From these state variables, the CPU computes the optimal control actions and drives it to the real-time simulator. Thus, the obtained results through these tests are considered more practical.

The practical results are obtained with nonlinear load, represented by a single-phase bridge diode rectifier feeding an inductive and resistive DC load (R_l, L_l), a single-phase AC source with line voltage fixed at 120V RMS and nominal grid frequency 50Hz. The sampling period of the proposed MPC is set to 50µs. The parameters of the tested system are presented in Table 2.2.

Figure 2.8 and 2.9 illustrate the experimental responses of the APF using MPUC5 inverter. It can be noticed that as soon as the filter is switched on, it starts to inject a harmonic current i_f into the grid. Consequently, the grid current i_s takes a pure sinusoidal form with low current distortion (Table 2.4) and the load current i_L is highly distorted as depicted in Figure 2.8.

Figure 2.9 shows the waveforms of the capacitor voltages (V_{dc1}, V_{dc2}) of the capacitors C_1 and C_2, respectively, with an accurate voltage balancing and the DC-link voltage V_{dc}, which is the sum of the two capacitor voltages. In addition, the AC grid voltage v_s is perfectly synchronized in the steady state with the grid current i_s, an indication of a high-power factor, as shown in Figure 2.10.

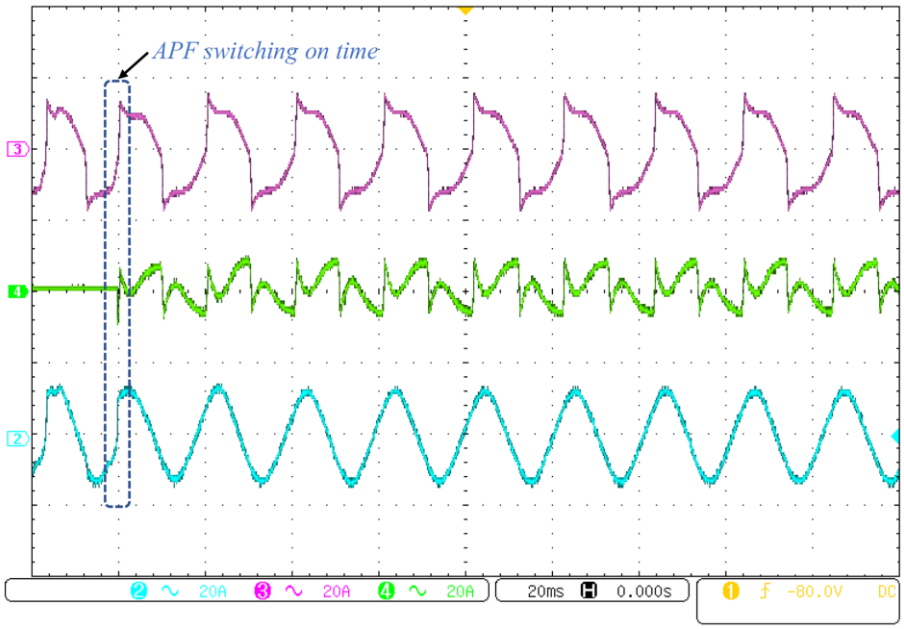

Figure 2.8: Experimental waveforms for load current ($\boldsymbol{i_L}$), filter current ($\boldsymbol{i_f}$) and grid current ($\boldsymbol{i_s}$), with the filter switched on.

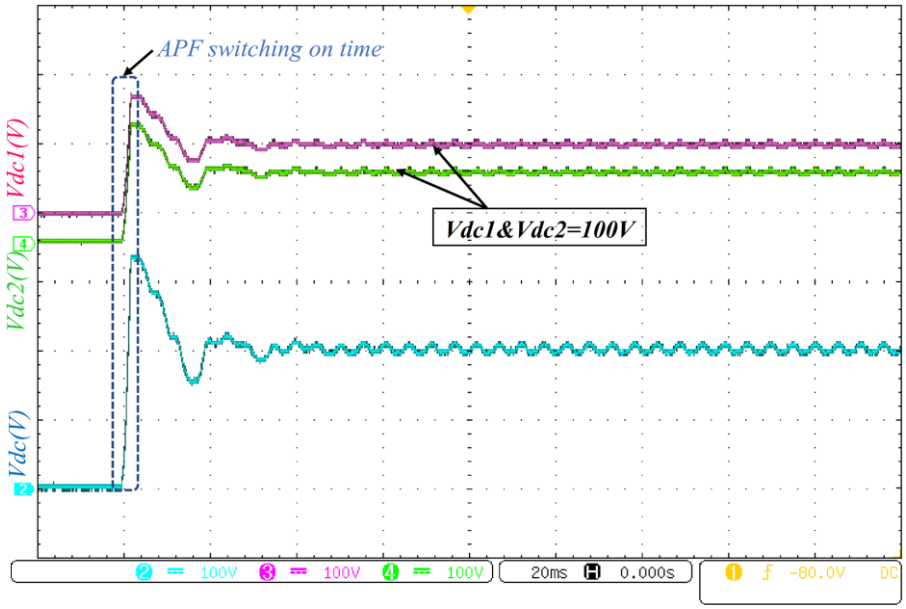

Figure 2.9: Experimental waveforms for DC-link capacitors voltages, the filter is switched on.

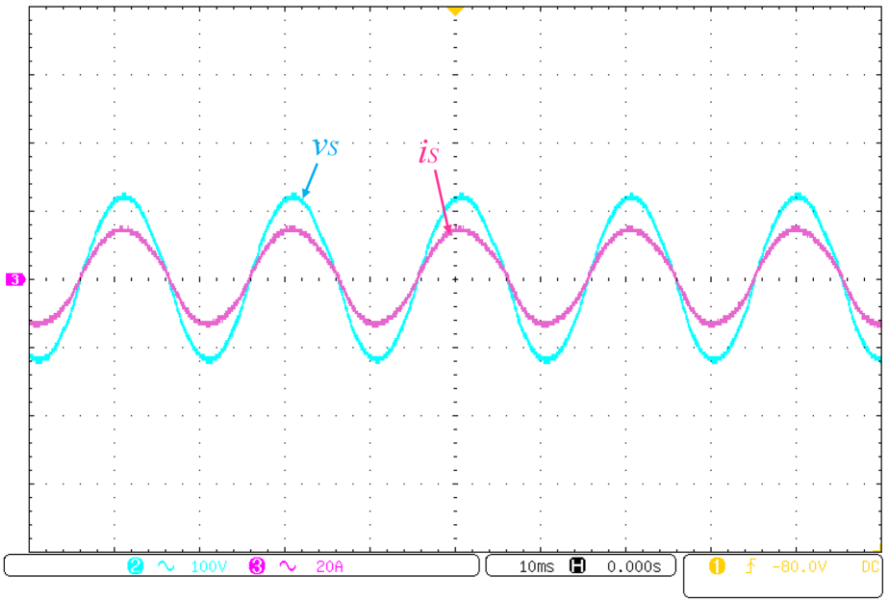

Figure 2.10: Experimental waveforms in steady state for grid voltage ($\boldsymbol{v_s}$) and grid current ($\boldsymbol{i_s}$).

Figure 2.11 depicts the experimental waveforms of the instantaneous active and reactive power of the grid (P_s, Q_s), where the APF provides reactive power to the nonlinear load, and the grid reactive power become null (Q_s=*0*). Consequently, the instantaneous active power continues to deliver the same active power required by the load.

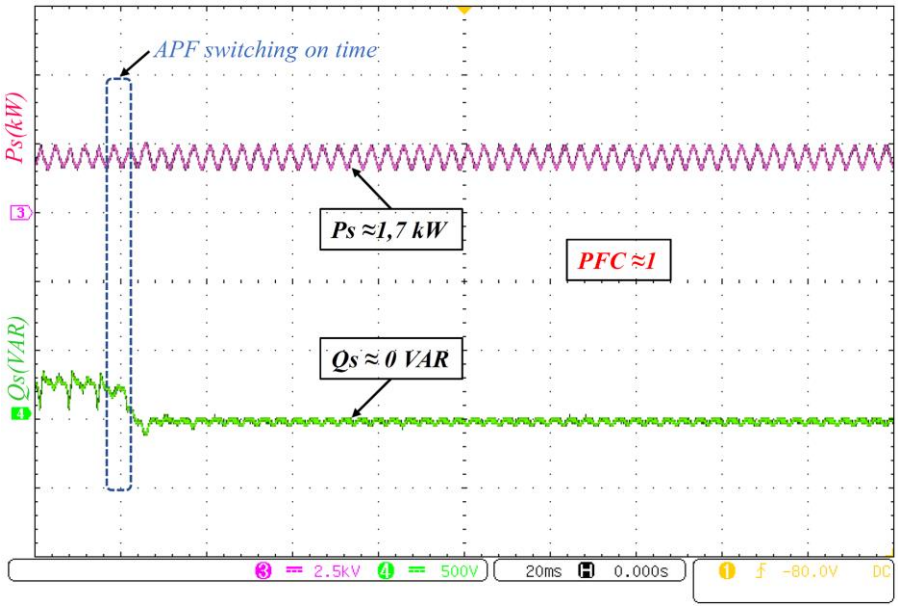

Figure 2.11: Experimental waveforms for instantaneous active and reactive power, the filter is switched on.

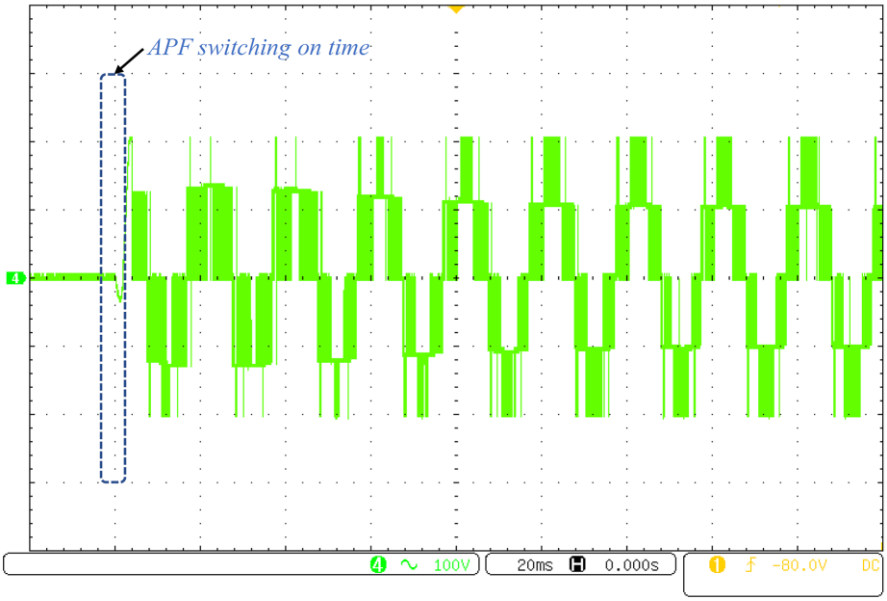

Figure 2.12: Experimental waveform for 5-level output voltage ($\boldsymbol{V_{in}}$), the filter is switched on.

Figure 2.12 illustrates the output voltage of the inverter when the filter is switched on, one can see that the 5-level voltage is perfectly shaped with low harmonic waveform which reduces the quantity of injected harmonic component at the PCC from the inverter and the APF could be connected to the PCC through a small inductor L_f.

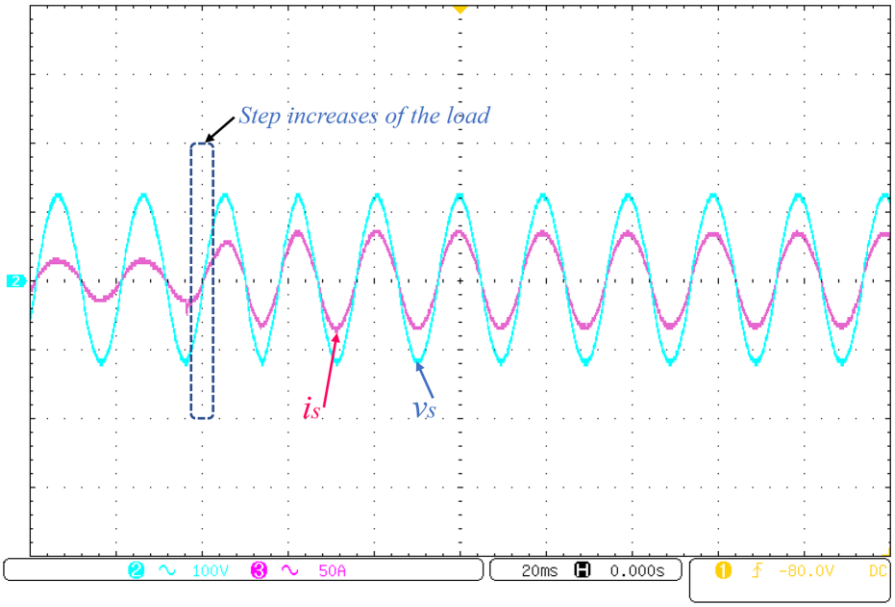

Figure 2.13: Experimental waveform for grid current ($\boldsymbol{i_s}$) and grid voltage ($\boldsymbol{v_s}$), step load change.

Figure 2.13 depicts the dynamic performance of the proposed configuration and implemented MPC by changing the load resistor R_l of the nonlinear load from 6Ω to 3Ω; it shows the grid current i_s and voltage v_s, it is clear that the current is always in phase with the voltage.

From those changes, it can be seen that the MPC controller guarantees a perfect balancing of capacitor voltages, and the DC-link voltages track their reference at the same time, as shown in Figure 2.14.

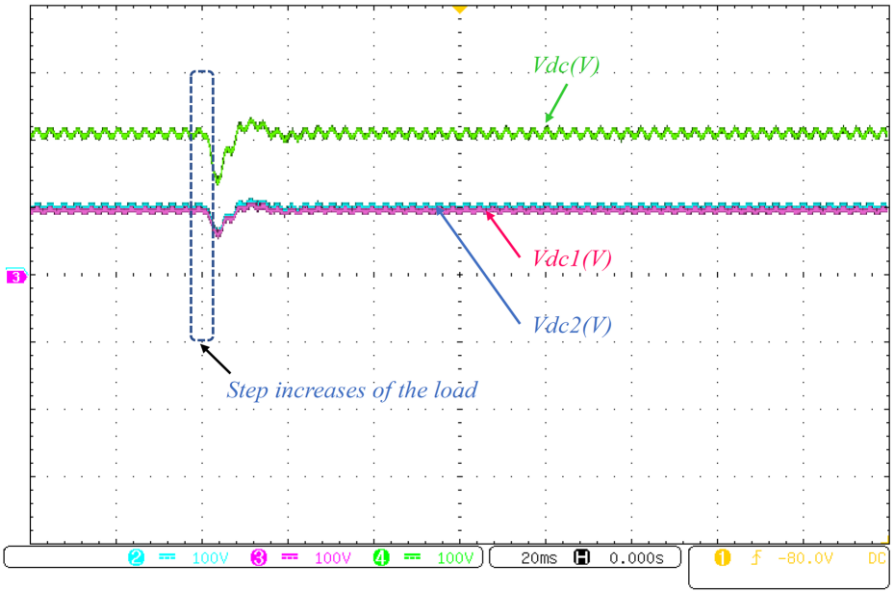

Figure 2.14: Experimental waveforms in dynamic state for DC-link capacitors voltages, step load change.

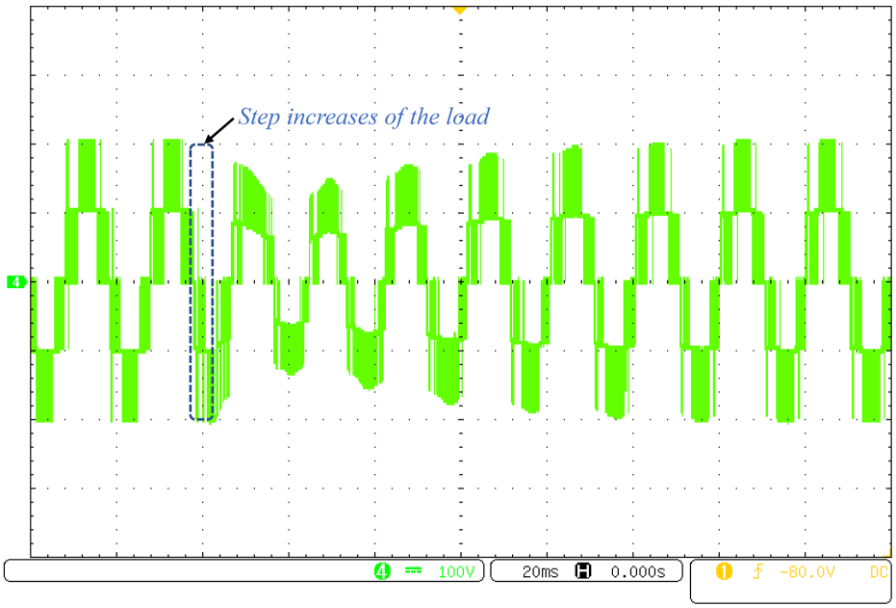

Figure 2.15: Experimental waveform for 5-level output voltage (V_{in}), step load change.

Figure 2.15 shows the dynamic state of the 5-level output voltage V_{in} when a change in the load has occurred, the inverter keeps providing the same voltage level at the output (5-level), which is an indication of the robustness of the proposed control strategy.

Experimental results show that the proposed APF ensures the power factor correction, the harmonic elimination, to less than 5% (Table 2.4), and compensates for the reactive power. This configuration guarantees compliance with IEEE STD 519 and IEC 61000-3-2 standards, and confirms the numerical simulation results obtained earlier. Also, it is worth mentioning that the MPUC5 topology reduces the DC voltage level on the two DC-link capacitors by dividing the DC stepped-up voltage over the two DC-links.

Table 2.4. THD analysis of grid current (*is*)

Case	Before filtering	After filtering	Load change
THDi(%)	*30,68%*	*2.06%*	*1.95%*

6. SUMMARY

In this chapter, a model predictive control (MPC) has been considered for 5-level modified PUC inverter control in single phase APF mode of operation, to reduce harmonic current at the PCC point caused by nonlinear loads. Simulations and experimental results through HIL system based on dSPACE 1104 control board, demonstrate the good functioning of the proposed MPC algorithm. It has a fast response and offers sinusoidal line currents with

low THD. Besides, it has been shown that the DC-link voltage is regulated with a perfect balancing of the two DC-link capacitor voltages and a 5-level voltage waveform of the MPUC inverter was generated at the output. Furthermore, the reactive power is compensated and a high-power factor correction has been obtained. Exhaustive tests have been carried out, including change in load, in order to confirm the good dynamic performance of the proposed controller for MPUC inverter in APF applications.

REFERENCES

[1] Z. Chen, F. Blaabjerg, J.K. Pedersen, A multi-functional power electronic converter in distributed generation power systems, in: Power Electron. Spec. Conf. 2005. PESC'05. IEEE 36th, IEEE, 2005: pp. 1738–1744.

[2] A. Micallef, M. Apap, C. Spiteri-Staines, J.M. Guerrero, Mitigation of harmonics in grid-connected and islanded microgrids via virtual admittances and impedances, IEEE Trans. Smart Grid. 8 (2017) 651–661.

[3] B. Singh, K. Al-Haddad, A. Chandra, A review of active filters for power quality improvement, IEEE Trans. Ind. Electron. 46 (1999) 960–971.

[4] W.M. Grady, M.J. Samotyj, A.H. Noyola, Survey of active power line conditioning methodologies, IEEE Trans. Power Deliv. 5 (1990) 1536–1542.

[5] S.K. Khadem, M. Basu, M.F. Conlon, Harmonic power compensation capacity of shunt active power filter and its relationship with design parameters, IET Power Electron. 7 (2013) 418–430.

[6] M. Angulo, D.A. Ruiz-Caballero, J. Lago, M.L. Heldwein, S.A. Mussa, Active power filter control strategy with implicit closed-loop current control and resonant controller, IEEE Trans. Ind. Electron. 60 (2013) 2721–2730.

[7] J. Tian, Q. Chen, B. Xie, Series hybrid active power filter based on controllable harmonic impedance, IET Power Electron. 5 (2012) 142–148.

[8] A. Sakthivel, P. Vijayakumar, A. Senthilkumar, L. Lakshminarasimman, S. Paramasivam, Experimental investigations on ant colony optimized PI control algorithm for shunt active power filter to improve power quality, Control Eng. Pract. 42 (2015) 153–169.

[9] P. Karuppanan, K.K. Mahapatra, PI and fuzzy logic controllers for shunt active power filter—A report, ISA Trans. 51 (2012) 163–169.

[10] V.F. Corasaniti, M.B. Barbieri, P.L. Arnera, M.I. Valla, Hybrid power filter to enhance power quality in a medium-voltage distribution network, IEEE Trans. Ind. Electron. 56 (2009) 2885–2893.

[11] A.S. Ray, A. Bhattacharya, Improved tracking of shunt active power filter by sliding mode control, Int. J. Electr. Power Energy Syst. 78 (2016) 916–925.

[12] A. Chaoui, J.-P. Gaubert, F. Krim, Power quality improvement using DPC controlled three-phase shunt active filter, Electr. Power Syst. Res. 80 (2010) 657–666.

[13] M.E. Ortúzar, R.E. Carmi, J.W. Dixon, L. Morán, Voltage-source active power filter based on multilevel converter and ultracapacitor DC link, IEEE Trans. Ind. Electron. 53 (2006) 477–485.

[14] M. Sharifzadeh, H. Vahedi, R. Portillo, M. Khenar, A. Sheikholeslami, L.G. Franquelo, K. Al-Haddad, Hybrid SHM-SHE pulse-amplitude modulation for high-power four-leg inverter, IEEE Trans. Ind. Electron. 63 (2016) 7234–7242.

[15] A. Draou, M. Benghanen, A. Tahri, Multilevel converters and VAR compensation, Power Electron. Handb. (2001) 615–622.

[16] H. Zhang, S.J. Finney, A. Massoud, B.W. Williams, An SVM algorithm to balance the capacitor voltages of the three-level NPC active power filter, IEEE Trans. Power Electron. 23 (2008) 2694–2702.

[17] S. Du, J. Liu, J. Lin, Hybrid cascaded H-bridge converter for harmonic current compensation, IEEE Trans. Power Electron. 28 (2013) 2170–2179.

[18] J. Dixon, L. Moran, Multilevel inverter, based on multi-stage connection of three-level converters scaled in power of three, in: IECON 02 [Industrial Electron. Soc. IEEE 2002 28th Annu. Conf. The], IEEE, 2002: pp. 886–891.

[19] F.Z. Peng, A generalized multilevel inverter topology with self voltage balancing, IEEE Trans. Ind. Appl. 37 (2001) 611–618.

[20] M.T. Chebbah, H. Vahedi, K. Al-Haddad, Real-time simulation of 7-level packed U-cell shunt active power filter, in: Ind. Electron. (ISIE), 2015 IEEE 24th Int. Symp., IEEE, 2015: pp. 1386–1391.

[21] H. Vahedi, P.-A. Labbé, K. Al-Haddad, Sensor-less five-level packed U-cell (PUC5) inverter operating in stand-alone and grid-connected modes, IEEE Trans. Ind. Informatics. 12 (2016) 361–370.

[22] H. Vahedi, A.A. Shojaei, L.-A. Dessaint, K. Al-Haddad, Reduced DC-Link Voltage Active Power Filter Using Modified PUC5 Converter, IEEE Trans. Power Electron. 33 (2018) 943–947.

[23] Y. Ounejjar, K. Al-Haddad, L.-A. Gregoire, Packed U cells multilevel converter topology: theoretical study and experimental validation, IEEE Trans. Ind. Electron. 58 (2011) 1294–1306.

[24] A.N. Babadi, O. Salari, M.J. Mojibian, M.T. Bina, Modified Multilevel Inverters With Reduced Structures Based on PackedU-Cell, IEEE J. Emerg. Sel. Top. Power Electron. 6 (2018) 874–887.

[25] S. Kouro, P. Cortés, R. Vargas, U. Ammann, J. Rodríguez, Model predictive control—A simple and powerful method to control power converters, IEEE Trans. Ind. Electron. 56 (2009) 1826–1838.

[26] J. Rodriguez, R.M. Kennel, J.R. Espinoza, M. Trincado, C.A. Silva, C.A. Rojas, High-performance control strategies for electrical drives: An experimental assessment, IEEE Trans. Ind. Electron. 59 (2012) 812–820.

[27] J. Rodriguez, P. Cortes, Predictive control of power converters and electrical drives, John Wiley & Sons, 2012.

[28] J. Rodriguez, M.P. Kazmierkowski, J.R. Espinoza, P. Zanchetta, H. Abu-Rub, H.A. Young, C.A. Rojas, State of the Art of Finite Control Set Model Predictive Control in Power Electronics, IEEE Trans. Ind. Informatics. 9 (2013) 1003–1016. doi:10.1109/TII.2012.2221469.

[29] J.I. Metri, H. Vahedi, H.Y. Kanaan, K. Al-Haddad, Real-time implementation of model-

predictive control on seven-level packed U-cell inverter, IEEE Trans. Ind. Electron. 63 (2016) 4180–4186.

[30] S. Vazquez, J.I. Leon, L.G. Franquelo, J. Rodriguez, H.A. Young, A. Marquez, P. Zanchetta, Model predictive control: A review of its applications in power electronics, IEEE Ind. Electron. Mag. 8 (2014) 16–31.

[31] S. Vazquez, J. Rodriguez, M. Rivera, L.G. Franquelo, M. Norambuena, Model Predictive Control for Power Converters and Drives: Advances and Trends, IEEE Trans. Ind. Electron. 64 (2017) 935–947. doi:10.1109/TIE.2016.2625238.

[32] P. Golchoubian, N.L. Azad, Real-Time Nonlinear Model Predictive Control of a Battery Supercapacitor Hybrid Energy Storage System in Electric Vehicles, IEEE Trans. Veh. Technol. 66 (2017) 9678–9688. doi:10.1109/TVT.2017.2725307.

[33] B. Talbi, F. Krim, T. Rekioua, S. Mekhilef, A. Laib, A. Belaout, A high-performance control scheme for photovoltaic pumping system under sudden irradiance and load changes, Sol. Energy. 159 (2018) 353–368.

Chapter 3

Review of Single-Phase Grid-Connected Photovoltaic Systems

1. INTRODUCTION

The predicted deficiency of fossil fuel-based energy sources and also the silent high consumption demand of energy in the modern society from industry and manufactory have been the major powerful forces to seek alternatives energy resources-based on renewables technologies. There is also an urgent need to solve the global warm and environmental concern, in order to reduce the emission of carbon dioxide (CO_2) [1]. Among various renewable technologies, the wind and solar PV energy are the most commercially implemented and widely adopted in today's energy paradigms across the world [1]. Therefore, many efforts have been made to better integrate various renewable energy sources of intermittency. In this chapiter an overview of photovoltaic energy integration in electrical grid has been introduced with an overview of the commonly used advancement of power electronics converters in single-phase grid-tied PV systems in residential applications. General control schemes in single phase system are also addressed with respect to power quality requirement and to better integration of this kind of renewable energy in future smart grids.

2. PHOTOVOLTAIC ENERGY SYSTEMS: TECHNOLOGY OVERVIEW AND PERSPECTIVES

Renewable energy systems and technologies are considered as some of the most promising solutions for the future, they need to be more developed in order to take over the greatest amount of the energy production. Many technologies have been developed and they have different levels of growth and the scale of their implementation is not also the same. Most

of the renewable technologies are reliant on meteorological conditions, and they are quite challenging especially in their integration into the electrical power system, which is the fundamental issue that needs to be resolved. In other terms, we should answer this question to solve this challenging problem: *how to make a power system able to handle a very high penetration of renewable energy systems (such as photovoltaics), which includes the development of smart grid systems as well?*

For photovoltaic energy, it can be used in different ways. The power generation is based on the PV effect [2], where the voltage or current level is very low for a single solar PV cell. Hence, in practical applications, a considerable number of solar PV cells have been connected in parallel and in series in order to gather PV panels and thus PV arrays.

Grid-tied PV systems illustrated in Figure 3.1, include a power electronics DC/DC converter, which ensures the harvesting of maximum solar energy produced by the PV panels through a maximum power point tracking (MPPT) control, and a DC/AC converter for interconnection to the main grid. Recently, the popularity of PV systems has increased not only for multi megawatts utility-scale power plants but also as rooftop installations on commercial and residential houses with small ratings of hundreds of Watts and in kW range.

The reduction in the price of PV cells contributed to these large-scale deployments. At the same time, technological evolution facilitated the increase in consistency, as results some PV systems now have an expected lifecycle length of 25 years or longer.

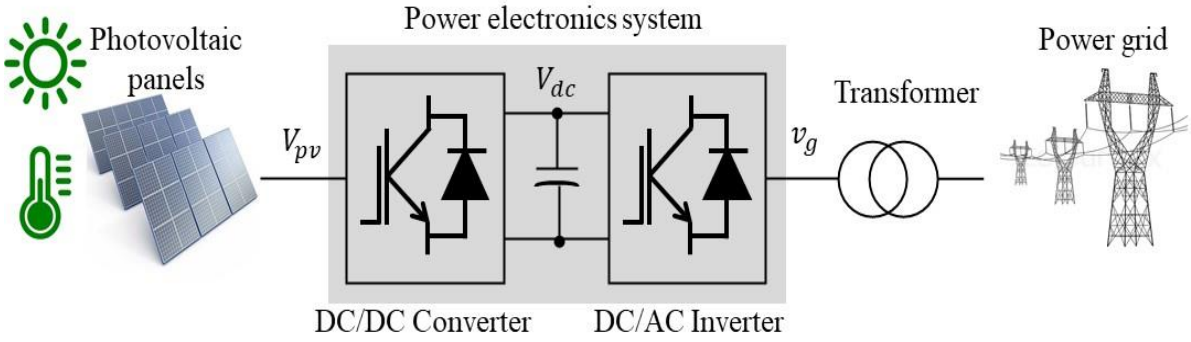

Figure 3.1: PV energy conversion system with DC/DC and DC/AC converters.
V_{pv}: photovoltaic voltage, V_{dc}: DC-link voltage, v_g : grid voltage

The renewable energy systems and devices are expected to become even more cost competitive with fossil fuel–based generators, by a technological enhancement of these installations. Furthermore, considerable efforts for integrating renewable energy systems into the electrical grid are also considered as general prospects, where, a proper balance between production and consumption is taken on consideration. Another challenge for research is to be

able to control the entire system (electrical power system, renewable energy and other energy resources) as a whole, which leads us to make a transition to smart grid functions and facilities.

3. GRID-CONNECTED PV SYSTEMS REQUIREMENTS

A rapid rate of PV power generation growth has been recorded in the past few years, where, it plays a substantial role in electricity production around the world.

Figure 3.2 illustrates the evolution of PV systems capacity in the past 19 years [3], where, a rapid growth of energy production from PV power systems has been noticed.

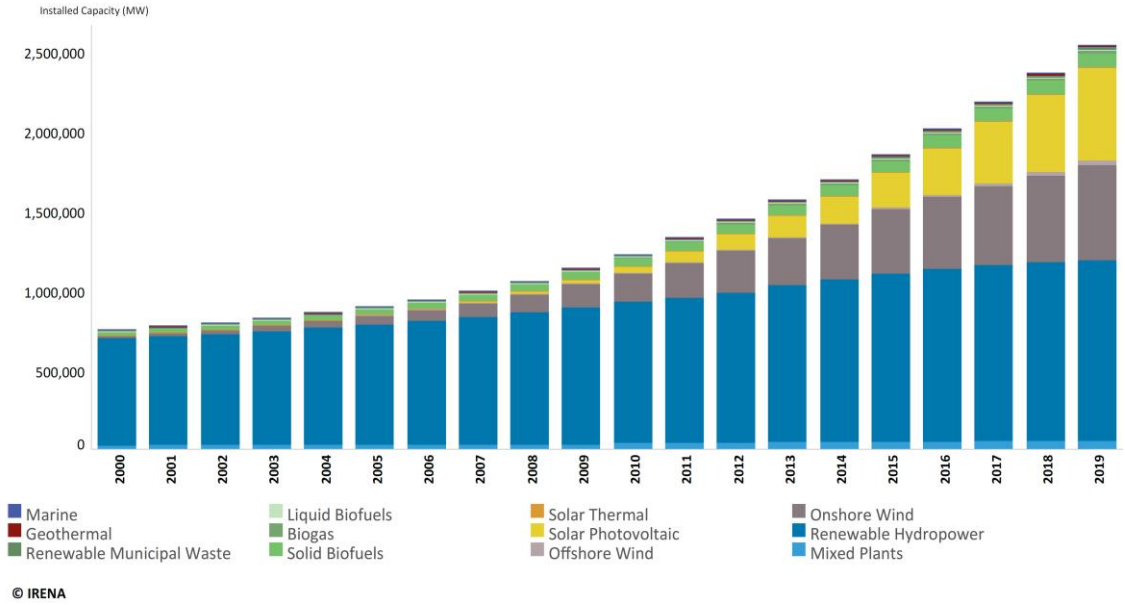

Figure 3.2: Evolution of global renewable energy capacity from 2000 to 2019 [3].

The technological advances in power electronics have been considered as an enabling technology for further development in grid connected PV systems and for more renewables into the grid [4], including the PV systems related by the improvements in power semiconductor devices [5], where, power electronics devices hold all the responsibility for a consistent and efficient energy conversion. As a result of that, numerous power converters for grid-connected PV systems have been developed and commercialized extensively [5– 7], where, their topologies vary in size and power —from small-scale (hundred watts) to large-scale PV power plants (hundreds of megawatts).

Furthermore, PV converters can be classified into four categories, module-level (AC-module inverter and DC-module converter), string, multistring, and central converters [8, 9]. The multistring and central converters are largely used for PV power plants as three-phase systems [10]. In contrast, the module and string converters are commonly used in residential

installations as single-phase systems [11]. Even though, the PV power converters functionalities are the same, including PV power maximization, DC/DC & DC/AC conversions, power transfer, synchronization, reactive power control and protection [12]. Where, advanced and intelligent control strategies are required in order to perform these features and also to encounter customized requirements, even more, monitoring, forecasting, and communication technology can also enhance the PV integration into the grid [12].

The requirements for PV systems can be specified at different stages. At the PV side, where, the PV panels output power should be maximized using maximum power point tracking (MPPT), where a DC/DC power converter is usually used in double-stage PV system as shown in Figure 3.3. In this case, the DC-link voltage should be maintained as a desirable value for the inverter. At the grid side, a desirable total harmonic distortion (THD) of the output current should be achieved (lower than 5%) to meet the specific standards for a good power quality as discussed in chapter 1.

In another side, high efficiency of PV systems is always required in order to maintain the cost as low as possible since the power generated by the PV panels is relatively low compared with the high cost of energy production, where, optimized energy harvesting is recommended. Furthermore, power electronics systems including passive components (capacitors, inductors, resistors) are considered as the most responsible components of power losses in the entire PV system. Therefore, to meet the efficiency requirement, improved semiconductor devices, advanced control, and power-lossless PV topologies are recommended to be used at large scale. Transformer-less grid connected PV technology is an example, where, transformer-less PV inverters can achieve a high conversion efficiency when the isolation transformers are not included in the installations [13].

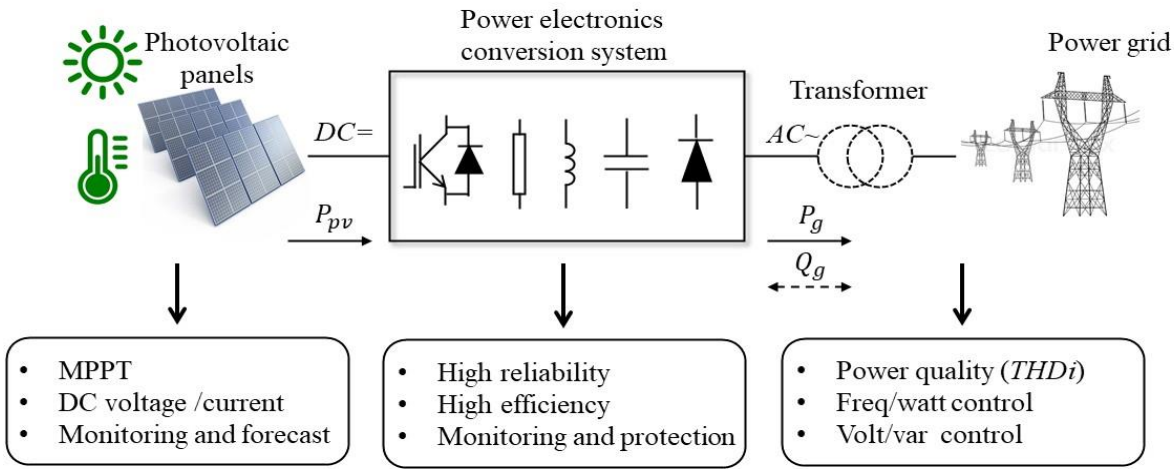

Figure 3.3: Grid-connected PV system requirements.
DC: direct current, *AC*: alternating current, P_{pv} : PV power, P_g: active power, Q_g: reactive power.

Hence, single phase PV systems in the residential installations are the most dominant and will be spread out largely in the future grid. Consequently, advances of single-phase grid-tied PV systems are reviewed in this chapter in order to designate the suitable technology for a desirable PV systems integration into the future power grid. The focus has been on power converter developments in single-phase grid-tied PV systems for low and medium power in residential applications.

4. POWER CONVERTER TECHNOLOGY FOR SINGLE-PHASE PV SYSTEMS

We count four principal organization concepts and configurations [9, 14] for single phase grid tied PV system as shown in Figure 3.4. Each grid-connected concept consists of a PV panel or PV string configured by power electronics converters (DC/DC converters and DC/AC inverters) in accordance with the PV panels output voltage as well as the power rating.

As it can be seen in Figure 3.4, the module concept, string inverter, and cascade topologies are the most used configurations in single-phase PV applications, where the important issue is the galvanic isolation for safety and protection of PV installations. Usually, the isolation can be adopted by including a transformer at the grid side as it is depicted in Figure 3.5 (a). Recently, in order to reduce the cost of these installations, research works have been proposed enhanced single-phase PV systems topologies as shown in Figure 3.5 (b) without isolation transformers.

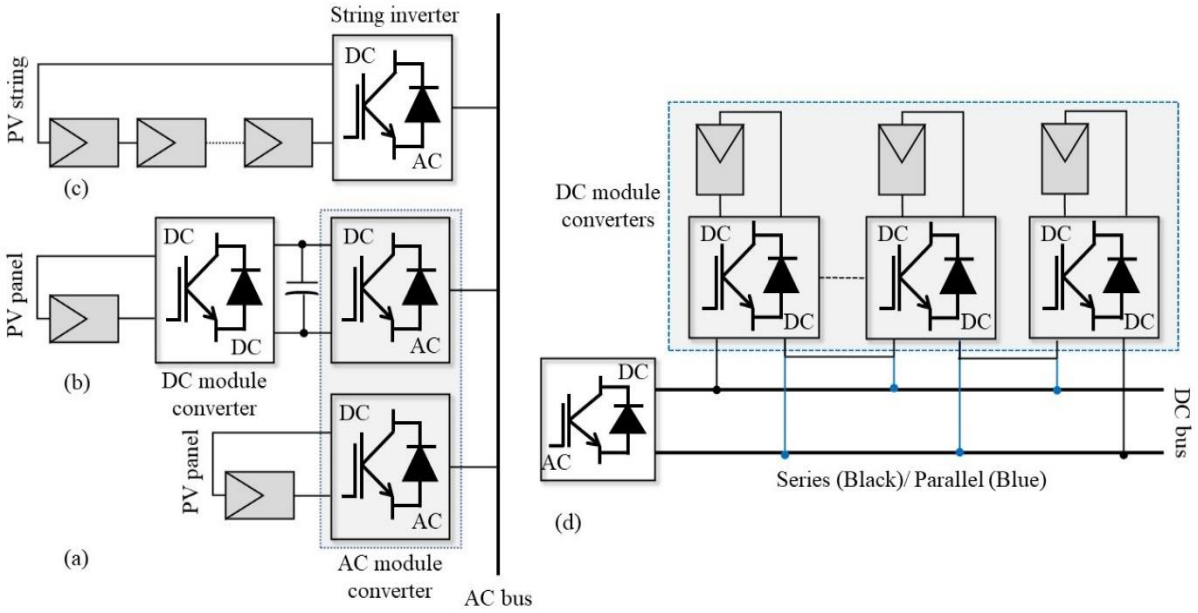

Figure 3.4: Single-phase grid-connected PV system configurations.
(a) AC module inverter, (b) DC & AC module converters, (C) String inverter, (d) Cascade topology.

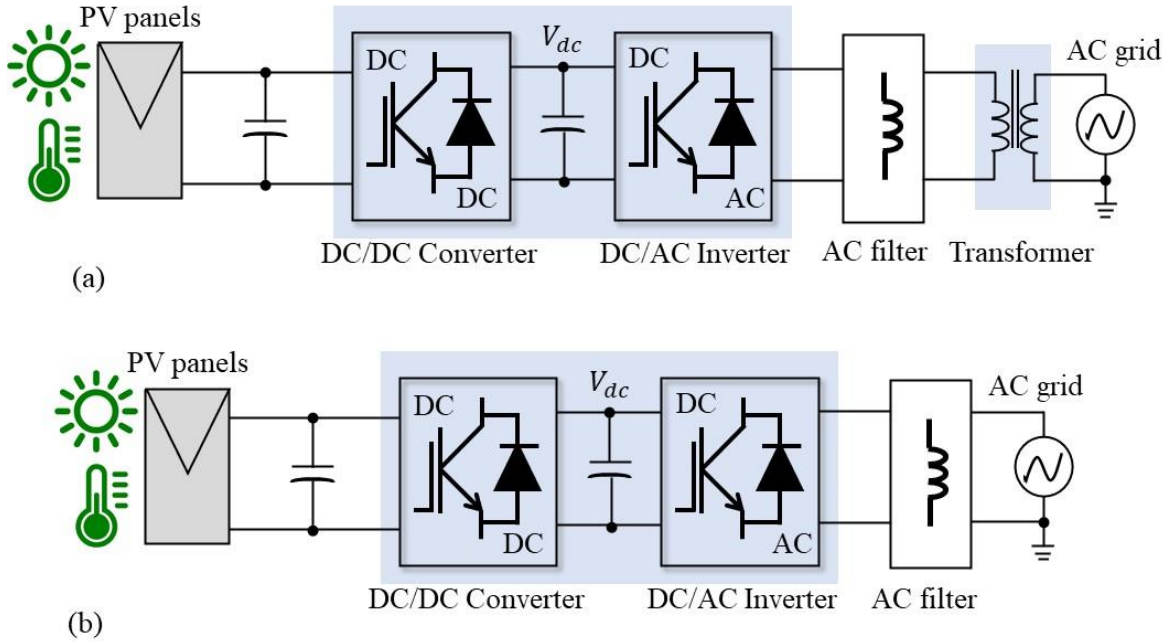

Figure 3.5: Single-phase grid-connected PV systems.
(a) with transformer, (b) without transformer.

4.1 Transformer-less single-stage AC-Module PV inverters

In the last years, considerable efforts have been devoted to decrease the number of power conversion stages in PV systems to increase the efficiency, to increase the power density of single-stage AC-module integrated PV inverters, and to reduce the cost of PV systems. Figure 3.6 shows the general scheme of single-stage grid-connected AC-module integrated PV inverter, where all the expected functionalities shown in Figure 3.3, have to be performed. It worth mentioned that the power decoupling in single-stage configuration is achieved through a DC-link capacitor, C_{dc}, in parallel with the PV panel [8].

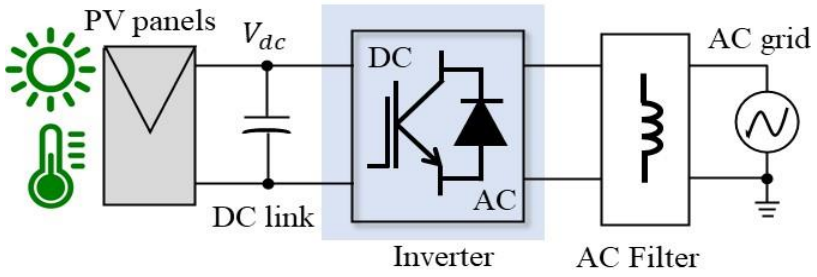

Figure 3.6: Transformer-less AC module inverters topology.

Since the produced power from PV panels is quite low and depends on the ambient conditions (i.e., solar irradiance and ambient temperature), a better solution is to integrate a boost or a buck–boost converter into the a full-bridge (FB) or half-bridge (HB) inverter in order

to achieve an acceptable DC-link voltage for the AC-module inverter [15–18]. Furthermore, the single-stage module-integrated PV converter can operate in a buck, boost, or buck–boost mode with a wide range of PV panel output voltages [15]. Figure 3.7 shows the modified topology of AC-module inverter, where an *LCL* filter is used instead of simple *L* filter in order to achieve a reasonable THD of the injected current into the grid. In [19], another modified topology of the AC-module inverter has been presented, which is a combination of a boost converter and an FB inverter. The major drawback in this topology is the zero-crossing current distortion, introduced by the integrated boost in the AC-module inverter. In order to resolve this drawback, an integrated buck–boost into the AC-module inverters is proposed in [16, 17].

Figure 3.8 shows an example of the buck–boost AC-module inverter topologies for single-phase grid-connected PV applications. In the AC-module inverter, presented in Figure 3.8, the buck–boost-integrated FB inverter generates a DC-biased unipolar sinusoidal voltage, which is 180° out of phase to the other in each half-cycle of the grid voltage to alleviate the zero-cross current distortions.

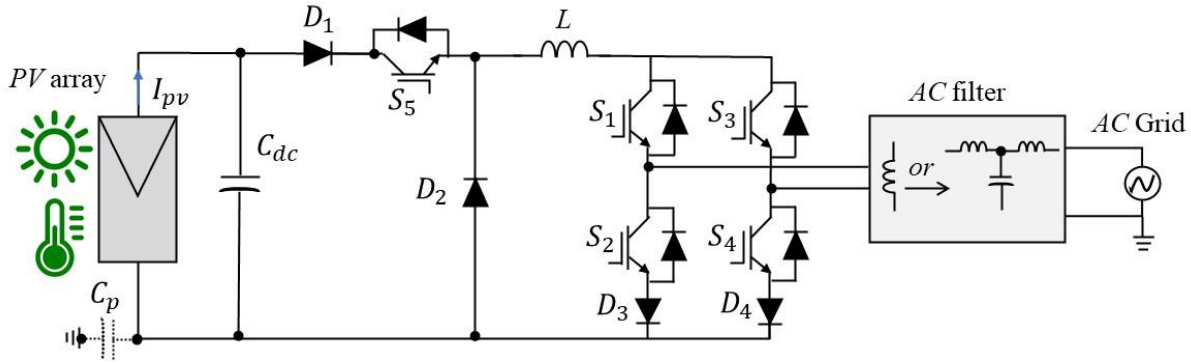

Figure 3.7: Universal single-stage single-phase grid connected PV system.
C_p: virtual parasitic capacitor, C_{dc}: DC-link capacitor.

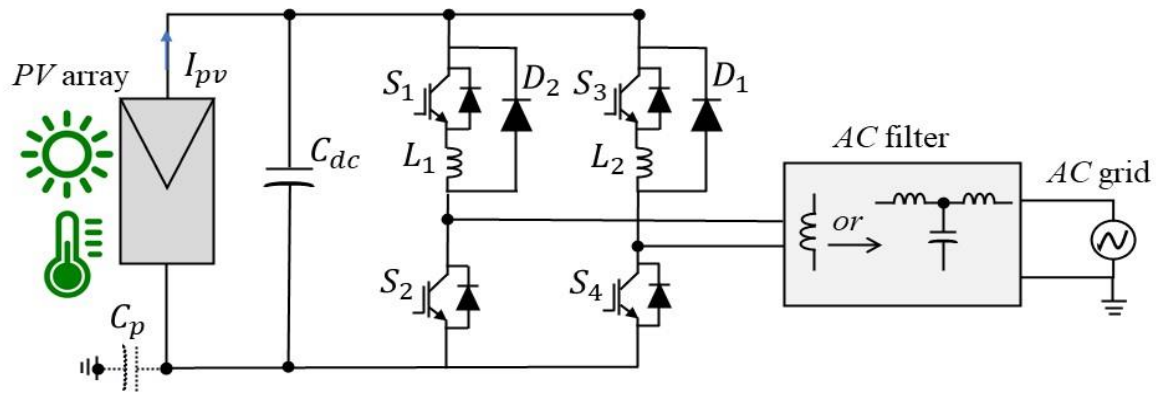

Figure 3.8: Single-stage configuration based on integrated buck-boost AC module inverter.

In addition to the topologies presented previously, where two relatively independent DC/DC converters integrated in an inverter, other topologies for AC-module inverters are also

proposed in the literature. Most of these topologies are developed in accordance with the impedance–admittance conversion theory and an impedance network [20–22]. The Z-source inverter is one example, which is able to boost up the voltage for an FB inverter by adding an *LC* impedance network, as it is demonstrated in Figure 3.9.

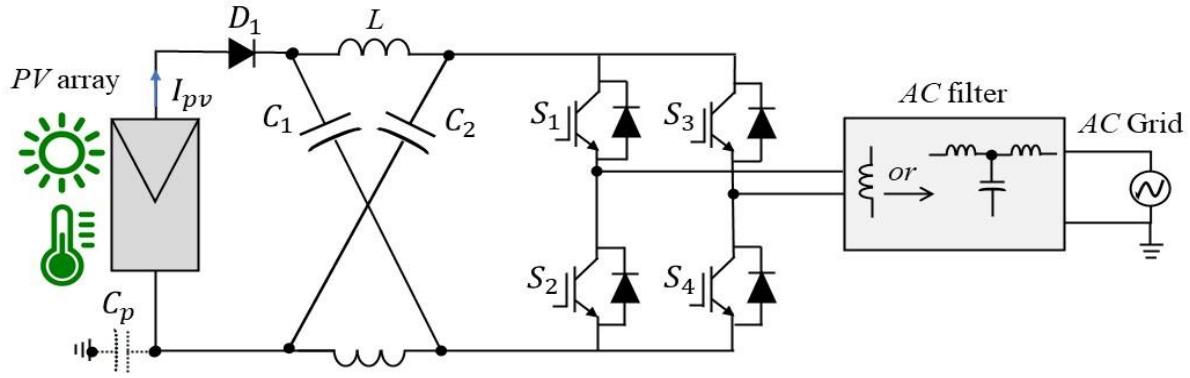

Figure 3.9: Single-stage configuration-based Z-source inverter.

4.2 Transformer-less single-stage string inverters

The AC-module inverters topologies presented before with an integration of a DC/DC boosting converter are appropriate only for use in low power applications (e.g., <1kW). When it comes to higher power ratings (e.g., 1–5 kW), the performance of AC-module inverters is not satisfactory. In such applications, single-phase FB string inverter is the most commonly used inverter topology due to its simplicity, where less power switching devices are used. Figure 3.10 shows the general schematics of a single-phase FB string inverter with an *LCL* or *L* filter for better power quality. Figure 3.10 shows also the leakage current circulating in the transformer-less topology, where a specifically designed modulation technique is always required in such topology in order to minimize the leakage current, such as the bipolar modulation, unipolar modulation, and hybrid modulation [23]. Considering the leakage current injection, the bipolar modulation scheme is preferable [24]. Furthermore, optimizing the modulation patterns is another alternative to eliminate the leakage currents [25].

Transformer-less topologies are mostly derived from the FB topology by adding supplementary power switching devices in order to create an AC path or a DC path [26- 28]. By doing so, an isolation is achieved between the PV modules and the grid during the zero-voltage states, consequently leading to a low leakage current injection such as the topologies proposed in [27]. Figure 3.11 shows an example of transformer-less string inverter based H6 topology, where two additional switching devices are added to the initial FB inverter topology to reduce the leakage current by creating a DC path.

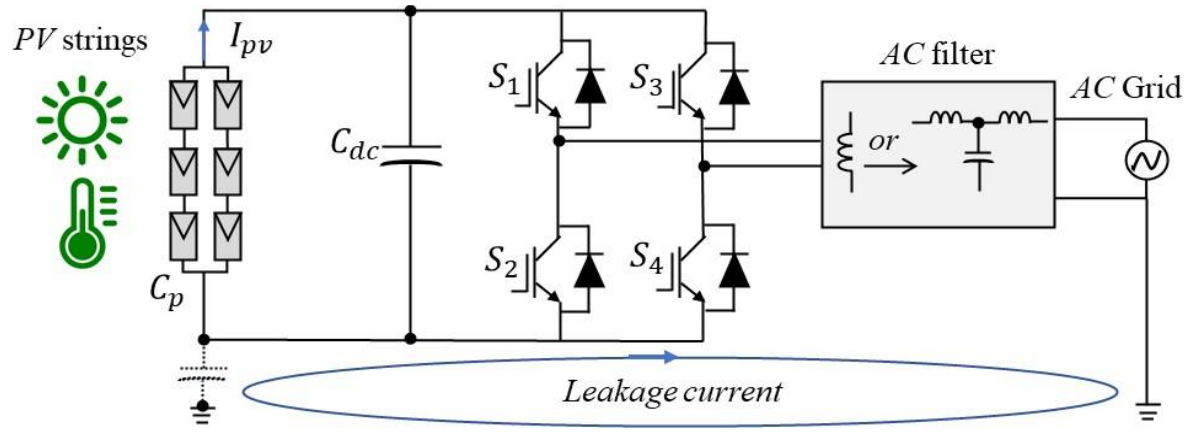

Figure 3.10: Single-stage transformer-less PV system-based FB string inverter.

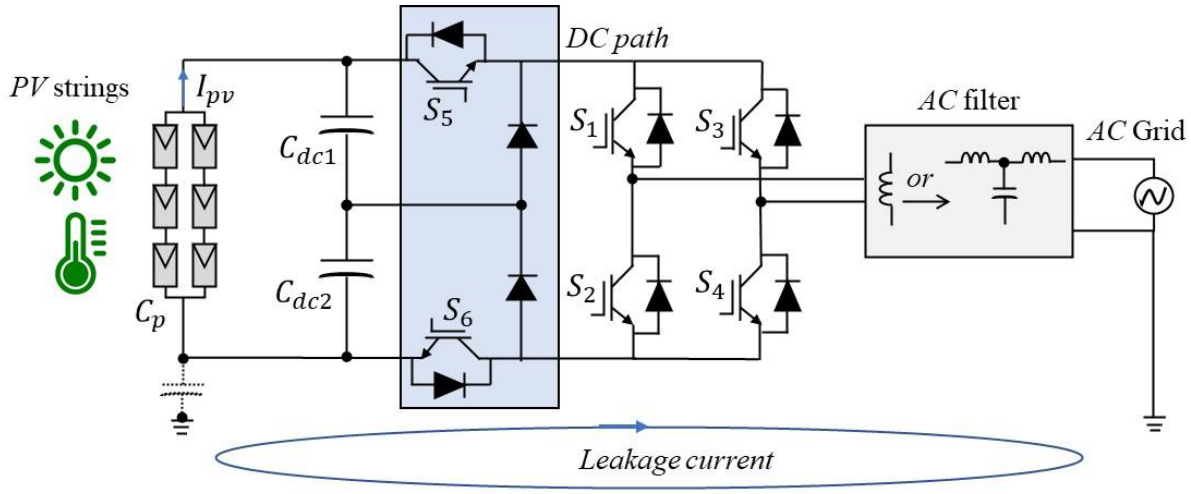

Figure 3.11: Single-stage Transformer-less string H6 inverter topology with a DC path derived from the FB inverter to eliminate leakage current.

Otherwise, the isolation can be achieved also at the grid side by adding an AC path. As it is demonstrated in Figure 3.12, the highly efficient and reliable inverter concept string inverter proposed in [28] has the same number of power switching devices as that of the H6 inverter, but it provides an AC path to eliminate the leakage current injection.

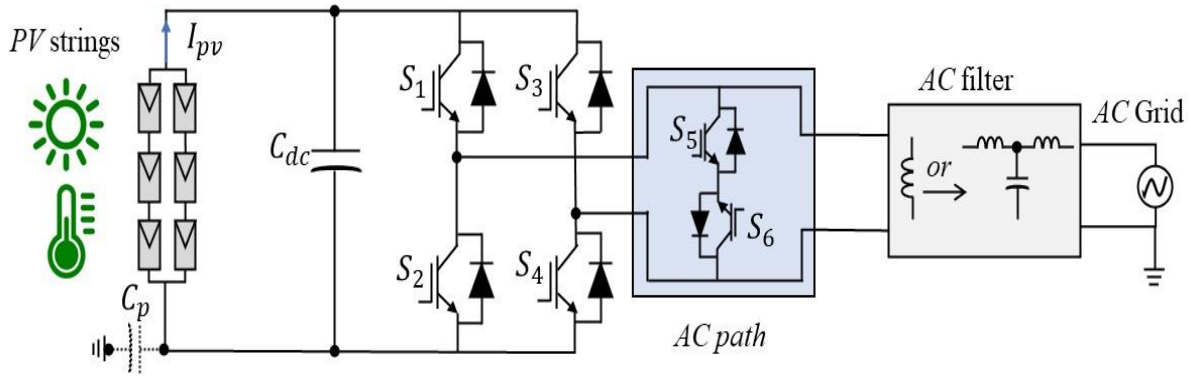

Figure 3.12: Single-stage transformer-less PV system-based enhanced FB inverter with AC path to eliminate leakage current.

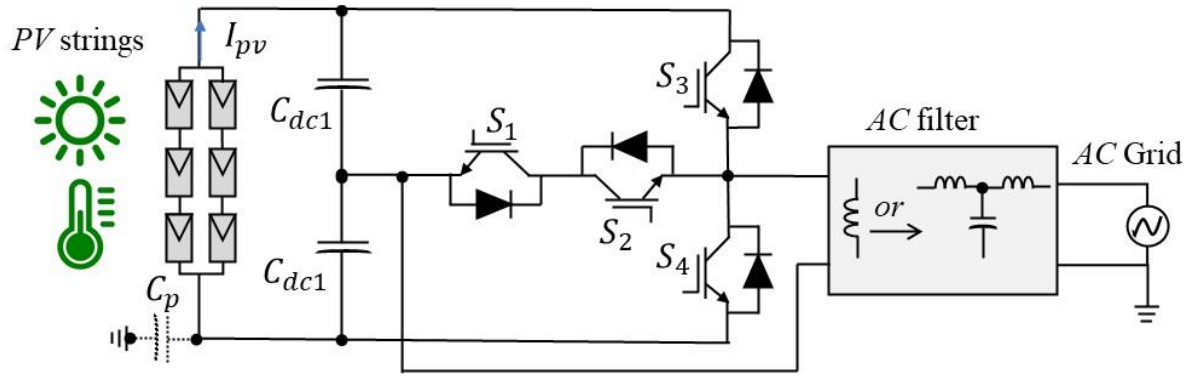

Figure 3.13: Single-stage transformer-less PV system-based multi-level NPC inverter.

Furthermore, single-phase transformer-less string inverter can be also developed based on the multilevel power converter topologies [23- 29] as shown in Figure 3.13.

4.3 DC-Module converters in transformer-less double-stage PV systems

A major drawback of the single-stage PV topologies is that the output voltage range of the PV panels/strings is limited especially in the low power applications (e.g., AC-module inverters), which consequently will affect the overall efficiency. The double-stage PV technology can solve this issue since it consists of a DC/DC converter that is responsible for increasing the voltage of the PV module to a desirable level for the inverter stage [30, 31]. Figure 3.14 shows the general block diagram of a double-stage single-phase PV topology, where the DC/DC converter performs the MPPT control of the PV panels. The DC-link capacitor C_{dc} shown in Figure 3.14 is used for power decoupling, while the PV capacitor C_{pv} is used for filtering.

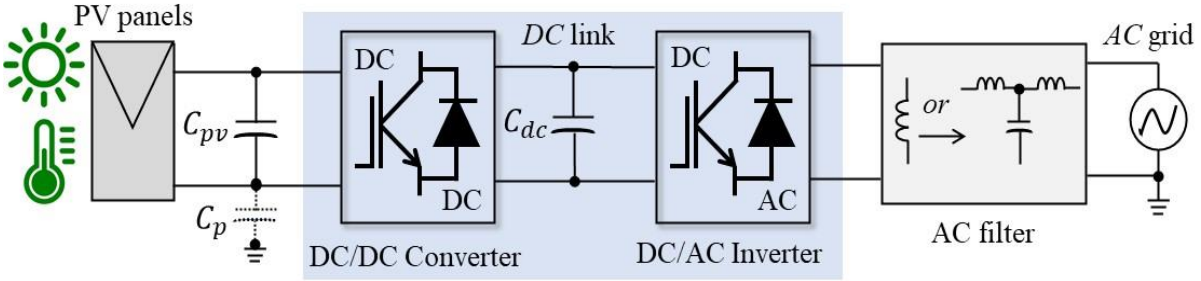

Figure 3.14: General scheme double-stage single-phase grid connected PV system
C_p: virtual parasitic capacitor, C_{dc}: DC-link capacitor.

In general, the DC/DC converter can be included between the PV panels and the DC/AC inverters. The inverters can be the string inverters as discussed earlier or a simple full-bridge inverter. Figure 3.15 shows a conventional double-stage single-phase PV system, consisting of a DC/DC converter and an FB string inverter. Where the leakage current needs to be minimized as well.

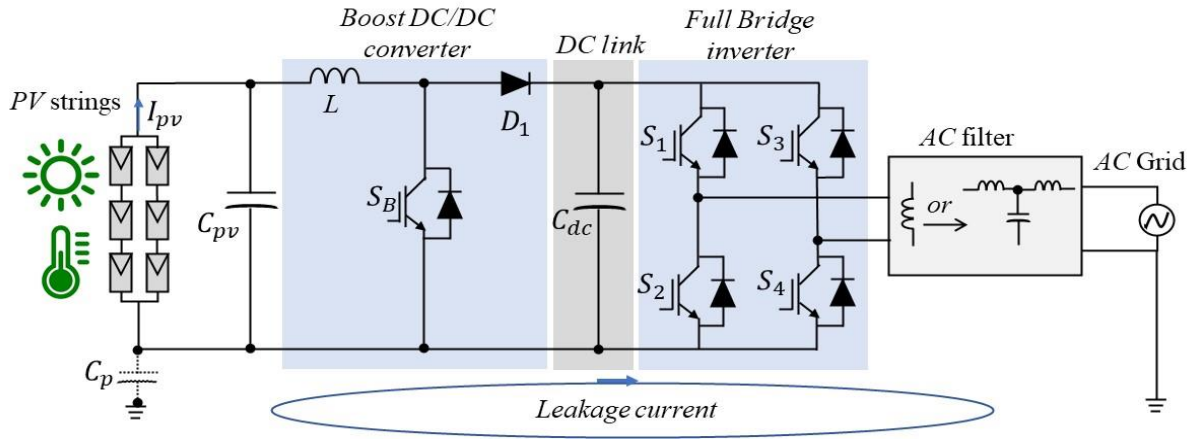

Figure 3.15: Conventional double-stage single-phase grid connected PV system using a boost converter and FB inverter.

5. Control of single-phase grid-connected PV systems

The control objectives of a single-phase grid-connected PV system [32] can be divided into two main parts: (1) PV-side control with the purpose to maximize the power from PV panels and (2) grid-side control performed on the PV inverters with the purpose of fulfilling the requirements to the power grid as shown in Figure 3.3. A conventional control structure for such a grid-connected PV system consists of a two-cascaded loop in order to fulfill the requirements [32]. An outer power/voltage control loop generates the current references and the inner control loop is responsible for shaping the current, so the power quality is preserved, and also it may perform various functionalities, as shown in Figure 3.16.

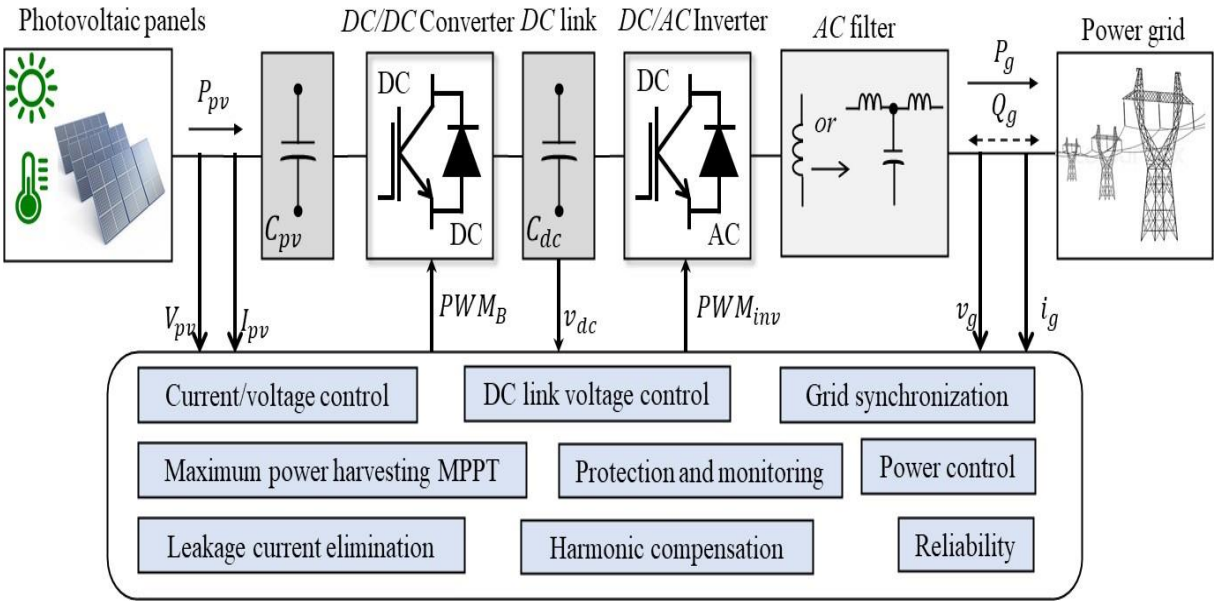

Figure 3.16: Single-phase grid connected PV system general control objectives.
PWM: pulse width modulation.

5.1 Grid synchronization

In grid connected PV systems the injected grid current should be synchronized with the grid voltage as required by the standards in this field [33]. As a result, grid synchronization is an essential grid monitoring task that will strongly contribute to the dynamic performance and the stability of the entire control system. The grid synchronization is even challenged in single-phase systems, as there is only one variable (i.e., the grid voltage) that can be used for synchronization. Nevertheless, different methods to extract the grid voltage information have been developed in [13, 33] like the zero-crossing method, the filtering of grid voltage method, and the phase-locked loop (PLL) techniques, which are important solutions.

Figure 3.17 shows the structure of the PLL-based synchronization system. It can be observed that the PLL system contains a phase detector (PD) to detect the phase difference, a PI-based loop filter (PI-LF) to smooth the frequency output, and finally a voltage-controlled oscillator (VCO).

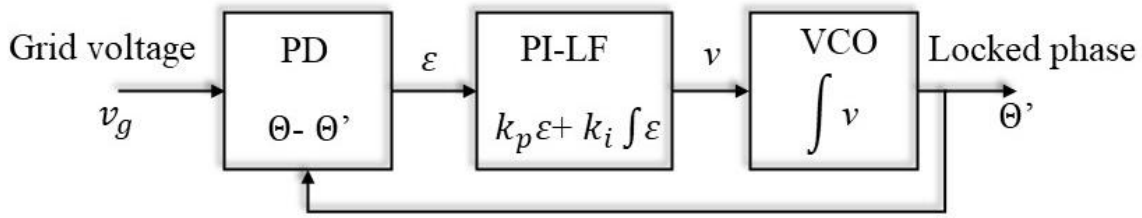

Figure 3.17: General structure of a PLL system.
θ: *grid voltage phase*, θ' *output lokked phase*.

Accordingly, the transfer function of the PLL system [13] can be obtained as

$$G_{pu}(s) = \frac{\theta'(s)}{\theta(s)} = \frac{k_p s + k_i}{s^2 + k_p s + k_i} \quad (1)$$

which is a second-order system with *kp* and *ki* being the proportional and integral gain of the PI-LF, respectively. Subsequently, the corresponding damping ratio ζ and undamped natural frequency ω*n* can be expressed, respectively, as

$$\zeta = \frac{k_p}{2\sqrt{k_i}} \; and \; \omega_n = \sqrt{k_i} \quad (2)$$

which can be used to tune the PI-LF parameters according to the desired settling time and resultant overshoot. More details about single-phase PLL synchronization techniques are presented in [13].

5.2 DC-link controller

The first conversion stage extracts the PV power from the PV arrays and transforms it to DC-link. The main objective at this point is to regulate the DC-link voltage at reference value and estimate the amplitude of grid currents as presented in Figure 3.18. To ensure a proper power injection control, the value of DC-link voltage reference must be chosen higher than the grid peak voltage.

Several research works have been employing the artificial intelligence (AI) such as fuzzy logic control (FLC) [34] and, neuro-fuzzy networks (NFIS) [35], in order to overcome the drawbacks provided by conventional PI regulator such as long-time response, large overshoot and significant voltage ripples during steady-state operation. Nevertheless, the implementation of these controllers requires a high computational burden and large capacity of the memory.

Despite these facts, simple PI regulator is the mostly used controller in the industrial Applications [36]. Hence, enhanced PI controllers have been developed to prevent performance degradation and also to maintain the simplest possible controller scheme of the PI controller especially in complex systems. Moreover, the hardware implementation of this type of controller is very easy which makes it the best choice in all industrial applications.

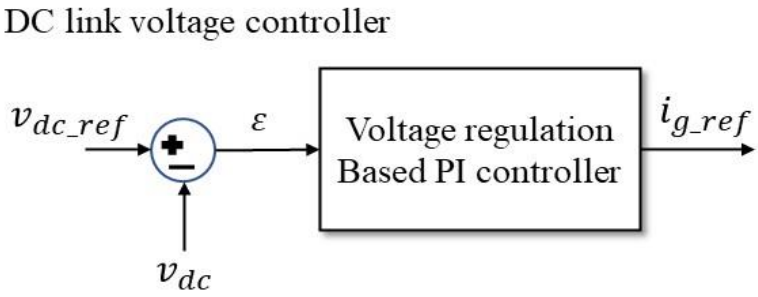

Figure 3.18: DC-link voltage controller-based PI regulator.

5.3 Maximum power point tracking

MPPT is one of the essential functions in PV systems. Considering the nonlinear current–voltage characteristics of PV cells, the maximum power delivered by the PV array is at a well-defined operating point named maximum power point (MPP). MPPT is one of the key functions that every grid connected PV inverter should have. There is a large number of publications dealing with MPPT, where the majority of the PV converters are able to extract around 99% of the available power from the PV installation, over a varied irradiance and temperature range— in steady and dynamic states.

An extensive overview of modern MPPT techniques has been presented in [37]. The most frequently applied MPPT algorithms are hill-climbing methods, such as the perturb and observe (P&O), and its alternate implementation (with identical behavior), the incremental conductance [38]. These methods are based on the fact that on the voltage–power characteristic (Figure 3.19), the variation of the power with respect to the voltage is positive ($dP/dV > 0$) in the left-hand side of the MPP, while it is negative ($dP/dV < 0$) on the right-hand side of MPP, as shown in Figure 3.19. The main advantages of these methods are that they are generic, that is, they are suitable for any PV array, they do not require any information about the PV array, they work reasonably well in most conditions, and they are simple to implement in a digital controller with minimum computational demand.

a) Perturbation and Observation MPPT

The perturbation and observation (P&O) MPPT method is based on the property that the derivative of the power–voltage characteristic of the PV module/array is positive on the left side and negative on the right side (see Figure 3.20), while at the MPP, it holds that

$$\frac{\Delta P_{pv}}{\Delta V_{pv}} = 0 \qquad (3)$$

where *Ppv* and *Vpv* are the output power and voltage, respectively, of the PV module/array.

During the execution of the P&O MPPT process, the output voltage and current of the PV module/ array are periodically sampled at consecutive sampling steps in order to calculate the corresponding output power and the power derivative with voltage. The MPPT process is performed by adjusting the reference signal of the DC/DC power converter PWM controller. Figure 3.21, presents the flowchart of the P&O MPPT [39].

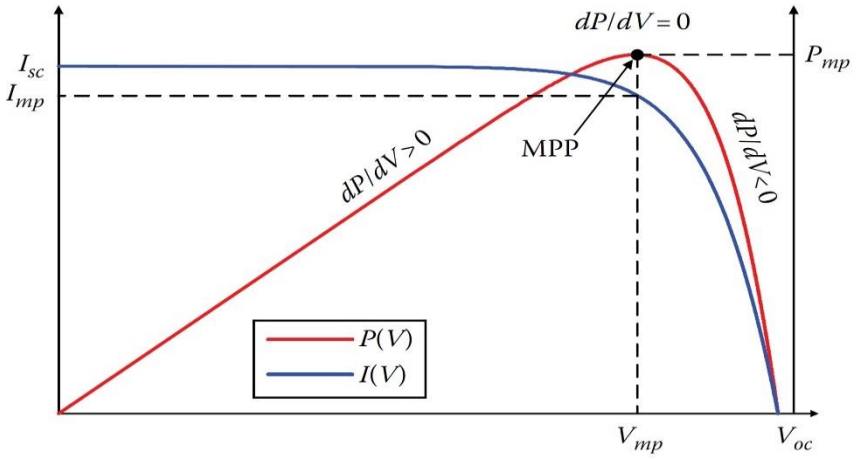

Figure 3.19: PV panel power/voltage & current/voltage curves showing the MPP.
I_{sc}: *short circuit current*, V_{oc}: *open circuit voltage*, I_{mp}: *current at MPP*, V_{mp}: *voltage at MPP*, P_{mp}: *peak power*.

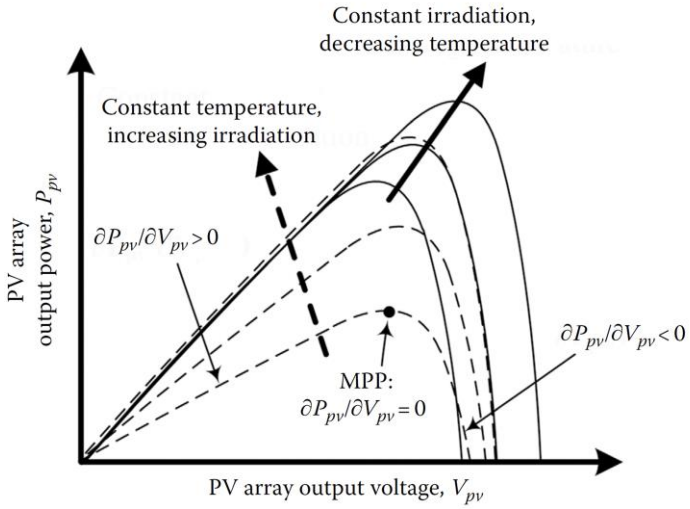

Figure 3.20: Power–voltage characteristics of a PV array.

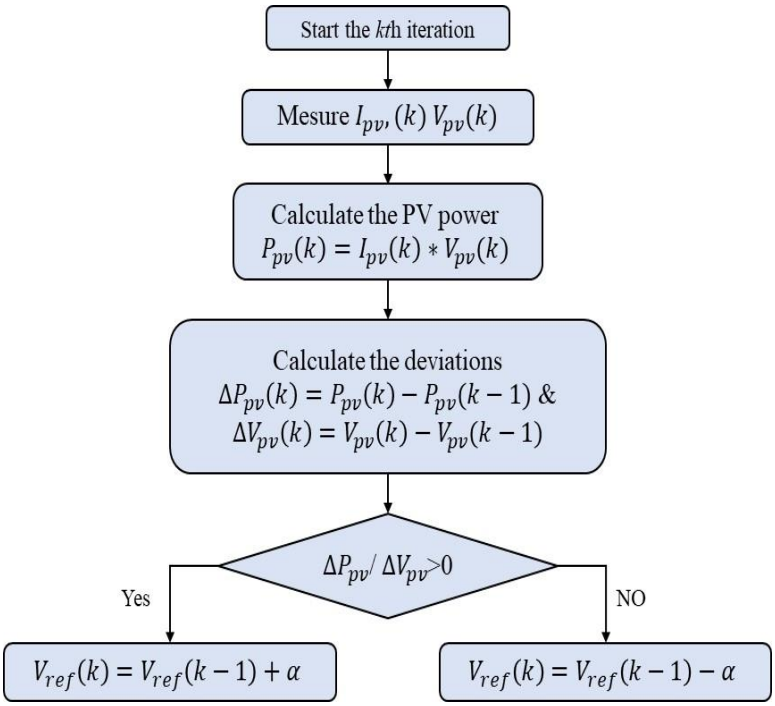

Figure 3.21: Flowchart of P&O MPPT algorithm.

The P&O method is characterized by its operationality and implementation simplicity. However, it exhibits a slow convergence speed under varying solar irradiation conditions and its performance may also be affected by system noise.

b) Incremental-Conductance MPPT

At the MPP of the PV source, it holds that

$$\frac{\Delta P_{pv}}{\Delta V_{pv}} = 0 \Rightarrow \frac{\Delta(I_{pv*}V_{pv})}{\Delta V_{pv}} = I_{pv} + \frac{\Delta I_{pv}}{\Delta V_{pv}} V_{pv} = 0 \Rightarrow \frac{\Delta I_{pv}}{\Delta V_{pv}} = -\frac{I_{pv}}{V_{pv}} \qquad (4)$$

The incremental-conductance (InC) MPPT technique operates by measuring the PV module/

array output voltage and current and comparing the value of $\frac{\Delta I_{pv}}{\Delta V_{pv}}$ with $-\frac{I_{pv}}{V_{pv}}$.

Then, the power converter is controlled based on the result of this comparison, according to the flowchart illustrated in Figure 3.22, which is based on the procedure presented in [40]. Similar to the P&O process, the execution of the algorithm shown in Figure 3.22 is iteratively repeated until the difference between $\frac{\Delta I_{pv}}{\Delta V_{pv}}$ and $-\frac{I_{pv}}{V_{pv}}$ is less than a predefined value, which indicates that the MPP has been tracked with an acceptable accuracy.

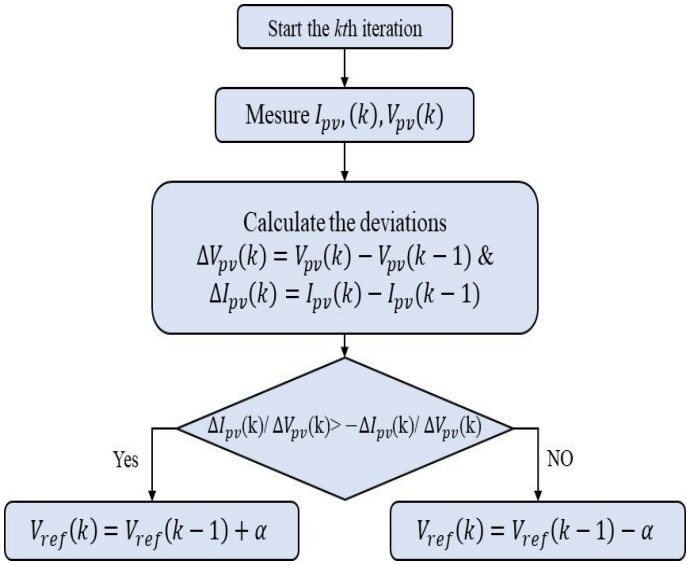

Figure 3.22: Flowchart of Inc MPPT algorithm.

However, the hill-climbing methods (PO & INC) have some inherent shortcomings as they have limited tracking capability during varying conditions and in the case of partial shadow, they may not find the global MPP, settling at a local maximum on the power–voltage curve. The MPPT methods that are mostly preferred by the industry are the hybrid or enhanced hill climbing ones, which have a P&O or INC algorithm as their core, with an improvement in combination, to overcome its limitations in variably and/or partially shaded conditions.

c) CURRENT-ORIENTED MPPT

The basic concept of current- oriented MPPT is presented in Figure 3.23. This MPPT involves MPPT current-based algorithm (C-MPPT) in cascade with current controller. The C-MPPT aims to generate the reference current that represents the MPP current, while the current controller aims to enforce the output PV current to track the reference current delivered by the C-MPPT [41, 42]. Generally, the P&O and INC algorithms presented in Figure 3.24 and 3.25 are the most employed algorithms as a core of this MPPT. The PI controller [41], is the most useful techniques as current controller in this method.

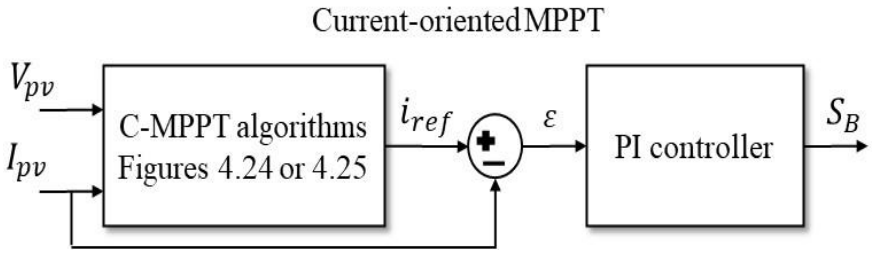

Figure 3.23: General structure of current-oriented MPPT.

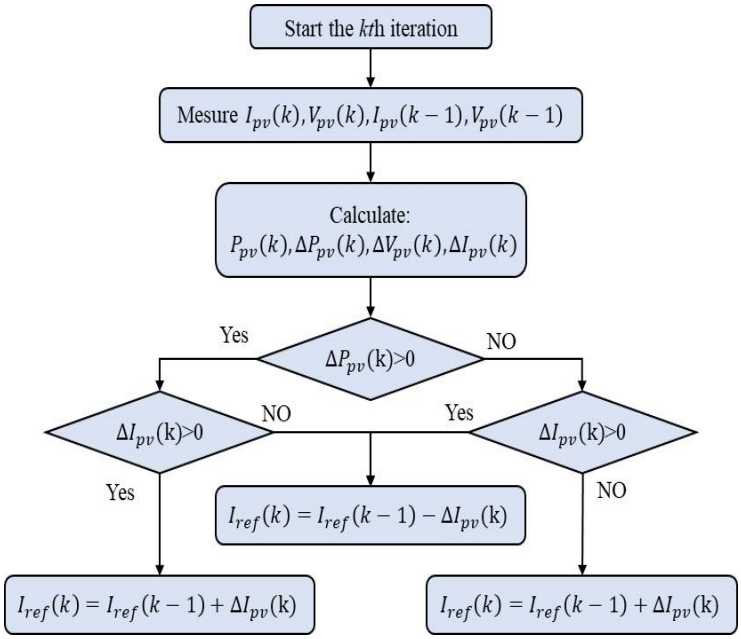

Figure 3.24: Current P&O algorithm flowchart.

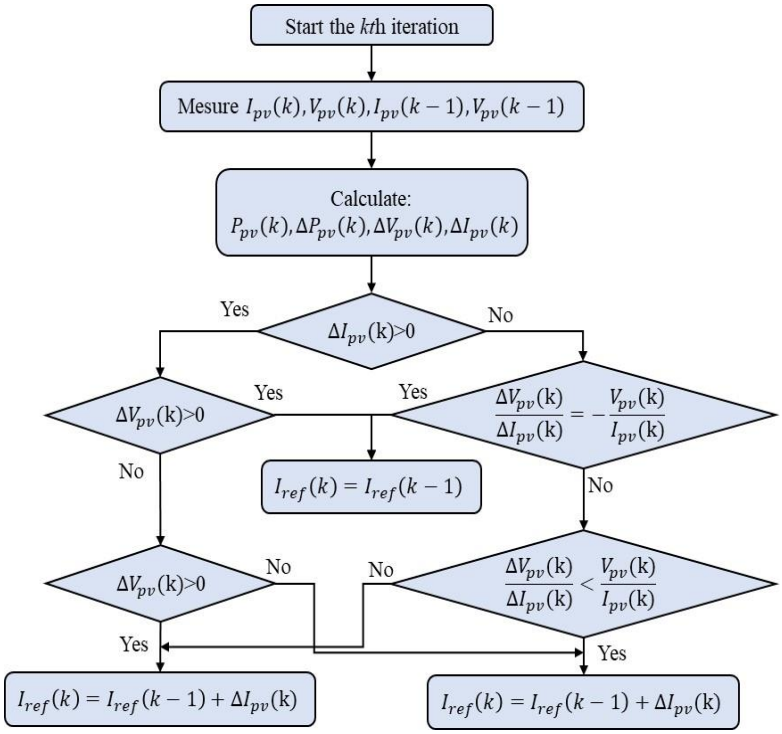

Figure 3.25: Current-Inc algorithm flowchart.

d) VOLTAGE- ORIENTED MPPT

The Voltage-oriented MPPT method consists of MPPT voltage-based algorithm (V-MPPT) in cascade with voltage controller as illustrated in Figure 3.26. the objective of V-MPPT is to deliver the reference voltage that represent the MPP voltage. While, the voltage controller aims to enforce the output PV voltage to track the reference voltage generated by the V-MPPT [42]. The P&O and INC algorithms presented in Figure 3.27 and 3.28 are widely employed as V-MPPT. Besides, the voltage regulator is performed usually by a simple PI controller.

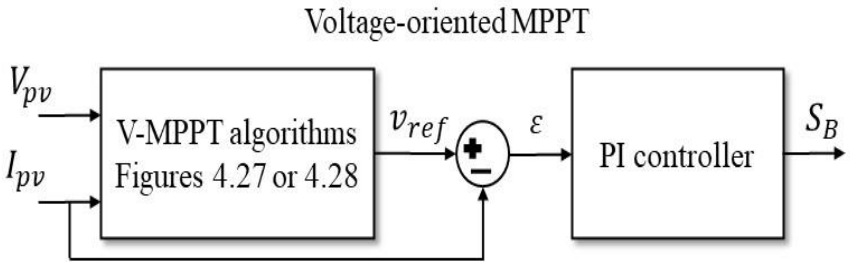

Figure 3.26: General structure of voltage-oriented MPPT.

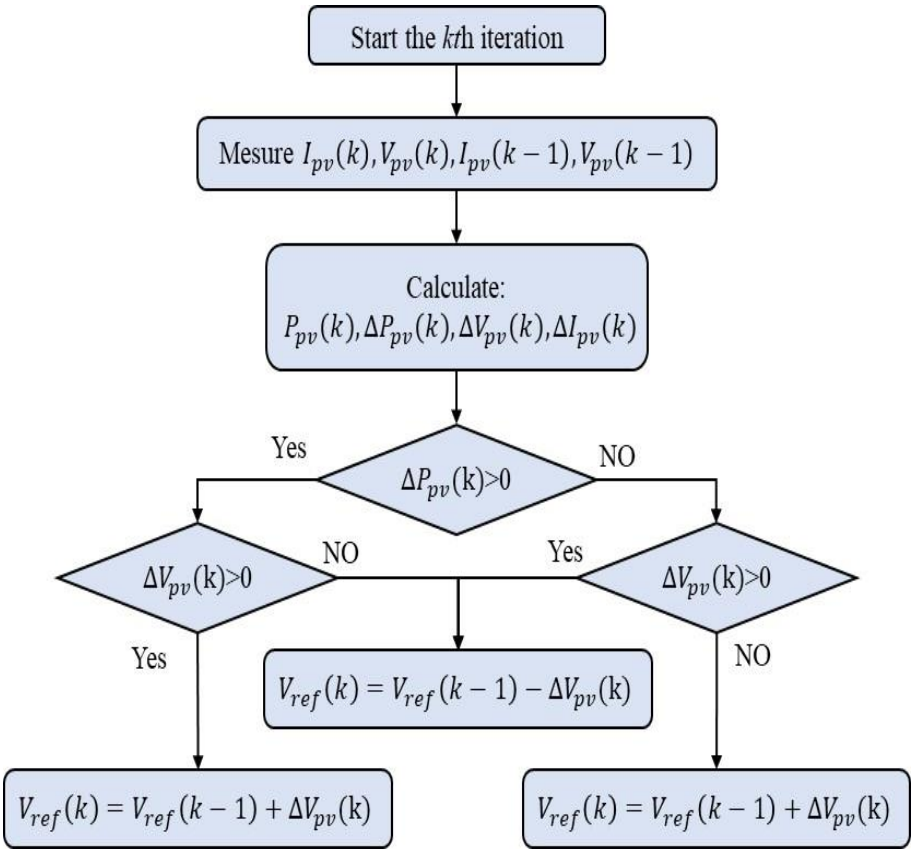

Figure 3.27: Voltage P&O algorithm flowchart.

Due to the PV voltage corresponding the MPP change slightly under sudden irradiation changes, VO-MPPT provides a fast MPP tracking compared to CO-MPPT.

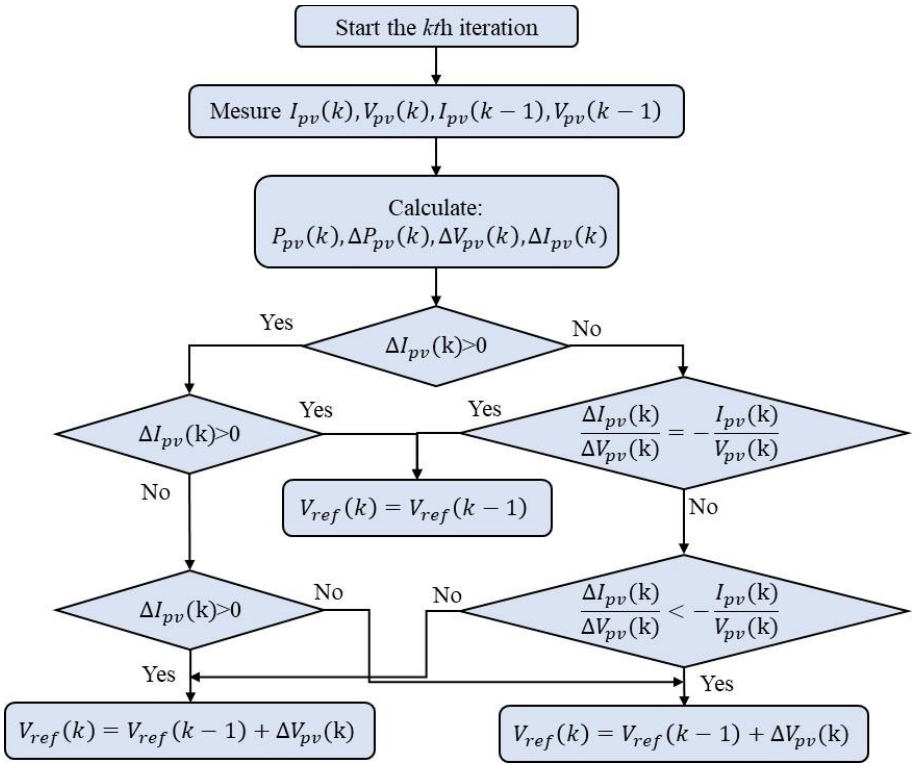

Figure 3.28: Voltage-Inc algorithm flowchart.

e) Other MPPT algorithms

Several recent research works have been investigated to introduce the artificial intelligence (AI) such as fuzzy logic control (FLC) [43] and neural networks (NN) [44], neuro-fuzzy networks (NFIS) [45], genetic algorithm (GA) [46], sliding mode control [47]. The AI-MPPT methods offer high performance operation in terms of good stability and fast response. However, the implementation of these MPPTs is limited in real time due to it require a high computational burden and large memory.

6. SUMMARY

In this chapter, a review of the recent technology of single-phase PV systems has been presented. Demands for the single-phase PV systems, including the grid-connected standards, the solar PV panel requirements, ground current requirements, efficiency, and reliability of the single-phase PV converters have been emphasized. Since achieving higher conversion efficiency is always of intense awareness, both the transformer-less single-stage (with an integrated (DC/DC converter) and the transformer-less double-stage (with a separate DC/DC converter) PV topologies have been discussed. The review reveals that the transformer-less double-stage (with a separate DC/DC converter) PV topologies are the most suitable for use in single-phase grid-tied systems, especially, when a DC/DC conversion stage is included, the

MPPT control becomes more convenient, where the enhanced hill climbing MPPTs are adopted to be the most suitable control techniques due to their simplicity. Finally, the general control structures for double-stage transformer-less PV systems are presented, as well as a brief discussion on DC-link regulation, synchronization and monitoring technologies. It is worth mentioning that all the review process is focused only on the most used techniques and topologies in residential applications.

REFERENCES

[1] O. Ellabban, H. Abu-Rub, and F. Blaabjerg, Renewable energy resources: Current status, future prospects and their enabling technology, Renew. Sust. Energy Rev., 39, 748–764, November 2014.

[2] J. Nelson, The Physics of Solar Cells, London, U.K.: Imperial College Press, 2003.

[3] International Renewable Energy Agency (IRENA), Renewable energy capacity statistics 2019, June 2019, http://www.irena.org/publications, last accessed June 8, 2019.

[4] F. Blaabjerg, K. Ma, and Y. Yang, Power electronics—The key technology for renewable energy systems, in Proceedings of EVER, pp. 1–11, Monte-Carlo, Monaco, March 2014.

[5] J.D. van Wyk and F.C. Lee, On a future for power electronics, IEEE J. Emerg. Sel. Top. Power Electron., 1(2), 59–72, June 2013.

[6] F. Spertino and G. Graditi, Power conditioning units in grid-connected photovoltaic systems: A comparison with different technologies and wide range of power ratings, Sol. Energy, 108, 219–229, October 2014.

[7] M.A. Eltawil and Z. Zhao, Grid-connected photovoltaic power systems: Technical and potential problems— A review, Renew. Sust. Energy Rev., 14(1), 112–129, January 2010.

[8] D. Meneses, F. Blaabjerg, O. Garcia, and J.A. Cobos, Review and comparison of step-up transformerless topologies for photovoltaic AC-module application, IEEE Trans. Power Electron., 28(6), 2649–2663, June 2013.

[9] S.B. Kjaer, J.K. Pedersen, and F. Blaabjerg, A review of single-phase grid-connected inverters for photovoltaic modules, IEEE Trans. Ind. Appl., 41(5), 1292–1306, September–October 2005.

[10] M. Morjaria, D. Anichkov, V. Chadliev, and S. Soni, A grid-friendly plant: The role of utility-scale photovoltaic plants in grid stability and reliability, IEEE Power Energy Mag., 12(3), 87–95, May–June 2014.

[11] Y. Xue, K.C. Divya, G. Griepentrog, M. Liviu, S. Suresh, and M. Manjrekar, Towards next generation photovoltaic inverters, in Proceedings of IEEE ECCE, pp. 2467–2474, Phoenix, AZ, September 17–22, 2011.

[12] Y. Yang, P. Enjeti, F. Blaabjerg, and H. Wang, Wide-scale adoption of photovoltaic energy: Grid code modifications are explored in the distribution grid, IEEE Ind. Appl. Mag., 21(5), 21–31, September–October 2015.

[13] R. Teodorescu, M. Liserre, and P. Rodriguez, Grid Converters for Photovoltaic and Wind Power Systems. Hoboken, NJ, Wiley, 2011.

[14] E. Romero-Cadaval, G. Spagnuolo, I. Garcia Franquelo, C.A. Ramos-Paja, T. Suntio, and W.M. Xiao, Grid-connected photovoltaic generation plants: Components and operation, IEEE Ind. Electron. Mag., 7(3), 6–20, September 2013.

[15] B.S. Prasad, S. Jain, and V. Agarwal, Universal single-stage grid-connected inverter, IEEE Trans.

Energy Convers., 23(1), 128‐137, March 2008.

[16] R.O. Caceres and I. Barbi, A boost DC‐AC converter: Analysis, design, and experimentation, IEEE Trans. Power Electron., 14(1), 134‐141, January 1999.

[17] C. Wang, A novel single-stage full-bridge buck-boost inverter, IEEE Trans. Power Electron., 19(1),150‐159, 2004.

[18] S. Jain and V. Agarwal, A single-stage grid connected inverter topology for solar PV systems with maximum power point tracking, IEEE Trans. Power Electron., 22(5), 1928‐1940, 2007.

[19] L.G. Junior, M.A.G. de Brito, L.P. Sampaio, and C.A. Canesin, Single stage converters for low Power stand-alone and grid-connected PV systems, in Proceedings of IEEE ISIE, pp. 1112‐1117, Gdansk, Poland, 2011.

[20] Y. Tang, S. Xie, and C. Zhang, Single-phase Z-source inverter, IEEE Trans. Power Electron., 26(12), 3869‐3873, 2011.

[21] Y.P. Siwakoti, F.Z. Peng, F. Blaabjerg, P.C. Loh, and G.E. Town, Impedance-source networks for electric power conversion Part I: A topological review, IEEE Trans. Power Electron., 30(2), 699‐716, February 2015.

[22] H. Liu, G. Liu, Y. Ran, G. Wang, W. Wang, and D. Xu, A modified single-phase transformerless Z-source photovoltaic grid-connected inverter, J. Power Electron., 5(5), September 2015.

[23] R. Teodorescu, M. Liserre, and P. Rodriguez, Grid Converters for Photovoltaic and Wind Power Systems. Hoboken, NJ, Wiley, 2011.

[24] Y. Yang, H. Wang, F. Blaabjerg, and K. Ma, Mission profile based multi-disciplinary analysis of power modules in single-phase transformerless photovoltaic inverters, in Proceedings of EPE, pp. 1‐10, Lille, France, September 2013.

[25] N. Achilladelis, E. Koutroulis, and F. Blaabjerg, Optimized pulse width modulation for transformerless active-NPC inverters, in Proceedings of EPE, pp. 1‐10, Lappeenranta, Finland, August 26‐28, 2014.

[26] M. Victor, F. Greizer, S. Bremicker, and U. Hubler, Method of converting a direct current voltage from a source of direct current voltage, more specifically from a photovoltaic source of direct current voltage, into a alternating current voltage, U.S. Patent 20050286281 A1, December 29, 2005.

[27] R. Gonzalez, J. Lopez, P. Sanchis, and L. Marroyo, Transformerless inverter for single-phase photovoltaic systems, IEEE Trans. Power Electron., 22(2), 693‐697, March 2007.

[28] H. Schmidt, C. Siedle, and J. Ketterer, DC/AC converter to convert direct electric voltage into alternating voltage or into alternating current, U.S. Patent 7046534, May 16, 2006.

[29] R. Gonzalez, E. Gubia, J. Lopez, and L. Marroyo, Transformerless single-phase multilevel-based photovoltaic inverter, IEEE Trans. Ind. Electron., 55(7), 2694‐2702, July 2008.

[30] K. Ogura, T. Nishida, E. Hiraki, M. Nakaoka, and S. Nagai, Time-sharing boost chopper cascaded dual mode single-phase sinewave inverter for solar photovoltaic power generation system, in Proceedings of IEEE PESC, pp. 4763‑4767, Aachen, Germany, 2004.

[31] Y. Kim, J. Kim, Y. Ji, C. Won, and Y. Jung, Photovoltaic parallel resonant dc-link soft switching inverter using hysteresis current control, in Proceedings of APEC, pp. 2275‑2280, Palm Springs, CA, 2010.

[32] Y. Yang, F. Blaabjerg, and H. Wang, Low voltage ride-through of single-phase transformerless photovoltaic inverters, IEEE Trans. Ind. Appl., 50(3), 1942‑1952, May/June 2014.

[33] F. Blaabjerg, R. Teodorescu, M. Liserre, and A.V. Timbus, Overview of control and grid synchronization for distributed power generation systems, IEEE Trans. Ind. Electron., 53(5), 1398‑1409, October 2006.

[34] Talbi, B., Krim, F., Rekioua, T., Mekhilef, S., Laib, A., & Belaout, A. (2018). "A high-performance control scheme for photovoltaic pumping system under sudden irradiance and load changes". Solar Energy, 159, 353-368.

[35] Singh, M., & Chandra, A. (2013). "Real-time implementation of ANFIS control for renewable interfacing inverter in 3P4W distribution network". IEEE Transactions on industrial electronics, 60(1), 121-128.

[36] Krama, A., Laid, Z., & Boualaga, R. (2017). "Anti-windup proportional integral strategy for shunt active power filter interfaced by photovoltaic system using technique of direct power control". Rev. Roum. Sci. Tech. Électrotech. Énerg, 62, 252-257.

[37] N. Femia, G. Petrone, G. Spagnuolo, and M. Vitelli, Power Electronics and Control Techniques for Maximum Energy Harvesting in Photovoltaic Systems. London, U.K.: CRC Press, 2012.

[38] D. Sera, L. Mathe, T. Kerekes, S. V. Spataru, and R. Teodorescu, On the perturb-and-observe and incremental conductance MPPT methods for PV systems, IEEE Journal of Photovoltaics, 3, 1070‑1078, July 2013.

[39] Hua, C., Lin, J., and Shen, C. Implementation of a DSP-controlled photovoltaic system with peak power tracking, IEEE Transactions on Industrial Electronics, 45(1), 99‑107, 1998.

[40] Elgendy, M.A., Zahawi, B., and Atkinson, D.J. Assessment of the incremental conductance maximum power point tracking algorithm, IEEE Transactions on Sustainable Energy, 4(1), 108‑117, 2013.

[41] Kollimalla SK, Mishra MK. "A novel adaptive P&O MPPT algorithm considering sudden changes in the irradiance". IEEE Transactions on Energy conversion 2014; 29(3): 602-610.

[42] Kakosimos PE, Kladas AG, Manias SN. Fast Photovoltaic-System Voltage- or Current-Oriented MPPT Employing a Predictive Digital Current-Controlled Converter. IEEE Trans Ind 385 Electron 2013; 60:5673–85. doi:10.1109/TIE.2012.2233700.

[43] Talbi, B., Krim, F., Rekioua, T., Laib, A., & Feroura, H. (2017). Design and hardware validation of modified P&O algorithm by fuzzy logic approach based on model predictive control for MPPT of PV systems. Journal of Renewable and Sustainable Energy, 9(4), 043503.

[44] Liu, Y.-H., Liu, C.-L., Huang, J.-W., Chen, J.-H., 2013. “Neural-network based maximum power point tracking methods for photovoltaic systems operating under fast changing environments”. Sol. Energy 89, 42–53.

[45] Chikh, A., Chandra, A., 2014. “Adaptive neuro-fuzzy based solar cell model”. IET Renew. Power Gener. 8(6), 679–686 .

[46] Shaiek, Y., Smida, M.B., Sakly, A., Mimouni, M.F., 2013. “Comparison between conventional methods and GA approach for maximum power point tracking of shaded solar PV generators”. Sol. Energy 90, 107–122.

[47] Kihal, A., Krim, F., Laib, A., Talbi, B., Afghoul, H. (2019). An improved MPPT scheme employing adaptive integral derivative sliding mode control for photovoltaic systems under fast irradiation changes. ISA transactions, 87, 297-306.

.

Chapter 4

Grid-Connected PV System Using Single-Phase Multilevel Inverter

1. INTRODUCTION

In the past decades, the utilization of renewable energy resources has been widely spread in the world in order to reduce the exorbitant use of the conventional sources, which causes environmental pollution problems. From the developed systems of renewable energy sources, the installation of solar energy systems has seen a fast increase in its request by the utilities. This reason led to more interest in grid-tied photovoltaic (PV) systems and related power conversion topologies [1].

In grid-tied process, the voltage source inverters (VSIs) contribute generally to improve the power quality by eliminating current harmonics and compensating the reactive power of the grid at the PCC, caused by local non-linear loads [2–4]. Much literature proposed a mixed topology of active filters and PV systems to increase the use of modern active filtering methods [5–10]. Those topologies can offer good quality for reactive power compensation and current harmonics elimination, but the use of two-level VSIs has few disadvantages such as an output voltage rich in harmonics and high switching losses [11].

In the past few years, research works on PV inverter structures shifted to multilevel inverters (MLIs), which are considered as the most suitable topologies for PV energy systems and integration to the grid, without using large passive output filters [12, 13].

The MLI topologies produce various and symmetrical output voltages which have the ability to deliver waveforms with low harmonic and less stress on semiconductor switches.

Therefore, the use of an inverter with a high number of output levels does not need large and expensive filter-side inductors to provide high-performance operation. Many recent research works deal with MLI topologies such as Flying Capacitors Inverter [14], Cascaded H-Bridge (CHB) inverter [15], and Packed U Cells (PUC) inverter [16–21].

Single-phase MLI can play a significant role in PV system applications by converting the PV array DC voltage to a practical AC voltage usable by the loads and grid with less harmonic filters and high efficiency [17, 22]. The five-level MPUC inverter has been proposed for such application with interesting advantages by using a low number of components as well as generating five levels of voltages at the output [18].

Various control strategies for grid-tied PUC inverter are proposed by using conventional PI controllers associated with modulation strategies [19, 20].

The authors of [19] propose a new self-voltage balance technique integrated through PWM modulator or modified five level packed Unit-cell converter (MPUC5) inverter to generate a five-level voltage in active power filter (APF) applications. However, this technique has few limitations on balancing capacitor voltages, complexity of PWM modulator and hard implementation.

Recently, multi-objective MPC strategies have been developed for PUC inverter [18, 21]. The MPC is a simple and effective strategy to control the MLIs. It has been intensively explored in power converters control [23–28], where the use of this strategy reduces the number of PI controllers and eliminates the need of modulation stage. Moreover, it is easy to include the DC-link capacitor voltages balancing in the control objective which makes the converter output very much cleaner. MPC technique is based on the calculation of the future behavior of the controlled variables for all switching cases by comparison to their references through a cost function in order to select the optimal state. Furthermore, the MPC has some interesting characteristics such as fast dynamic response, accurate tracking and ability to include non-linearities and constraints in the design of the controller [27, 28].

In this chapter, a Transformer-less single-phase grid-tied PV system is developed using MPUC5 MLI controlled by a novel MPC strategy with the aim to compensate a contaminating load with poor power factor, to enhance reactive power in the grid, to eliminate harmonic currents at the PCC and to inject the produced PV power into the grid under various levels of solar irradiation. The proposed MPC algorithm is employed to reduce the computational burden, to minimize the switching frequency and to provide high power factor correction, in

addition to ensure the balance of the DC-link capacitor voltages. To confirm the good performance of the proposed configuration, detailed simulations are carried out in Matlab/Simulink^{TM} environment and validated experimentally by means of a test bench based on dSPACE1104 control board.

The main contributions of this chapter are summarized as follows:

i. A new multifunctional single-phase grid-connected MPUC5 inverter interfaced with PV system configuration is presented.

ii. A novel MPC algorithm is deployed for MPUC5 inverter to work properly, where, the proposed algorithm does not introduce any additional complexity.

iii. The proposed control algorithm is implemented and checked using a real-time hardware in the loop (HIL) system that is entirely based on dSPACE 1104 control board.

The remaining of this chapter is organized as follows: after an introduction and an overview on the proposed system, section 3 introduces the MPUC5 topology configuration. Section 4 gives a brief description of the MPPT algorithm used to control DC/DC Cùk converter and the DC-link regulator. The proposed MPC technique for the MPUC5 inverter in APF and grid-tied applications is presented in Section 5. Simulation results and discussions are presented in Section 6. Experimental results with HIL implementation using Matlab/Simulink^{TM} and dSPACE 1104 control board are discussed in Section 7 to confirm the good performance of the proposed MPC controller, after which conclusions are drawn in Section 8.

2. OVERVIEW OF THE PROPOSED SINGLE-PHASE GRID-TIED PV SYSTEM WITH APF APPLICATION

The proposed structure of transformer-less single-phase grid-tied PV system in addition to its control scheme including the proposed MPC controller are shown in Figure 4.1. The studied system consists of an AC source, a non-linear load in series and the MPUC5 inverter in parallel to the grid through a line inductor *(L_f)* at the PCC. The PV system is connected to one DC-link capacitor of the MPUC5 inverter through a DC/DC Cùk converter, which can boost the PV array voltage up to a high DC-link voltage.

The main goals of this configuration are the injection of the produced PV power into the

grid with high grid current quality, compensation of the reactive power and elimination of the harmonic components caused by non-linear loads at the PCC under various levels of solar irradiation.

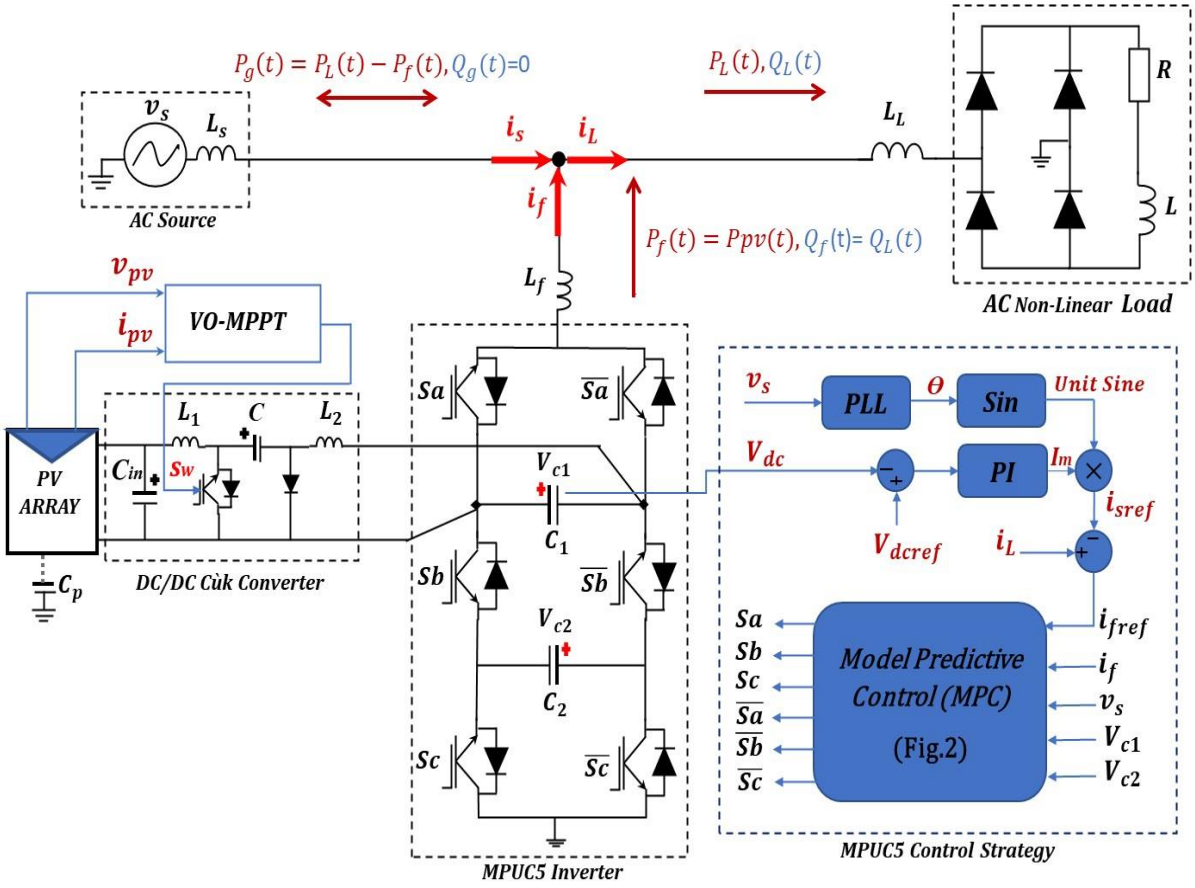

Figure 4.1: Synoptic of the proposed single-phase grid-tied PV system based on MPUC5 inverter.

3. MODELLING OF MPUC5 INVERTER IN APF APPLICATION

The MPUC5 inverter can be employed in the field of renewable energy conversion system where a PV array is connected to one DC-link capacitor of the MPUC inverter through DC/DC Cùk converter.

According to Figure 4.1, MPUC5 inverter topology has 6 active switches and two DC-link capacitors. The main advantage of this structure is that MPUC5 inverter generates five level voltage amplitude values, higher than the PCC voltage. Where the inverter output voltage amplitude is equal to the sum of two DC-link capacitor voltages amplitude ($V_{AN} = V_{c1} + V_{c2}$). Therefore, the capacitors will be charged by equal voltage amplitude to ensure the capacitors voltages balancing at the DC side of the MPUC5 inverter [19, 20] to guarantee boost operation of the inverter and to inject into the grid the compensating current during solar irradiation

periods, as well as the produced power from PV array. By assuming (V_{c1}= V_{c2} = E), the switching states and the corresponding output voltage levels of the MPUC5 inverter could be illustrated as in Table 4.1.

Furthermore, in the MPUC5 inverter topology, the zero-voltage level in freewheeling period can be achieved without using extra power switches as depicted in Table 4.1. Therefore, the common mode voltage will be zero during the freewheeling period; as a result, the ground leakage current will be declined significantly [29]. This makes it the best choice for non-isolated single-phase PV applications.

Table 4.1. Switching states and voltage levels of the MPUC5 Inverter.

Switching State (*St*)	S_a	S_b	S_c	$\overline{S_a}$	$\overline{S_b}$	$\overline{S_c}$	**Voltage levels generated by MPUC5 (V_{AN})**
State 1	0	1	0	1	0	1	V_{AN}= ***-2E***
State 2	1	0	1	0	1	0	V_{AN} = ***+2E***
State 3	1	1	1	0	0	0	V_{AN} = ***0***
State 4	0	0	0	1	1	1	V_{AN} = ***0***
State 5	0	1	1	1	0	0	V_{AN} = ***-E***
State 6	1	1	0	0	0	1	V_{AN} = ***-E***
State 7	0	0	1	1	1	0	V_{AN} = ***+E***
State 8	1	0	0	0	1	1	V_{AN} = ***+E***

The mathematical model of single-phase APF system using MPUC5 is given below

$$\frac{di_s(t)}{dt} = \frac{1}{L}[V_{AN} - v_s - R_f i_f] \tag{1}$$

$$\begin{cases} \dfrac{dV_{cx}(t)}{dt} = \dfrac{1}{C_x} i_f \\ x = 1,2. \end{cases} \tag{2}$$

where i_s and v_s are the grid current and voltage respectively. V_{cx} are the DC-link capacitor voltages, i_f the filter current, V_{AN} is the output voltage of the MPUC inverter, R_f and L_f are the resistance and inductance of the filter, respectively, and C_x are the DC-link capacitors.

4. VO-MPPT ALGORITHM AND DC-LINK VOLTAGE CONTROL

PV array is connected to the MPUC5 inverter through a DC/DC Cùk converter, working with VO-MPPT (Voltage-oriented maximum power tracking) algorithm to draw maximum power under solar irradiation change.

The Cùk converter has been employed for interfacing the PV array and the MPUC5 inverter due to its low switching losses and the highest efficiency among non-isolated DC/DC converters [33, 34]. Moreover, the Cùk converter has the advantage that it can provide isolation between the PV array and the MPUC5 inverter [30].

On the other hand, the VO-MPPT is composed of a voltage MPPT algorithm and voltage control loop [31, 32]. The PV voltage is regulated to its reference generated by a voltage MPPT P&O algorithm based on the conventional PI regulator. While the DC-link voltage is controlled by a conventional PI controller as shown in Figure 4.1.

More details about PV system modeling and DC/DC Cùk converter design can be found in Appendix A.

5. PROPOSED MPC FOR MPUC5 INVERTER

In general, MPC is an advanced and effective strategy to control the power converters [23–28]. It is based on the mathematical model of the studied system in order to predict the future behavior of the controlled variables. Then to form these predictions, a cost function is defined and evaluated in order to select the optimal control action [18, 21].

In this section, a novel MPC which aims to control the filter current, to guarantee the balance of the two DC-link capacitor voltages and to minimize the switching frequency is proposed. The proposed MPC allows to control MPUC5 inverter in dual-function; single-phase PV system and APF mode. The functionality of the proposed MPC is summarized in the flowchart of Figure 4.2.

From the measured values of the filter current (i_f), grid voltage (v_s), filter reference current (i_{fref}), and the capacitor voltages (V_{c1}, V_{c2}); the predicted value of filter current ($i_f(k+1)$) is calculated for all eight switching states (Table 4.1).

The future behavior of the capacitor voltages ($V_{c1}(k+1)$, $V_{c2}(k+1)$) are calculated only for four switching states which have an effect on the capacitor voltages (State 5, 6, 7 & 8), where the MPUC output voltage (V_{AN}=*+E or -E*) as presented in Table 4.1, otherwise, the

predicted capacitor voltages remain the same ($V_{c1}(k+1) = V_{c1}(k)$ = & $V_{c2}(k+1) = V_{c1}(k)$) in the other states, as shown in the proposed MPC flowchart. After that, a cost function (g) is evaluated in order to select the optimal switching state corresponding to the minimum value.

The optimal switching state selected is applied to the MPUC5 inverter during the next sampling time through the switching pulses, which are produced according to the appropriate switching state chosen by the MPC from the switching table (Table 4.1).

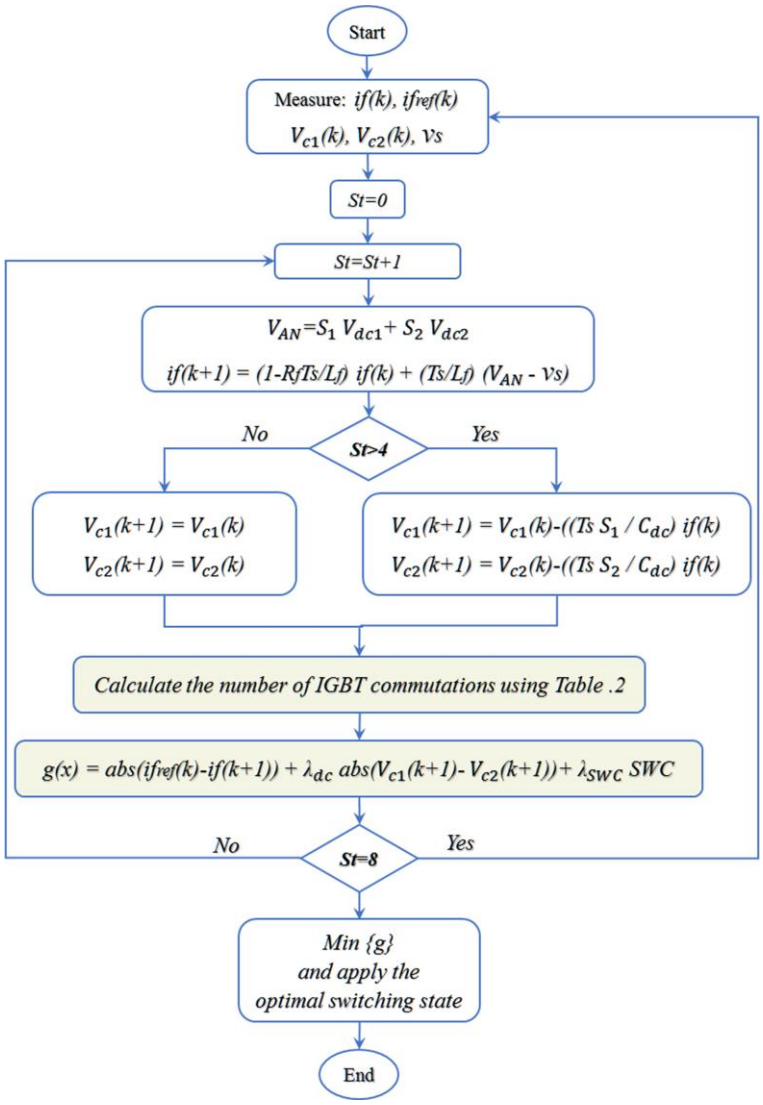

Figure 4.2: Flowchart of the proposed MPC.

The variables that have to be controlled by the proposed MPC are the future filter current i_f , capacitor voltages V_{c1}, V_{c2} and switching frequency. These control objectives are included in the cost function (g) as follows:

$$g = abs(i_{fref} - i_f(k+1)) + \lambda_{dc} abs(V_{c1}(k+1) - V_{c2}(k+1)) + \lambda_{SWC} SWC \qquad (3)$$

where i_{fref} and $i_f(k+1)$ are the reference and future behavior of filter current respectively,

$V_{c1}(k+1)$ & $V_{c2}(k+1)$ are the future behavior of DC-link capacitor voltages. SWC is the number of switching change,$\lambda_{dc}$and λ_{SWC} are the weighting factors for the DC-link capacitor voltages balance and switching frequency minimization, respectively.

These weighting factors are selected using the guidelines given in [36]; where a good balancing of the DC-link capacitor voltages is required. A very high value for λ_{dc} will create the perfect balance of the capacitor voltages, but with higher tracking errors. Likewise, a low value for λ_{dc}, leads to a drift in the capacitor voltages. A suitable compromise is to select λ_{dc} such that the drift in capacitor voltages is around 5% of nominal DC-link capacitor voltage.

On the other hand, the selection of λ_{SWC} is specific to our application; where the device switching frequency should be maintained below 10 kHz to allow a proper heat dissipation and less switching losses.

From Figure 4.1, the filter reference current can be estimated by using Kirchhoff current law,

$$i_f = i_L - i_s \tag{4}$$

Therefore, the filter reference current can be expressed as follows

$$i_{fref} = i_L - i_{sref} \tag{5}$$

where i_{sref} is the grid reference current generated by the DC-link voltage controller (PI-Controller) and i_L is the measured load current at the PCC. More details about design PI controller design can be found in Appendix B.

From Eq. (1) and by using the Euler Forward approximation, the future behavior of filter current can be expressed as

$$i_f(k+1) = (1 - R_f T_s/L_f) i_f(k) + (T_s/L_f)(V_{AN} - v_s) \tag{5.6}$$

where, V_{AN} is the voltage vector generated by the 5-level MPUC inverter, T_S the sampling period and v_s the AC source voltage.

In order to estimate the value of V_{AN} with simplified computational burden, two variables are introduced, namely, S_1 and S_1 to simplify the use of the inverter switching states S_a, S_b and S_c. Which are evaluated by using Eq. (7) and Eq. (8).

$$S_1 = S_a - S_b \tag{7}$$

$$S_2 = S_c - S_b \tag{8}$$

The voltage vector generated by the 5-level MPUC inverter can be calculated as follows.

$$V_{AN} = S_1 V_{c1} + S_2 V_{c2} \tag{9}$$

Using again Euler approximation and Eq. (2), the behavior of the two capacitor voltages during the next sampling time $V_{c1}(k+1)$ and $V_{c1}(k+1)$ can be predicted by sending the appropriate switching variables S_1 and S_2, as follows:

$$V_{c1}(k+1) = V_{c1}(k) - ((T_s S_1)/C_{dc}) if(k) \tag{10}$$

$$V_{c2}(k+1) = V_{c2}(k) - ((T_s S_2)/C_{dc}) if(k) \tag{11}$$

where, ($C_{dc} = C_1 = C_2$) are the DC-link capacitors.

The SWC is the number of IGBT commutations illustrated by the number of switch changes between the actual switching state applied to MPUC5 inverter and the predicted switching state, which can be calculated as detailed in Table 4.2.

Table 4.2. Number of switch changes calculation.

SWC	***St(K+1)***							
	1	***2***	***3***	***4***	***5***	***6***	***7***	***8***
St(K)= State1	0	3	2	1	1	1	2	2
St(K)= State2	3	0	1	2	2	2	1	1
St(K)= State3	2	1	0	3	1	1	2	2
St(K)= State4	1	2	2	0	2	2	1	1
St(K)= State5	1	2	1	2	0	2	1	3
St(K)= State6	1	2	1	2	2	0	3	1
St(K)= State7	2	1	2	1	1	3	0	2
St(K)= State8	2	1	2	1	3	1	2	0

6. ANALYTICAL STUDIES AND DISCUSSION

Numerical simulations of the proposed system, using MATLAB/Simulink environment, are carried out under various solar irradiation levels with a non-linear load connected to the PCC point. The key simulation parameters are shown in Table 4.3.

Table 4.3. Test parameters.

PV array Siemens SM110	**Values (STC)**
Maximum power (*Pmpp*)	120*Watts*
Open circuit voltage (*Voc*)	42.1*V*
Short circuit current (*Isc*)	3.87*A*
Voltage at *Pmax*	*33.7*
Current at *Pmax*	*3.56*
Number of cells connected in parallel (*Np*)	1
Number of cells connected in series (*Ns*)	72
Number of modules connected in series (*Nss*)	2
Number of modules connected in parallel (*Npp*)	2
Cùk Converter	**Values**
Inductance L_1	5 *mH*
Inductance L_2	5 *mH*
Capacitance *C*	220 μF
Input capacitance C_{in}	1100 μF
Grid parameters	**Values**
Grid Voltage (*Vs*)	70 *V*
Grid Frequency (*fs*)	50 *Hz*
Grid Side Inductor (*Ls*)	0.566 *mH*
MPUC inverter parameter	**Values**
DC Capacitors (*C1&C2*)	1100 μF
DC voltage reference Vdcref	150 V
Filter parameter	**Values**
Filter Side Inductor (*Lf*)	2 *mH*
Non-Linear Load parameters	**Values**
Rectifier AC Side Inductor (L_L)	2 *mH*
Load DC Side Resistor (*R*)	6 Ω
Load DC Side Inductor (*L*)	2 *mH*
Sampling Times	**Values**
MPPT sampling Time *Tp*	0.1 *ms*
Ds 1104 control board sampling time	50μs
MPC sampling Time *Ts*	50μs

It is worth to mention that, the power sizing of the whole system should be analyzed, to ensure the good performance of the proposed topology. Where the non-linear load is sized in order to consume an amount of $P_L = 370\,W, Q_L = 120\,VAR$ of active and reactive powers respectively. Therefore, the PV system is sized also to produce a maximum real power $P_{PV} = 480\,W$ at $1000\,W/m^2$ of irradiation level. Hence the inverter is dimensioned to inject the total real power produced by the PV system, and in the same time compensates the reactive power demanded by the non-linear load, so the inverter is sized for $500\,VA$ of apparent power S.

Simulation results thus allow the performance evaluation of transformer-less single-phase grid-connected PV system using multi-level MPUC5 inverter (APF with PV array). So, the injection of the generated PV power into the grid and non-linear load, compensation of reactive power and elimination of harmonic grid current are observed simultaneously in this section.

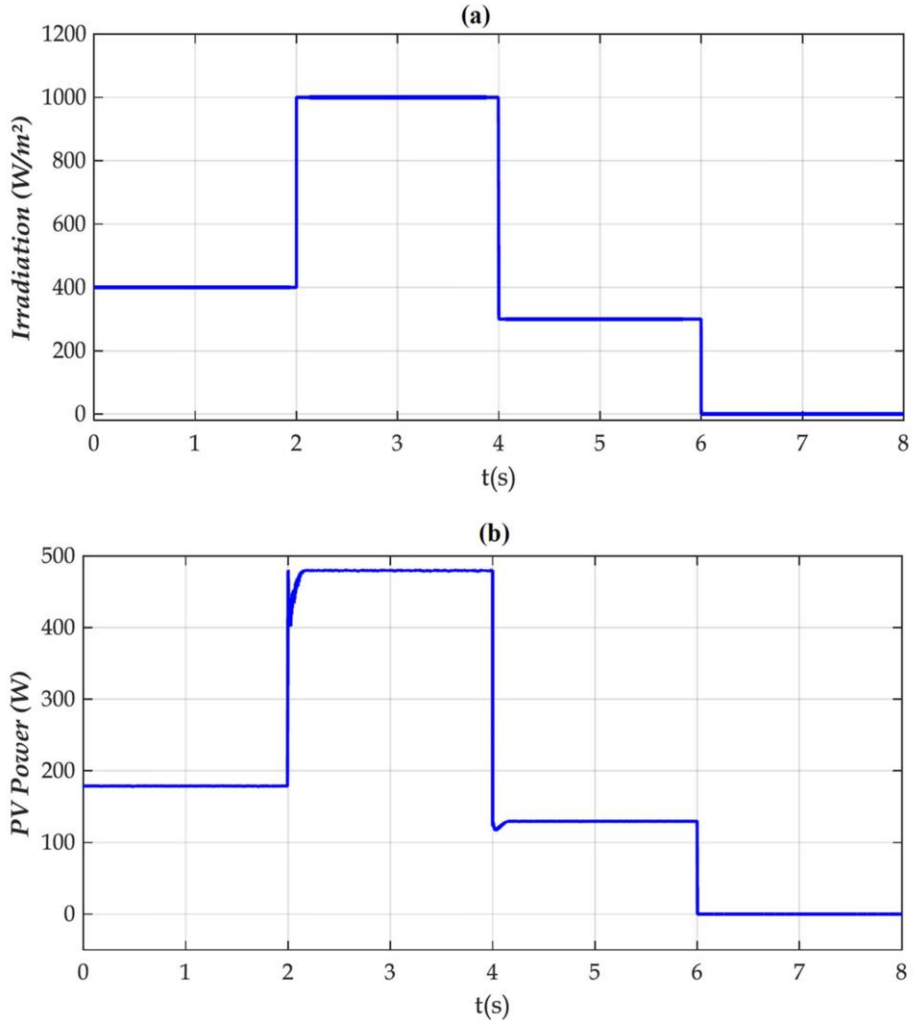

Figure 4.3: Waveforms of: **(a)** Irradiation levels, **(b)** PV array power under variable irradiation profile.

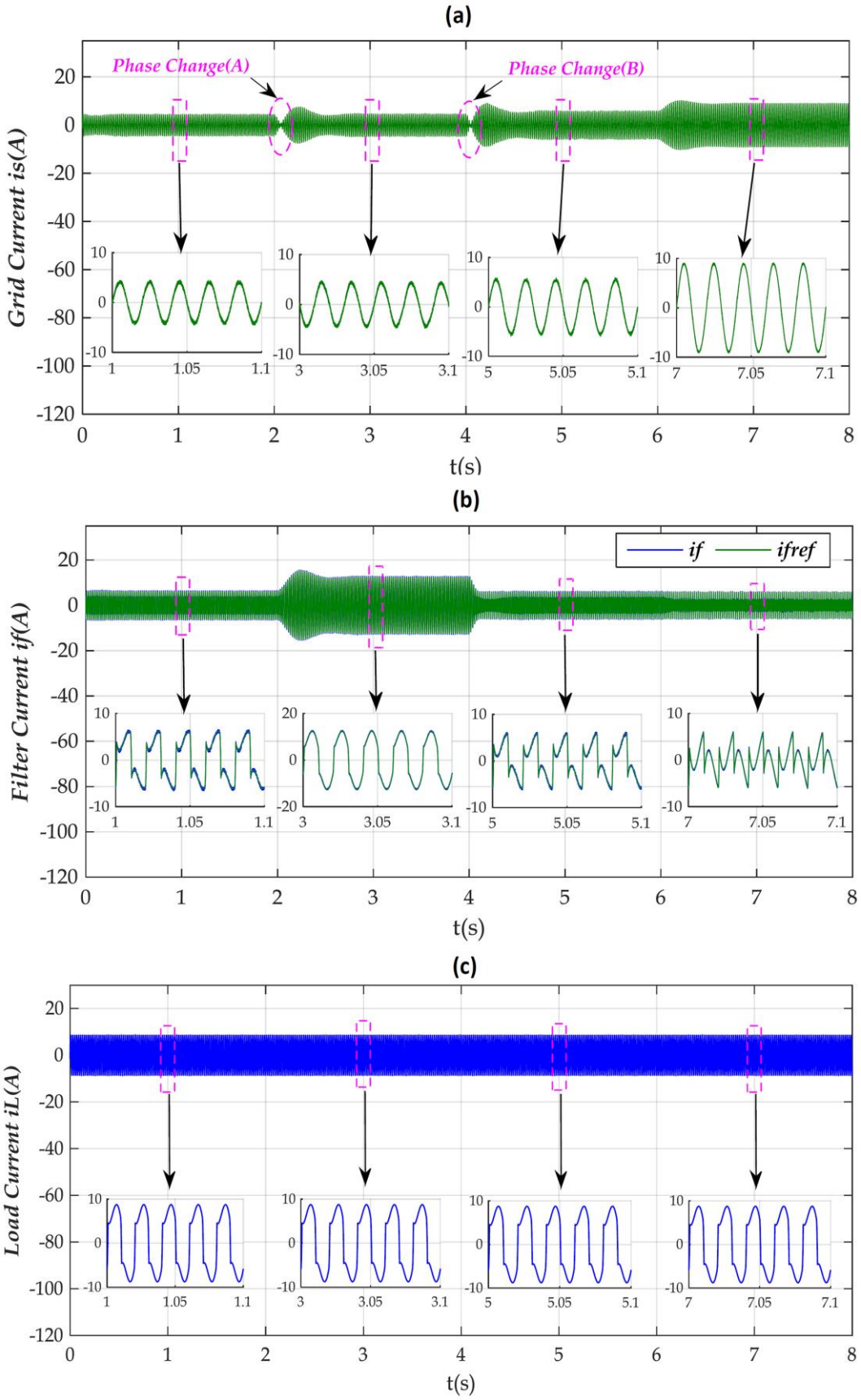

Figure 4.4: Waveforms of: **(a)** grid current (i_S), **(b)** filter current (i_L) and **(c)** load current (i_L), under solar irradiation changes.

Figure 4.3(b) shows the PV array power behavior under variable irradiation profile (Figure 4.3(a)). Firstly, constant irradiation is applied ($400W/m^2$) during 2 seconds, the PV power output is at the maximum power point ($175W$) and remains constant owing to the VO-MPPT.

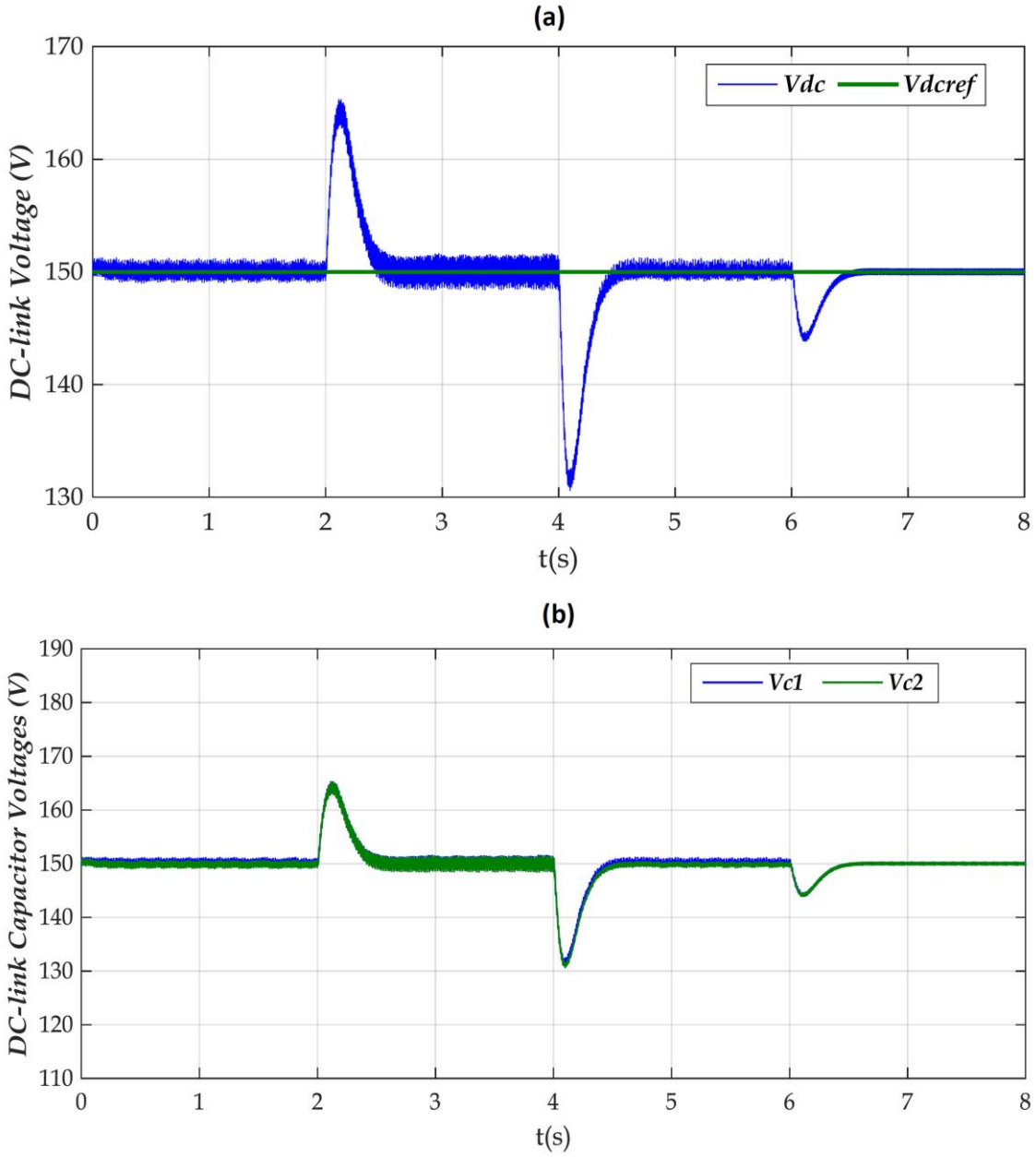

Figure 4.5: Waveforms of: **(a)** DC-link voltage, **(b)** DC-link capacitor voltages, under solar irradiation changes.

The injected filter current is shown in Figure 4.4(b). As a result, the grid current becomes sinusoidal (*see* Figure 4.4(a)) while the non-linear load continues to absorb a distorted current (*see* Figure 4.4(c)). The DC-link voltage V_{dc} is regulated to its reference value with small

voltage ripple (less than 5%) as shown in Figure 4.5(a). In addition, a perfect balance of the two capacitor voltages V_{c1} *and* V_{c2}, is achieved (*see* Figure 4.5(b)).

Then, a rising step in solar irradiation from $400W/m^2$ to $1000W/m^2$ is done at instant t= 2s and then remains constant during 2 s, the PV power output reaches the new MPP ($480W$) preceded by a small deviation which proves the efficiency of the VO-MPPT, while the filter continues to inject a current into the grid and non-linear load, in addition to ensure the elimination of current harmonics as depicted in Figure 4.4(b). An overshoot of the DC-link voltage over its reference occurs due the sudden change in the solar irradiation as shown in Figure 4.5(a) and both capacitor voltages get balanced perfectly (*see* Figure 4.5(b)), which demonstrates the good performance of the proposed MPC. After a phase change, the grid current waveform becomes sinusoidal again as presented in Figures 4.4(a), 4.6(a) & 4.6(c).

After that, a falling step in solar irradiation from $1000W/m^2$ to $300W/m^2$ is done at t=4s and remains constant during 2 s, the PV power output reaches the new MPP ($125W$) again. The filter continues to eliminate harmonics current at the PCC and ensure the injection of PV power into non-linear load as shown in Figure 4.4(b). Consequently, the grid current becomes again in phase with the grid voltage (*see* Figure 4.6(b)) and with a sinusoidal shape (*see* Figure 4.4(a) & 4.6(c)). However, we observe that the DC-link voltage oscillating around the reference after a small overshoot. While, the capacitor voltages get perfectly balanced (*see* Figures 4.5(a) & 4.5(b)).

Finally, to highlight the APF operation mode of the proposed system, the solar irradiation is removed at t=6s, so there is no PV power available. The filter continues to inject a compensation current at the PCC according to Figure 4.4(b). As a result of that, the grid current waveform remains sinusoidal as shown in Figure 4.4(a) and well synchronized with the grid voltage as depicted in Figure 4.6(c). Moreover, the DC-link keeps the same behavior as previously (*see* Figure 4.5(a)) and the capacitor voltages remain completely balanced (*see* Figure 4.5(b)).

Figure 4.7(a) shows the flux of grid active power (P_{grid}), filter power (P_{filter}) and load power (P_{load}) under variable irradiation profile (*see* Figure 4.3(a)). It is worth mentioning, that during low solar irradiance intervals, t=0s to t=2s and t=4s to t=6s, the load active power remains constant and is supplied by both the PV array and grid simultaneously because the active power delivered by the PV array is not sufficient to meet the power requirement of the load.

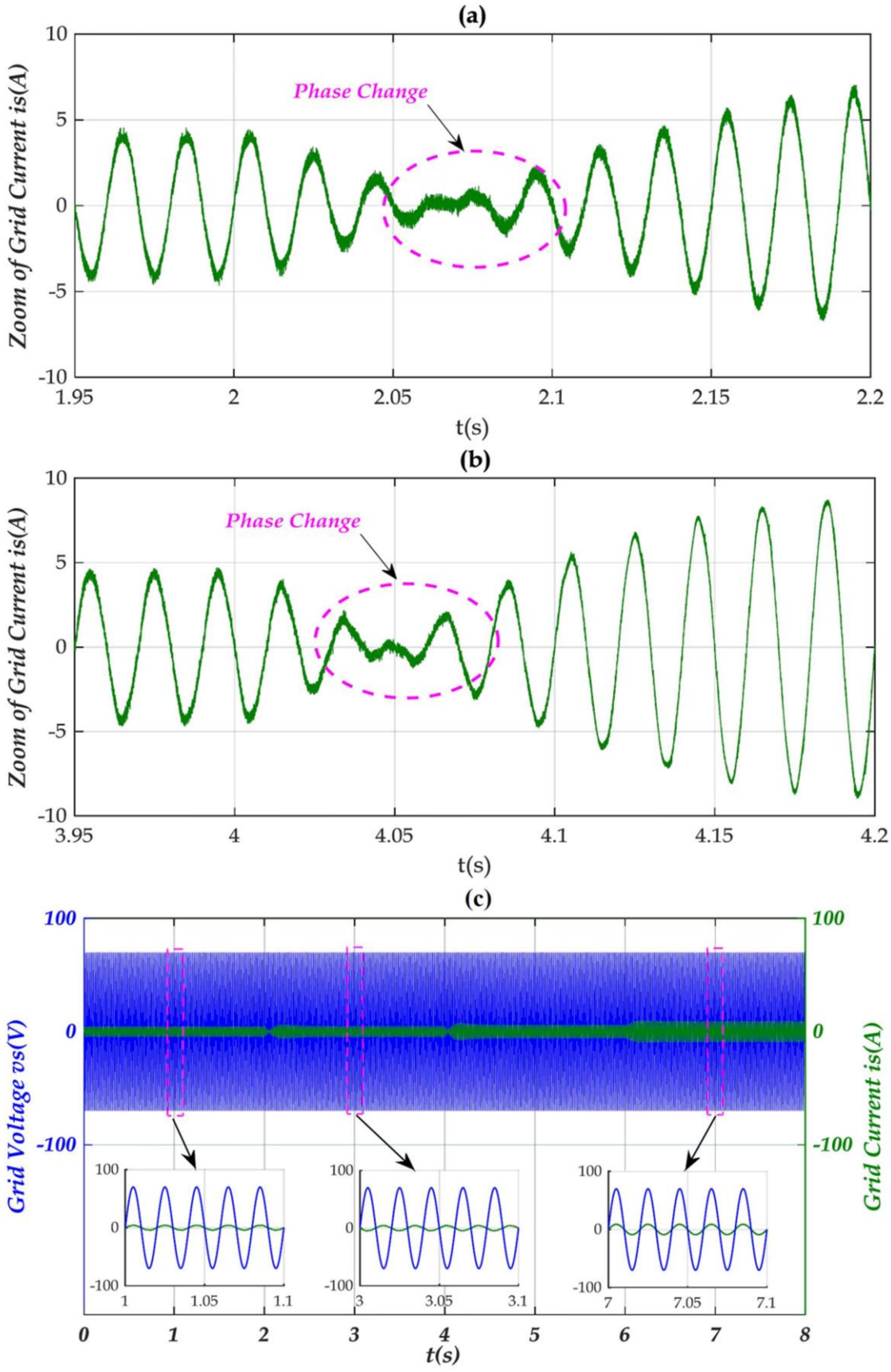

Figure 4.6: Waveforms of: (a), (b) current (i_S) during phase change, (c) grid voltage (v_S) and grid current (i_S) under solar irradiation changes.

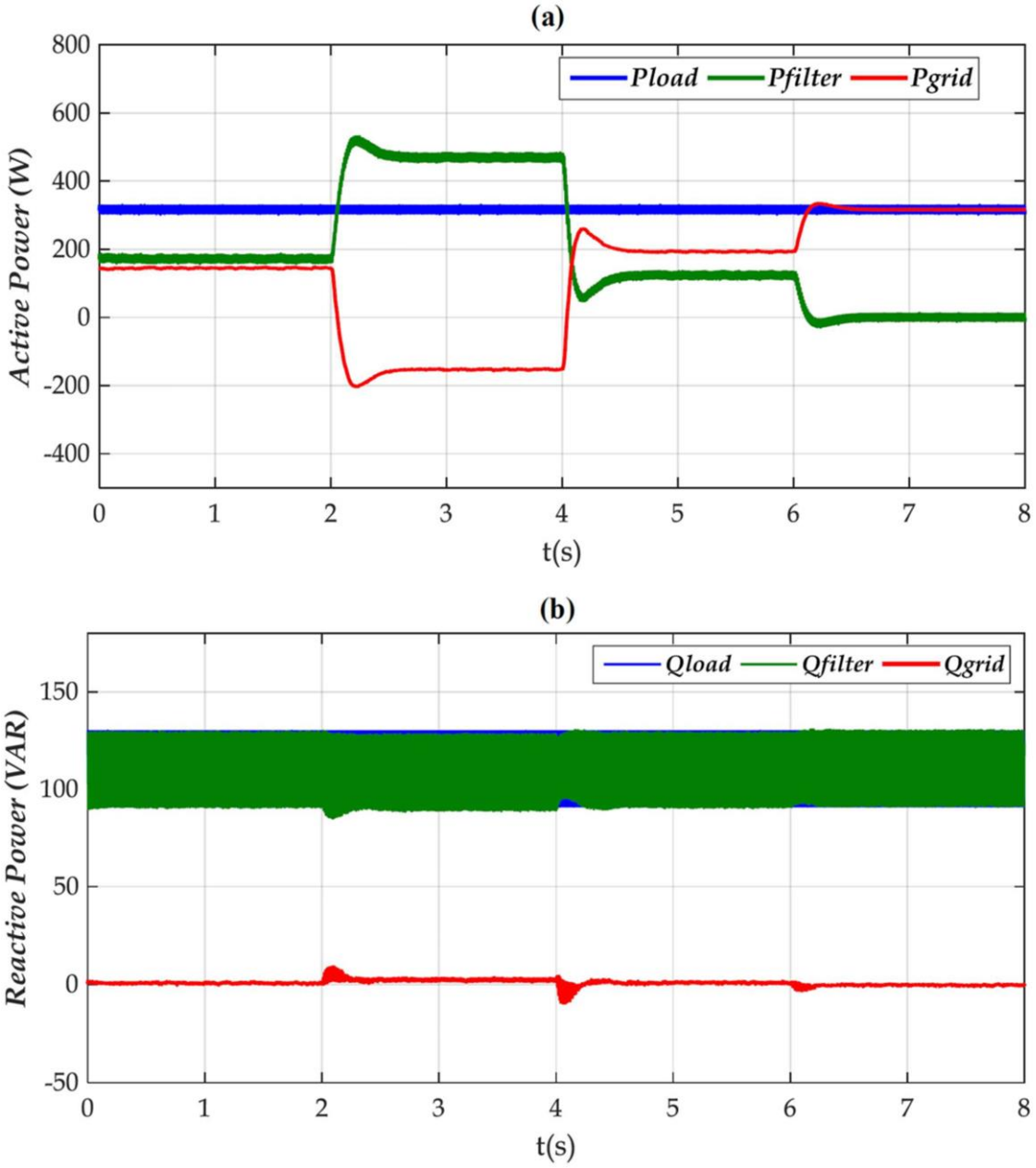

Figure 4.7: Waveforms of: **(a)** Instantaneous active powers, **(b)** Instantaneous reactive powers, under solar irradiation changes.

At t=2s, solar irradiation level rises from $400W/m^2$ to $1000W/m^2$, then the active grid power value decreases once receiving power from the PV array, because the generated PV power guarantees the power requirement of the load, so the extra power is injected into the grid.

During the interval where solar irradiation is not available (from t=6s to t=8s), there is no PV power, then an increase in grid active power value is observed, in order to provide the necessary power to the load. In this case the multilevel inverter MPUC5 acts only as an active power filter.

Reactive power of the whole system is represented in Figure 4.7(b) under variable irradiation profile (*see* Figure 4.3(a)). It is worth mentioning that it is only the filter, which supplies reactive power to the load, so the grid reactive power remains zero all the time.

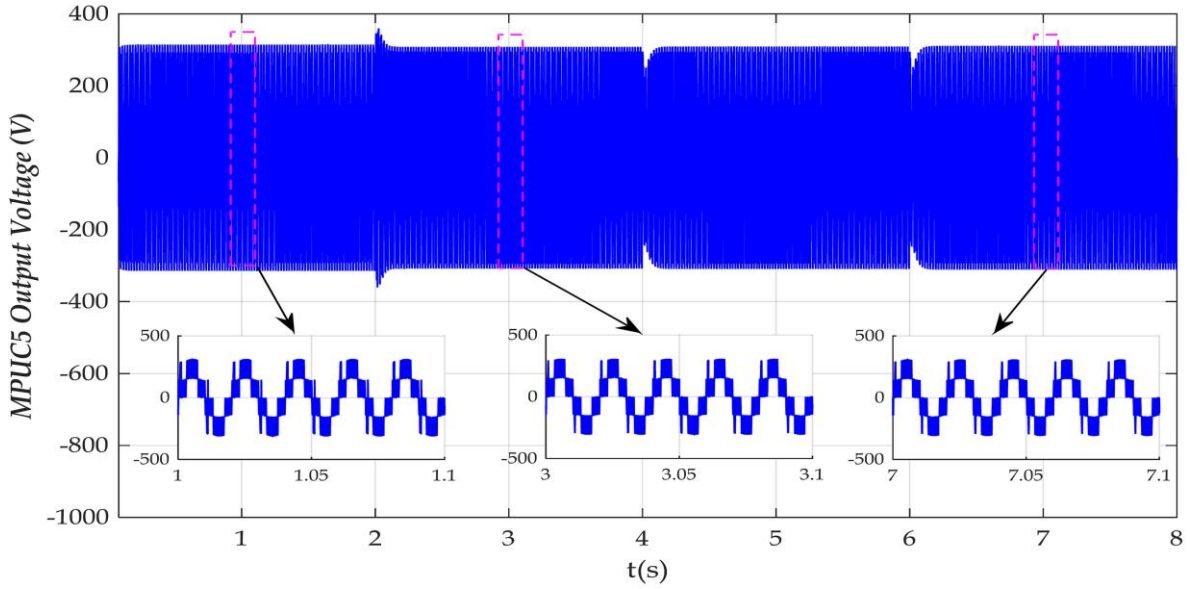

Figure 4.8: Waveform of MPUC5 inverter output voltage (V_{AN}) under solar irradiation changes.

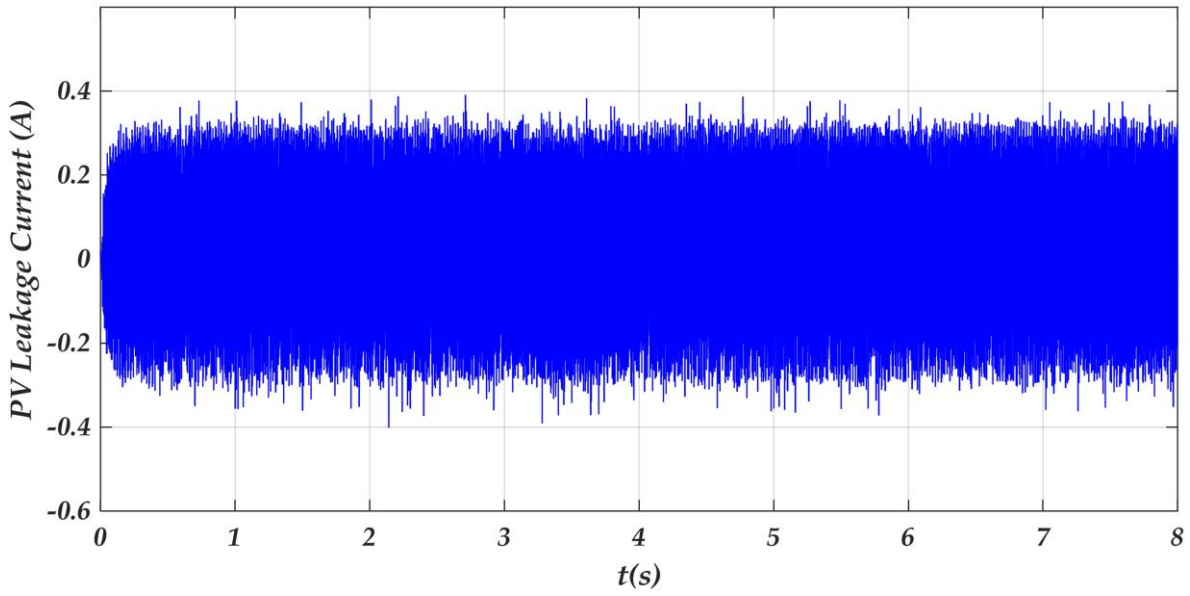

Figure 4.9: Waveform of the PV leakage current (I_{leak}).

It is also important to note that the MPC controller guarantees a perfect balance of the capacitor voltages since the 5-level output voltage waveform of the MPUC is perfectly regular and symmetrical according to Figure 4.8. Hence, the proposed system-based MPUC5 inverter shows a low leakage current as shown in Figure 4.9, which demonstrate that MLI MPUC

topology is a good choice for low and medium power conversion system-based PV sources for transformer-less single-phase applications.

Furthermore, to show the good performance of the proposed MPC algorithm, the average device switching frequency f_{SW} is calculated for all operating scenarios. The proposed MPC maintains the $THDi\%$ below 5% with unity power factor according to the IEEE STD 519 and IEC 61000-3-2 standards discussed previously in chapter 1. In addition, it increases the reliability of the semiconductor switches, where the switching frequency f_{SW} is sustained below 10 kHz as reported in Table 4.4.

Table 4.4. Analysis of grid current THD and the average switching frequency $\boldsymbol{f_{SW}}$.

Irradiation G (W/m²)	**G=400**	**G=1000**	**G=300**	**G=0**
THDi(%)	*1.85*	*2.17*	*1.71*	*1.32*
f_{SW} *(Khz)*	*4.8514*	*6.8562*	*4.6523*	*3.9562*

7. EXPERIMENTAL RESULTS

To validate the obtained simulation results, experimental tests are performed. The proposed system shown in Figure 4.1 has been implemented in the laboratory LEPCI, Sétif through a test bench based on dSPACE 1104 control board using hardware in the loop (HIL).

The DS1104 controller Board is a cost-effective entry-level system with I/O interfaces and a real-time processor on a single board that can be plugged directly into a PC for rapid control prototyping suitable for controller's development in power converters field. HIL system based on DS1104 controller board consists of an independent control processing unit (CPU) based on DS1104 controller board to build the control algorithms. A real-time simulator interface provides Matlab/ Simulink^{TM} blocks for graphical I/O configuration in order to simulate the plant model and a communication channel between the simulator and the DS1104 controller board. For each sample time, the DS1104 controller board receives the state variables from the real-time simulator through the communication channel. From these state variables, the CPU computes the optimal control actions and drives it to the real-time simulator. Thus, the obtained results through these tests are considered more practical. The control and system parameters used in the implementation are identical to the parameters used in simulation. The results are recorded using a 500 MHz Instek oscilloscope, as well as Control Desk interface, under variable irradiation profile as in the simulation.

Figure 4.10 shows the grid current behavior under variable solar irradiation. Figure 4.11 illustrates zoom of grid current filter current and load current, where the filter injects a current i_f into the grid, consequently, the grid current is taking a good sinusoidal shape and the load current i_L remains the same, which demonstrate the good compensation of reactive power by the proposed system.

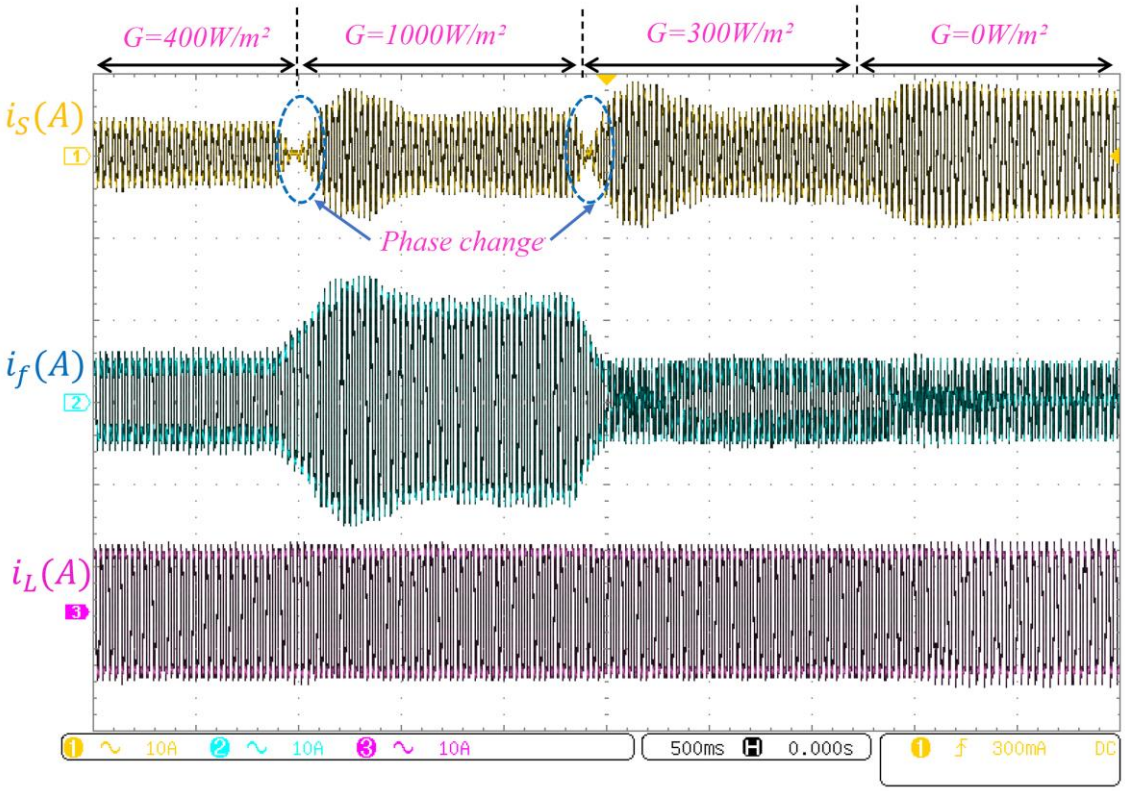

Figure 4.10: Experimental waveform for: grid current (i_S), filter current (i_f) and load current (i_L), under solar irradiation changes.

Figure 4.12 illustrates the zoom of grid current and voltage waveforms under different irradiation changes. It is worth mentioning that the grid current waveform during all changes in solar irradiation remains sinusoidal and in phase with the grid voltage during low irradiation level (*see* Figures 4.12 (a) & (c)), while in opposite phase with the grid voltage under high solar irradiation (*see* Figures 4.12 (b)). The grid current presents a low current distortion in all cases of solar irradiation levels ($THDi < 5\%$). Furthermore, the switching frequency f_{sw} is maintained below 10 kHz in all operating cases as summarized in Table 4.5.

Figure 4.13 depicts the capacitor voltages waveforms (V_{c1}, V_{c2}) of the capacitors C_1 and C_2, respectively, along with the five-level output voltage V_{AN} of the MPUC inverter. It is

observed clearly that the capacitor voltages are in accurate balancing, which proves the good performance of the proposed MPC algorithm.

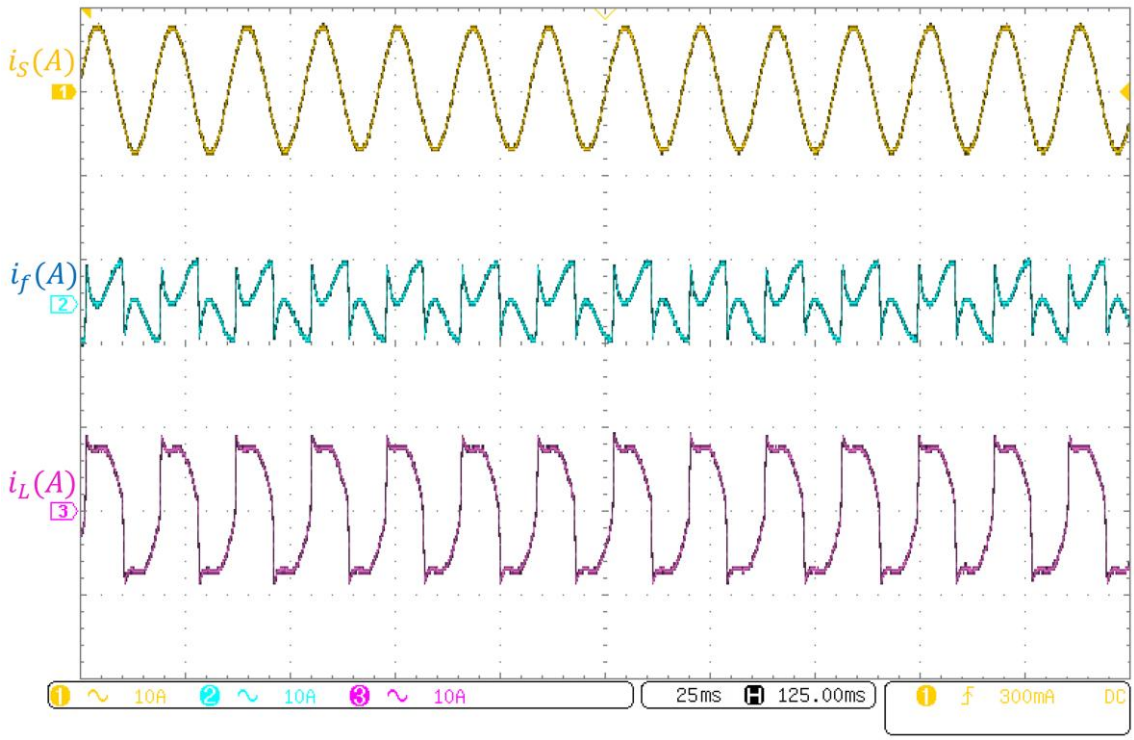

Figure 4.11: Zoom of grid current (i_S), filter current (i_f) and load current (i_L).

Figure 4.14 illustrates the experimental waveforms of the instantaneous active grid power, load power, filter power and DC-link voltage V_{dc} regulation during solar irradiation changes. It is clear that during low irradiation, the active power needed by the non-linear load is provided by both the PV array and the grid or only by the grid in case where there is no PV power. Besides, the PV array ensures the power requirement of the load and injects the extra power into the grid during high solar irradiation levels. Moreover, the DC-link voltage V_{dc} is completely regulated.

Figure 4.15 depicts the experimental waveforms of the instantaneous reactive powers of the grid, non-linear load and filter. The filter provides reactive power to the load all time, which imposes the reactive power grid to remain zero.

In conclusion, Figures 4.14 and 4.15 confirm experimentally the good performance of the proposed topology and MPC controller in terms of active power injection and reactive power compensation.

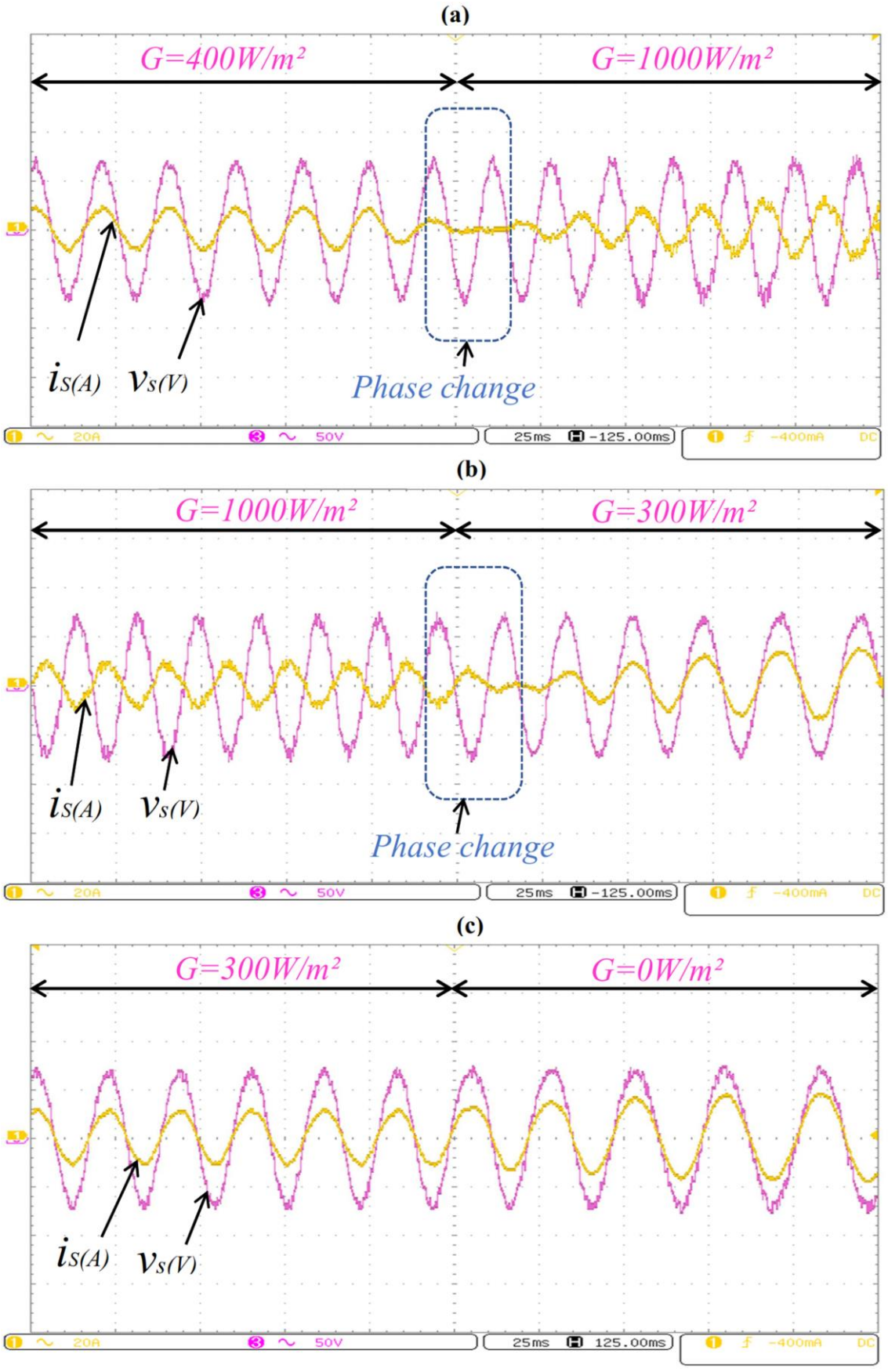

Figure 4.12: Zoom of grid current and voltage under different levels of solar irradiation.
(a) G: 400– 1000 W/m^2, **(b)** G: 1000 – 300 W/m^2, **(c)** G: 300 – 0 W/m^2

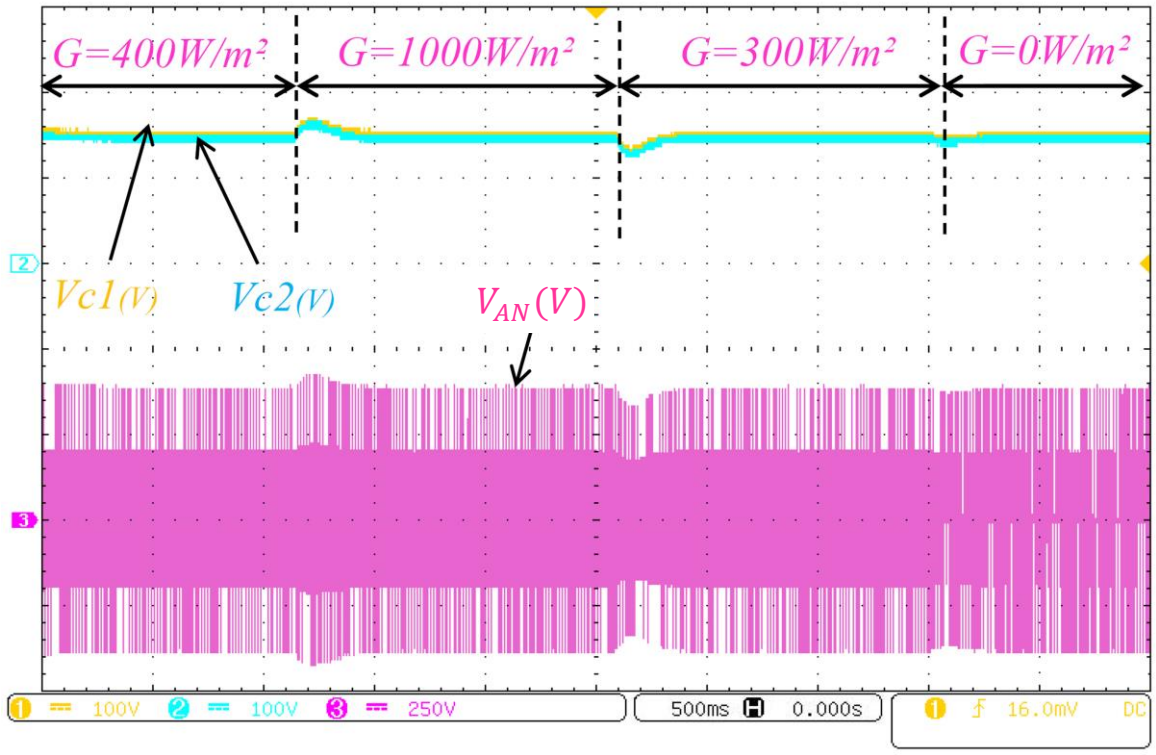

Figure 4.13: Experimental waveforms for DC-link capacitor voltages and MPUC5 output voltage (V_{AN}).

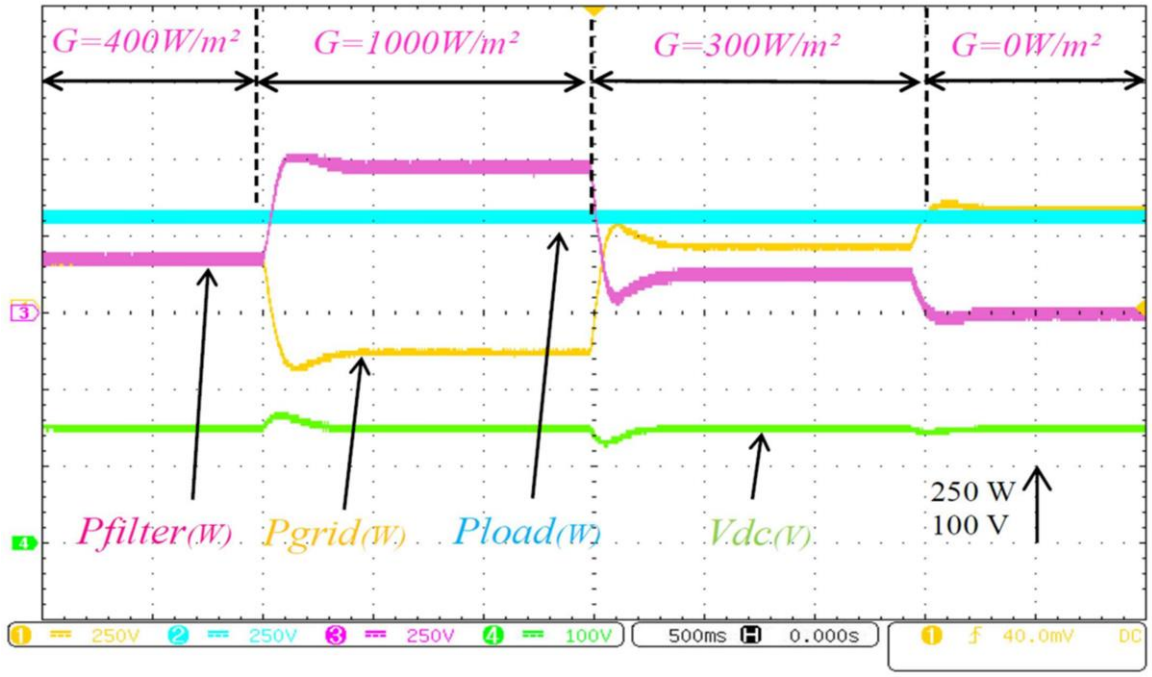

Figure 4.14: Experimental waveforms for instantaneous active powers with DC-link voltage (V_{dc}).

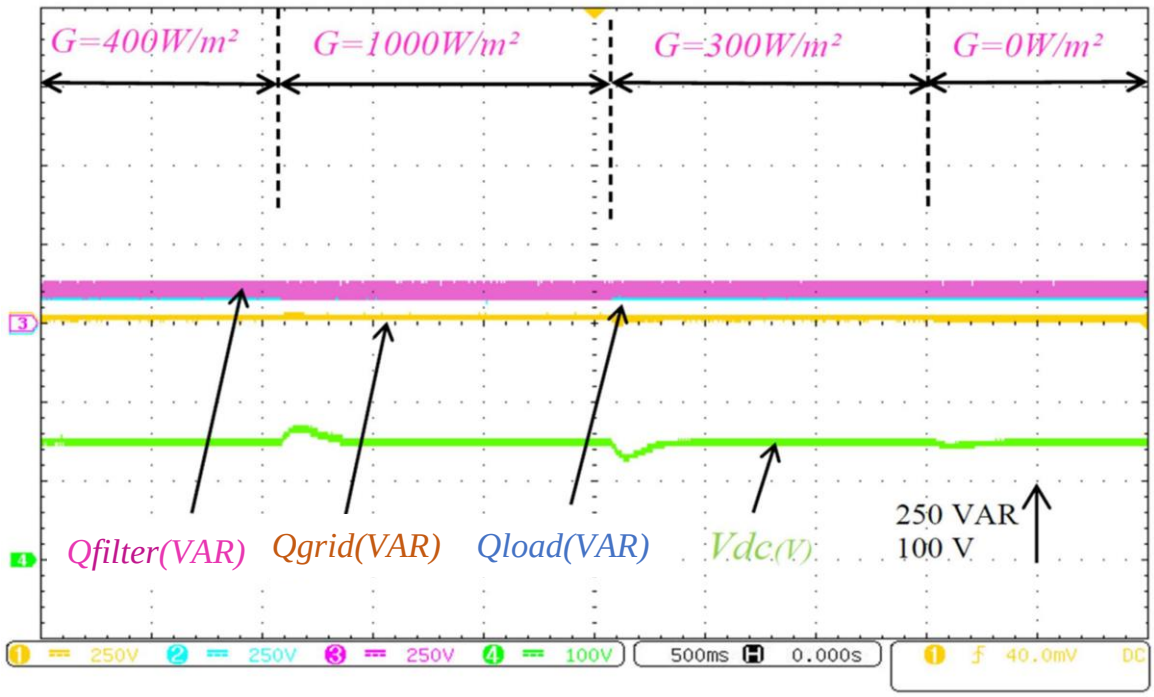

Figure 4.15: Experimental waveforms for instantaneous reactive powers and DC-link voltage (V_{dc}).

TABLE 4.5: Analysis of grid current THD and the average switching frequency f_{sw}.

Irradiation G (W/m²)	**G=400**	**G=1000**	**G=300**	**G=0**
THDi(%)	*3,11*	*4.19*	*3.02*	*2.19*
f_{sw} *(Khz)*	*6.2356*	*8.6852*	*5.1123*	*4.6825*

8. SUMMARY

A Transformer-less single-phase dual stage grid-connected PV system using five-level MPUC inverter controlled by a novel MPC was presented in this chapter. The system is able to perform a dual-function, namely the reduction of harmonic currents and injection of the power produced by the PV array into the grid or to the load regardless of the solar irradiation levels. Moreover, simulation results demonstrated the good performance of the proposed MPC method regarding the grid current quality, and DC-link capacitor voltages balance. Besides, the DC-link voltage regulation was achieved by means of a simple PI regulator. Consequently, the proposed topology exhibits a good flexibility for solar irradiation change regarding the active power injection, reactive power compensation, and power factor correction.

Furthermore, the proposed transformer-less single-phase double stage PV system based-multi-level inverter MPUC topology shows a low leakage current in comparison with the conventional topologies presented previously in chapter 3, which demonstrate that the proposed MLI MPUC topology is a good choice for low and medium power conversion system. Experimental results obtained through HIL system based on dSPACE 1104 control board, confirm all the simulation results, which prove the feasibility and validity of the proposed system.

REFERENCES

[1] Eltawil MA, Zhao Z. Grid-connected photovoltaic power systems: Technical and potential problems—A review. Renew Sustain Energy Rev 2010;14:112–29.

[2] Wang X, Zhuo F, Li J, Wang L, Ni S. Modeling and Control of Dual-Stage High-Power Multifunctional PV System in d-Q-Coordinate. IEEE Trans Ind Electron 2013;60:1556–70.

[3] Chen Z, Blaabjerg F, Pedersen JK. A multi-functional power electronic converter in distributed generation power systems. Power Electron. Spec. Conf. 2005. PESC'05. IEEE 36th, IEEE; 2005, p. 1738–44.

[4] Micallef A, Apap M, Spiteri-Staines C, Guerrero JM. Mitigation of harmonics in grid-connected and islanded microgrids via virtual admittances and impedances. IEEE Trans Smart Grid 2017;8:651–61.

[5] Ouchen S, Betka A, Abdeddaim S, Menadi A. Fuzzy-predictive direct power control implementation of a grid connected photovoltaic system, associated with an active power filter. Energy Convers Manag 2016;122:515–25.

[6] Liu L, Li H, Xue Y, Liu W. Decoupled active and reactive power control for large-scale grid-connected photovoltaic systems using cascaded modular multilevel converters. IEEE Trans Power Electron 2015;30:176–87.

[7] Tripathi RN, Singh A, Hanamoto T. Design and control of LCL filter interfaced grid connected solar photovoltaic (SPV) system using power balance theory. Int J Electr Power Energy Syst 2015;69:264–72.

[8] Hanif M, Khadkikar V, Xiao W, Kirtley JL. Two degrees of freedom active damping technique for $ LCL $ filter-based grid connected PV systems. IEEE Trans Ind Electron 2014;61:2795–803.

[9] Barater D, Buticchi G, Lorenzani E, Concari C. Active Common-Mode Filter for Ground Leakage Current Reduction in Grid-Connected PV Converters Operating With Arbitrary Power Factor. IEEE Trans Ind Electron 2014;61:3940–50.

[10] Patel H, Agarwal V. Investigations into the performance of photovoltaics-based active filter configurations and their control schemes under uniform and non-uniform radiation conditions. IET Renew Power Gener 2010;4:12–22.

[11] Ortúzar ME, Carmi RE, Dixon JW, Morán L. Voltage-source active power filter based on multilevel converter and ultracapacitor DC link. IEEE Trans Ind Electron 2006;53:477–85.

[12] Abu-Rub H, Holtz J, Rodriguez J, Baoming G. Medium-voltage multilevel converters--state of the art, challenges, and requirements in industrial applications. IEEE Trans Ind Electron 2010;57:2581–96.

[13] Abu-Rub H, Malinowski M, Al-Haddad K. Power electronics for renewable energy systems, transportation and industrial applications. John Wiley & Sons; 2014.

[14] Trabelsi M, Ghazi KA, Al-Emadi N, Ben-Brahim L. An original controller design for a grid connected PV system. IECON 2012-38th Annu. Conf. IEEE Ind. Electron. Soc., IEEE; 2012, p. 924–9.

[15] Chavarria J, Biel D, Guinjoan F, Meza C, Negroni JJ. Energy-Balance Control of PV Cascaded Multilevel Grid-Connected Inverters Under Level-Shifted and Phase-Shifted PWMs. IEEE Trans Ind Electron 2013;60:98–111. doi:10.1109/TIE.2012.2186108.

[16] Vahedi H, Kanaan HY, Al-Haddad K. PUC converter review: Topology, control and applications. Ind. Electron. Soc. IECON 2015-41st Annu. Conf. IEEE, IEEE; 2015, p. 4334–9.

[17] Vahedi H, Sharifzadeh M, Al-Haddad K. Modified Seven-Level Pack U-Cell Inverter for Photovoltaic Applications. IEEE J Emerg Sel Top Power Electron 2018.

[18] Trabelsi M, Bayhan S, Ghazi KA, Abu-Rub H, Ben-Brahim L. Finite-control-set model predictive control for grid-connected packed-U-cells multilevel inverter. IEEE Trans Ind Electron 2016;63:7286–95.

[19] Vahedi H, Shojaei AA, Dessaint L-A, Al-Haddad K. Reduced DC-Link Voltage Active Power Filter Using Modified PUC5 Converter. IEEE Trans Power Electron 2018;33:943–7.

[20] Vahedi H, Labbé P-A, Al-Haddad K. Sensor-less five-level packed U-cell (PUC5) inverter operating in stand-alone and grid-connected modes. IEEE Trans Ind Informatics 2016;12:361–70.

[21] Metri JI, Vahedi H, Kanaan HY, Al-Haddad K. Real-time implementation of model-predictive control on seven-level packed U-cell inverter. IEEE Trans Ind Electron 2016;63:4180–6.

[22] Nademi, H., Das, A., Burgos, R., et al.: 'A new circuit performance of modular multilevel inverter suitable for photovoltaic conversion plants', IEEE J. Emerg. Sel. Top. Power Electron., 2016, 4, pp. 393–404

[23] Rodriguez J, Cortes P. Predictive control of power converters and electrical drives. vol. 40. John Wiley & Sons; 2012.

[24] Kouro S, Cortés P, Vargas R, Ammann U, Rodríguez J. Model predictive control—A simple and powerful method to control power converters. IEEE Trans Ind Electron 2009;56:1826–38.

[25] Rodriguez J, Kennel RM, Espinoza JR, Trincado M, Silva CA, Rojas CA. High-performance control strategies for electrical drives: An experimental assessment. IEEE Trans Ind Electron 2012;59:812–20.

[26] Rodriguez J, Kazmierkowski MP, Espinoza JR, Zanchetta P, Abu-Rub H, Young HA, et al. State of the Art of Finite Control Set Model Predictive Control in Power Electronics. IEEE Trans Ind Informatics 2013;9:1003–16. doi:10.1109/TII.2012.2221469.

[27] Vazquez S, Leon JI, Franquelo LG, Rodriguez J, Young HA, Marquez A, et al. Model predictive control: A review of its applications in power electronics. IEEE Ind Electron Mag 2014;8:16–31.

[28] Vazquez S, Rodriguez J, Rivera M, Franquelo LG, Norambuena M. Model Predictive Control for Power Converters and Drives: Advances and Trends. IEEE Trans Ind Electron 2017;64:935–47. doi:10.1109/TIE.2016.2625238.

[29] Pakdel, M., Jalilzadeh, S.: 'A new family of multilevel grid connected inverters based on packed U cell topology', Sci. Rep., 2017, 7, (1), p. 12396.

[30] Mohamed, A.A., Berzoy, A., Mohammed, O.A.: 'Design and hardware implementation of FL-MPPT control of PV systems based on GA and smallsignal analysis', IEEE Trans. Sustain. Energy, 2017, 8, (1), pp. 279–290

[31] Kakosimos PE, Kladas AG, Manias SN. Fast Photovoltaic-System Voltage- or Current-Oriented MPPT Employing a Predictive Digital Current-Controlled Converter. IEEE Trans Ind Electron 2013;60:5673–85. doi:10.1109/TIE.2012.2233700.

[32] Kihel A, Krim F, Laib A. MPPT voltage oriented loop based on integral sliding mode control applied to the boost converter. 2017 6th Int. Conf. Syst. Control, 2017, p. 205–9. doi:10.1109/ICoSC.2017.7958687.

[33] Safari A, Mekhilef S. Simulation and Hardware Implementation of Incremental Conductance MPPT With Direct Control Method Using Cuk Converter. IEEE Trans Ind Electron 2011;58:1154–61. doi:10.1109/TIE.2010.2048834.

[34] Tekeshwar Prasad S, Dixit T V. Modelling and analysis of Perturb & Observe and Incremental Conductance MPPT algorithm for PV array using cuk converter. Electr. Electron. Comput. Sci. (SCEECS), 2014 IEEE Students' Conf., 2014, p. 1–6. doi:10.1109/SCEECS.2014.6804468.

[35] Sahli, A., Krim, F., Belaout, A.: 'Energy management and power quality improvement in grid-connected photovoltaic systems'. 2017 Int. Renewable and Sustainable Energy Conf. (IRSEC), 2017 IEEE, 2017, pp. 1–7

[36] Cortes, P., Kouro, S., La Rocca, B., et al.: 'Guidelines for weighting factors design in model predictive control of power converters and drives'. IEEE Int. Conf. on Ind. Tech. (ICIT), Gippsland, Australia, February 2009, pp. 1–7

General Conclusion

1. GENERAL CONCLUSION

In recent years, most world countries face the great challenge of modernizing an aging grid infrastructure toward a new smart grid, which has special features that would improve the overall effectiveness of the power system to make it environment friendly with low carbon emission, improve power quality to correspond to new demands, become more reliable, resilient, flexible and sustainable. Furthermore, renewable energy systems (RESs), which are considered environmentally friendly, have extensively investigated. Therefore, the use of new and renewable sources of energy such as wind and solar has become a necessity. Hence, the power system is facing a great change due to many reasons, such as environmental concerns, energy system security, fossil fuel problems, and economical and operation cost issues. For these raisons, many countries have decided to increase the integration level of RESs in their energy system.

To do so, in this thesis we focus on two potential promises of the smart grid that include improved power quality and capability to integrate more renewable energy resources, where, power quality and reliability are attracting much attention in such systems; In order to meet the grid specification requirements, especially, with the ability to accommodate more renewables into the system, which make the grid more vulnerable to power quality issues.

Among the technologies that reinforced power quality and integration of renewable energy, power electronics has been representing a major technology enabler. It is extensively used and rapidly expanded, becoming more integrated in the grid-based systems to address power quality issue and to improve the grid power quality by eliminating current harmonics and compensating the reactive power. In this dissertation, the presented research works have brought several investigations of suitable conversion topologies and effective control schemes

for single phase grid-connected PV systems and for power quality enhancement in the future grid.

Single phase multi-level packed unit-cell inverter for active power filtering and for grid connected PV system has been presented and adopted in these contributions as the most effective inverter topology to be used.

Furthermore, Model predictive control (MPC) has been extensively investigated as the most promising control strategy for power converter in both applications, where the major drawbacks of the MPC have been tacked on consideration.

On other hand, transformer-less single-phase double stage grid-tied PV system based multi-level MPUC inverter has been presented to overcome the drawbacks of the conventional topologies where, the proposed system is able to perform a dual-function, namely the reduction of harmonic currents and injection of the power produced by the PV array into the grid or to the load regardless of the solar irradiation levels.

Finally, to show the performance improvement of the proposed systems, a completed simulation models have developed using MATLAB/Simulink^{TM} environment and confirmed through real-time hardware in the loop (HIL) system. The obtained results indicated the excellent performance of the proposed control schemes.

2. AUTHOR'S CONTRIBUTIONS

The major contributions of this research work can be summarized as follows:

- A multilevel modified packed U-Cell (MPUC5) converter is proposed for APF system.
- A model predictive control (MPC) for single phase APF using MPUC5 is discussed.
- The MPC algorithm is proposed to solve the balancing of the DC-Link capacitor voltages issue.
- Transformer-less grid-tied single-phase PV System with unity power factor is presented.
- Modified multilevel packed U-Cell MPUC5 inverter is also employed in the studied system.

- An improved model predictive control (MPC) for MPUC5 inverter is proposed taking in consideration the DC- Link capacitor voltages balancing issue, where the proposed inverter operates under minimized switching frequency

3. FUTURE WORKS

The following future research works are suggested as an extension to the knowledge presented in this thesis:

a) Comparison of proposed controllers with the classical control techniques

To contribute to the ongoing research on predictive control, and to clearly distinguish this method from classical control techniques, comparison studies can be carried out.

b) Active damping of the LCL filters

The proper design of predictive controller with LCL filters should be studied for further enhancement in grid tied PV system, in order to lessen more the harmonic current.

c) Investigation of other multilevel converters

Investigation of other multilevel converters for PV system with power quality enhancement where the control approach presented in this thesis can be extended.

d) Performance improvement

Performance improvement of the predictive strategy, where more investigations are needed such as weighting factor selection and variable switching frequency.

Appendix A: PV system modeling

In this Appendix, a brief description about PV array modeling and DC/DC Cùk converter employed in this thesis are presented.

A.1 PV array Modeling

PV cell is a 'p-n' junction fabricated in a thin semiconductor wafer. The solar energy is directly converted to electricity through photovoltaic effect. For simplicity and accuracy, single diode model is the most used in the industry. The equivalent circuit of this model is presented in Figure A.1, with a photo-current source in parallel with a diode, a shunt resistance R_{sh} and a series resistance R_s.

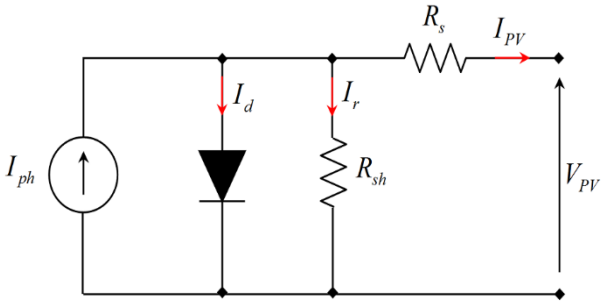

Figure A.1: PV cell equivalent circuit.

This equivalent circuit can be mathematically described by the following equation:

$$I_{PVc} = I_{ph} - I_d - I_r = I_{ph} - I_o\left(e^{\frac{V_{PVc}+R_sI_{PVc}}{nV_t}} - 1\right) - \frac{V_{PVc} + R_{sc}I_{PVc}}{R_{shc}} \quad \text{(A.1)}$$

where:

I_{PV}: is the cell output current (A).
I_{ph}: is the cell photocurrent (A).
I_d : is the diode current (Shockley equation) (A).
I_r : is the derived current by the shunt resistance (A).
I_0 : is the reverse saturation current of the diode (A).
V_{PVc}: is the cell output voltage (V).
R_{sc}: is the cell series parasitic resistance (Ω).
R_{shc}: is the cell shunt parasitic resistance (Ω).
n: is the diode ideality factor
V_t: is the thermal voltage given by:

$$V_t = \frac{kT}{q} \quad \text{(A.2)}$$

where:

k: is the Boltzmann constant (1.38×10^{-23} J/K).

T: is the absolute temperature (K).

q : is the electronic charge (1.6×10^{-19} C)

In order to produce the required power from PV cells, these later are connected in series-parallel configuration to form a PV module.

The equivalent circuit of the PV module can be mathematically described by the following equation, where all used cells are identical:

$$I_{PVm} = N_p I_{ph} - N_p I_o \left(e^{\frac{N_s V_{PVm} + (N_s/N_p) R_s I_{PVm}}{n N_s V_t}} - 1 \right) - \frac{N_s V_{PVm} + (N_s/N_p) R_s I_{PVm}}{(N_s/N_p) R_{shm}} \quad \text{(A.3)}$$

where:

I_{PVm}: is the module output current (A).
V_{PVm}: is the module output voltage (V).
N_s : is the number of cells connected in series
N_p : is the number of cells connected in parallel

To form a PV array or panel from PV modules, these later are connected in series-parallel configuration to obtain the desired voltage and current at the PV panel output. The PV panel output current and voltage are obtained from equations (A.4) and (A.5) respectively:

$$I_{PVa} = N_{pp} I_{PVm} \quad \text{(A.4)}$$

$$V_{PVa} = N_{ss} V_{PVm} \quad \text{(A.5)}$$

where:

I_{PVa}: is the array output current (A).
V_{PVa}: is the array output voltage (V).
N_{ss} : is the number of modules connected in series
N_{pp}: is the number of modules connected in parallel

A.2 DC/DC Cùk converter

The proposed PV system employs a Cùk converter as the first power-processing stage, which can boost a low voltage of the PV array up to a high DC link voltage. Figure A.2 shows the equivalent circuit of the proposed converter. The DC-DC Cùk converter is used to maximize the energy transfer from the PV generator to the load by adjusting the PV generator output voltage to a reference value *Vref*, at which the PV generator supplies the maximum power, with low switching losses and high efficiency. It can also provide a better output current characteristic due to the inductor on the output stage.

The conversion ratio *M* is the relations between output and input currents and voltages

given in the following equations, which is the function of duty cycle D:

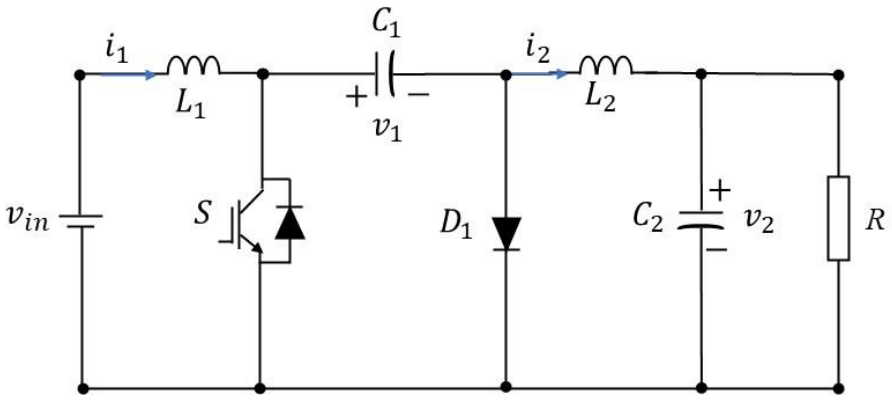

Figure A.2: DC-DC Cùk converter topology.

$$M(D) = \frac{v_{out}}{v_{in}} = \frac{i_{in}}{i_{out}} = -\left(\frac{D}{1-D}\right) \tag{A.6}$$

The Cùk converter exhibits two different modes of operation. The first mode is obtained when the IGBT is ON and instantaneously, the diode *D* is inversely polarized generating a circuit topology shown in Figure A.3. During this period, the current through the inductor *L*1 is drawn from the voltage source *E*. This mode represents the *charging* mode.

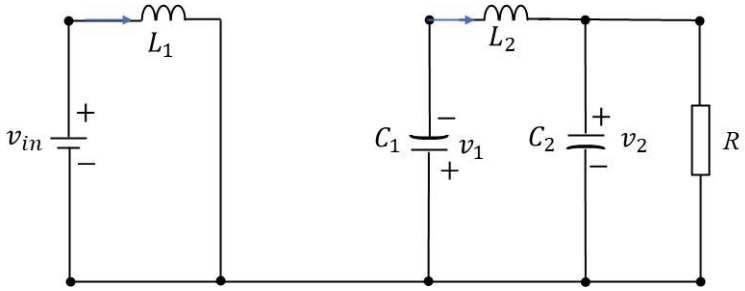

Figure A.3: Equivalent circuits of the Cùk converter (Switch ON).

The equations for the switch conduction mode are as follows:

$$v_{L1} = v_{in} \tag{A.7}$$

$$v_{L2} = -v_1 - v_2 \tag{A.8}$$

$$i_{c1} = i_{c2} \tag{A.9}$$

$$i_{c2} = i_{2-}\frac{v_2}{R} \tag{A.10}$$

The second mode of operation starts when the switch is OFF and the diode *D* is directly polarized generating the circuit topology shown in Figure A.4. This stage or mode of operation is known as the *discharging* mode since all the energy stored in *L*1 is now transferred to the load *R*.

The equations for the discharging mode are as follows:

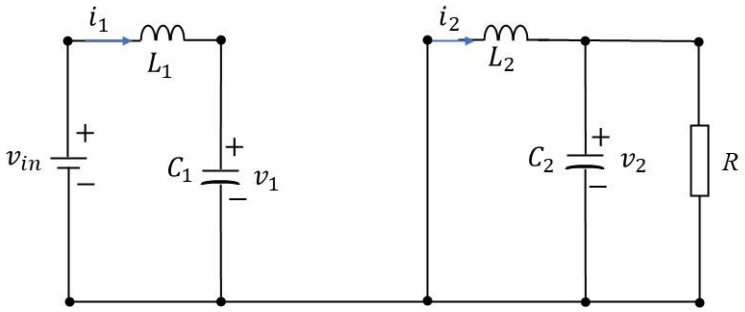

Figure A.4: Equivalent circuits of the Cùk converter (Switch OFF).

$$v_{L1} = v_{in} - v_1 \tag{A.11}$$

$$v_{L2} = -v_2 \tag{A.12}$$

$$i_{c1} = i_1 \tag{A.13}$$

$$i_{c2} = i_{2-}\frac{v_2}{R} \tag{A.14}$$

where v_1 and i_1 are, respectively, the voltage across the capacitor $C1$ and the current in the inductor $L1$, while v_2 and i_2 are, respectively, the voltage across the parallel branches formed by the capacitor $C2$ and the load R, and the current through the inductor $L2$.

Appendix B: Capacitors sizing and Controller design

In this Appendix, a detailed description about PI controller design and DC capacitor values selection employed in this thesis are presented.

B.1 DC capacitors values selection

The capacitor design is based on the maximum real power rating of the PV system. The design equation based on this principle is derived as follows.

Let the peak power rating of the grid be P_max (W) and the RMS utility voltage be (V_S). Therefore, the maximum energy that the capacitor has to supply in the worst case of transient is given by:

$$E_{max} = P\_max \times T \tag{B.1}$$

where $T = 20ms$

Vdc_min preset lower limit of the voltage of energy-storage capacitor, Therefore,

$$E_{max} = \frac{1}{2} C_{dc} V_{dc} - \frac{1}{2} C_{dc} V_{dc\_min} \tag{B.2}$$

where V_{dc} is the DC-link voltage, C the DC-link capacitor value and could be obtained by:

$$C = \frac{2\,E_{max}}{V_{dc}^2 (1 - \left(\frac{V_{dc\_min}}{V_{dc}}\right)^2)} \text{ Farads} \tag{B.3}$$

By assuming that the minimum voltage, $V_{dc\_min} = 10\% V_{dc}$ and $V_{dc} \geq 2V_S$

1- Numerical application for PV application in chapter 4:

The values of $V_S = 120\ volts,$ and the value of $V_{dc} \geq 2V_S$.

So, the value of $V_{dc}$is chosen to be $150\ volt$, on the other hand, the nonlinear load has been sized to consume 120 VAR of reactive power and 370 W of active power. Therefore, the PV array is sized to produce a 480 W max at 1000w/m² of solar irradiation level so we get:

$$C = 888\mu F$$

So, the chosen normalized value is: $C = 1100\ \mu F$. For ensure the good performance of the overall system and to avoid oscillations in the DC-link voltage.

B.2 PI Voltage controller

To reduce the DC-link capacitor fluctuation voltages and compensate the system loss regarding the power exchange between the PV system and main grid, a proportional-integral controller (PI) is used to decrease to voltage fluctuation in the DC-link, and regulate it at a

desired value, Figure B.1 shows the synaptic of the PI controller, when the input is the error between the DC-link capacitor voltage *Vdc* and the estimation value *Vdcref*, the output of the regulator is the reference current is_ref.

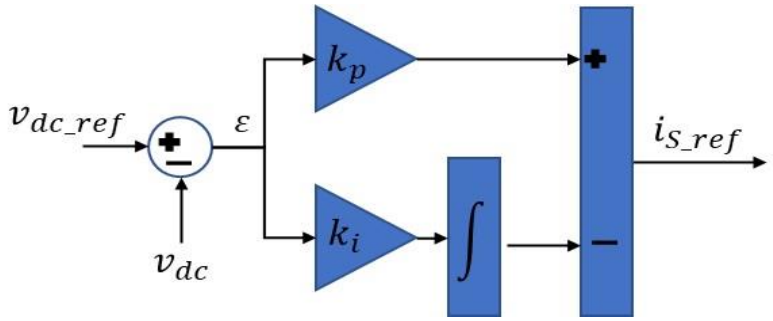

Figure B.1: PI Controller system.

The PI controller can be modelled as a second-order system as fellow:

$$G_{Vdc(PI)}(S) = \frac{K_p.S + K_i}{KS^2 + K_p.S + K_i} = \frac{K_p/K(s + \frac{K_i}{K_p})}{S^2 + \frac{K_p}{K}.S + K_i/K} = \frac{Vdc}{Vdcref} \quad \text{(B.4)}$$

$$K = \frac{\sqrt{2}.C_{dc}Vdcref}{3.Vs} \quad \text{(B.5)}$$

The transfer function *Gvdc(PI)* is a second order transfer function and the characteristic equation can be expressed as:

$$dc(S) = S^2 + \frac{K_p}{K}.S + \frac{K_i}{K} = S^2 + 2\xi\omega_n.S + {\omega_n}^2 \quad \text{(B.6)}$$

$$\omega_n = 2\pi\, f_c \quad \text{(B.7)}$$

Where ω_n is the natural frequency.

So, the gain *Ki* and *Kp* can be expressed as:

$$\Rightarrow \begin{cases} K_i = K{\omega_n}^2 \\ K_p = 2\xi\omega_n K \end{cases} \quad \text{(B.8)}$$

Where, $\xi = 0.707$ is the damping coefficient.

Where, *fc* is the cut frequency at -3db in bode diagram correspond to 25Hz which means half of nominal frequency of the system. So, fc=fs/4.

Appendix C: Scientific production

The following list includes all papers published by the author during his research studies. Papers designated by " * " are directly related with research results presented in this thesis.

Journal Papers

*[1] **Abdeslem Sahli**, Fateh Krim, Abdelbaset Laib, Billel Talbi, (2019). Energy management and power quality enhancement in grid-tied single-phase PV system using modified PUC converter. IET Renewable Power Generation, 13(14), 2512-2521. (Impact Factor: 3.894).

*[2] **Abdeslem Sahli**, Fateh Krim, Abdelbaset Laib, Billel Talbi (2020). Model predictive control for single phase active power filter using modified packed U-cell (MPUC5) converter. Electric Power Systems Research, 180, 106139. (Impact Factor: 3.211).

[3] Abdelbaset Laib, Fateh Krim, Billel Talbi, **Abdeslem Sahli**, (2020). A predictive control scheme for large-scale grid-connected PV system using high-level NPC inverter. Arabian Journal for Science and Engineering, 45(3), 1685-1701. (Impact Factor: 1.711).

[4] Billel Talbi, Fateh Krim, Abdelbaset Laib, **Abdeslem Sahli**, (2020). Model predictive voltage control of a single-phase inverter with output LC filter for stand-alone renewable energy systems. Electrical Engineering, 1-10. (Impact Factor: 1.180).

[5] Abbas Kihal, Fteh Krim, Billel Talbi, Abdelbaset Laib, **Abdeslem Sahli**. (2018). A robust control of two-stage grid-tied PV systems employing integral sliding mode theory. Energies, 11(10), 2791. (Impact Factor: 2.702).

[6] Abdelouhab Benhamadouche, Farid Djahli, Adel Ballouti, **Abdeslem Sahli**. (2019). FPGA-based hardware-in-the-loop for multi-domain simulation. International Journal of Modeling, Simulation, and Scientific Computing, 10(04), 1950020.

[7] Abdelouhab Benhamadouche, Farid Djahli, Adel Ballouti, **Abdeslem Sahli**. (2018). FPGA based Hardware-in-the-Loop Simulation for Digital Control of Power Converters using VHDL-AMS. international journal of advanced computer science and applications, 9(12), 524-529.

Conference Papers

[8] **Abdeslem Sahli**, Fateh Krim, Abdesslam Belaout. (2017, December). Energy management and power quality improvement in grid-connected photovoltaic systems. In 2017 International Renewable and Sustainable Energy Conference (IRSEC) (pp. 1-7). IEEE.

[9] Abdelbaset Laib, Fateh Krim, Billel Talbi, Abbes Kihal, **Abdeslem Sahli**. (2017, November). Predictive Control Strategy for Double-Stage Grid Connected PV Systems. In International Conference on Electrical Engineering and Control Applications (pp. 314-327). Springer, Cham.

[10] Billel Talbi, Fateh Krim, Abdelbaset Laib, **Abdeslem Sahli**, Hamza Feroura. (2019, November). Sensorless Predictive Current Controlled DC-DC Boost Converter for PV MPPT Applications. In 2019 7th International Renewable and Sustainable Energy Conference (IRSEC) (pp. 1-6). IEEE.

[11] Abdesslam Belaout, Fateh Krim, **Abdeslem Sahli**, Adel Mellit. (2017, October). Multi-class neuro-fuzzy classifier for photovoltaic array faults diagnosis. In 2017 5th International Conference on Electrical Engineering-Boumerdes (ICEE-B) (pp. 1-4). IEEE.

[12] Abdelkader Lakhdari, Fateh Krim, Abdelkrim, T., Borni, A., **Abdeslem Sahli**. (2016). PV Power Injection Associated with a Reactive Power Compensator. 4ème Séminair International sur les Energies Nouvelles et Renouvelables SIENR.

[13] Habib Bey, Fateh Krim, Billel Talbi, **Abdeslem Sahli**. (2020). FPGA based HIL simulation for direct current control of active power filter. In 2020 International Conference on Electrical Engineering (ICEE) (pp. 1-5). IEEE.

[14] Billel Talbi, Fateh Krim, Abdelbaset Laib, **Abdeslem Sahli**, Abdelbasset Krama. (2020). PI-MPC Switching Control for DC-DC Boost Converter using an Adaptive Sliding Mode Observer. In 2020 International Conference on Electrical Engineering (ICEE) (pp. 1-5). IEEE.

Résumé

La qualité d'énergie et l'intégration des énergies renouvelables sont les points essentiels pour le développement des smart grids, assurent l'amélioration de la qualité d'énergie et la capacité d'intégrer d'avantage des ressources d'énergie renouvelables.

Dans cette thèse, un onduleur modifié à cinq niveaux de cellule U emballée (MPUC5) avec une stratégie de contrôle prédictif (MPC) est proposé pour une application de filtrage de puissance active monophasé (APF), qui est appliquée pour éliminer les harmoniques du courant et compenser la puissance réactive au point de couplage commun (PCC), causée par les charges non linéaires locales connectées au réseau. La configuration de l'onduleur MPUC5 se compose de nombreux condensateurs DC-link qui doivent être équilibrés. Dans ce contexte, un nouveau modèle de contrôle prédictif (MPC) a été conçu et mis en œuvre pour assurer l'équilibrage de la tension des condensateurs DC-link et générer une tension à cinq niveaux à la sortie. Pour l'application de l'APF, l'onduleur doit pouvoir fournir la puissance réactive demandée au PCC et assurer une correction élevée du facteur de puissance.

D'autre part, cette étude introduit le convertisseur MPUC5 dans un système photovoltaïque (PV) monophasé connecté au réseau à double étage sans transformateur, avec un facteur de puissance unitaire. Le système proposé fonctionne comme un filtre actif monophasé capable de compenser la puissance réactive générée par les charges non linéaires raccordées au réseau, d'alimenter la charge non linéaire par la puissance PV produite et d'injecter le surplus de puissance dans le réseau, où l'algorithme FCS-MPC proposé est conçu pour assurer une qualité élevée du courant de réseau, en tenant compte de la question de l'équilibrage des tensions des condensateurs et de la minimisation de la fréquence de commutation de l'onduleur. En outre, cette topologie montre une grande amélioration de la sécurité et de la protection du système PV avec une élimination du courant de fuite en mode commun dans un système non isolé.

Pour montrer l'amélioration des performances des systèmes proposés, des modèles de simulation complets ont été développés à l'aide de l'environnement MATLAB/SimulinkTM et confirmés en temps réel par un système HIL (Hardware in the loop). Les résultats obtenus ont indiqué l'excellente performance des systèmes de contrôle proposés.

Mots-clés : Smart grid ; Optimisation de la qualité d'énergie ; Système photovoltaïque (PV) ; Onduleur Multi-niveaux MPUC5 ; Commande prédictif FCS-MPC ; Système HIL (Hardware in the loop).

Abstract

Power quality and renewable energy integration are two potential promises for the smart grid expansion, including power quality improvement and capability to integrate more renewable energy resources.

In this thesis, a modified packed U-cell five-level inverter (MPUC5) with Model predictive control (MPC) strategy is proposed for a single-phase active power filter (APF) application, which is applied to eliminate harmonic current and compensate reactive power at the point of common coupling (PCC), caused by local non-linear loads connected to the grid. In this context, a new model predictive control (MPC) has been designed and implemented to ensure the voltage balancing for the DC-link capacitors, and generate five-level voltage at the output to ensure high power factor correction.

On the other hand, this study introduces the MPUC5 converter in transformer-less single-phase double stage grid-tied photovoltaic (PV) system. The proposed system operates as a single-phase APF able to compensate reactive power generated by non-linear loads connected to grid, feeds the non-linear load by the generated PV power, and injects the extra power into the grid, where the proposed FCS-MPC algorithm is designed to ensure a high grid current quality, taking into consideration the issue of the capacitor voltages balancing and the switching frequency minimization. Furthermore, this topology shows a great enhancement in safety and protection of the PV system with an elimination of the common mode leakage current in non-isolated system.

To show the performance improvement of the proposed systems, completed simulation models have been developed using MATLAB/Simulink^{TM} environment and confirmed through real-time hardware in the loop (HIL) system. The obtained results indicated the excellent performance of the proposed control schemes.

Keywords: Smart grid ; Energy quality optimization; Photovoltaic system (PV); Multi-level inverter MPUC5; Predictive control FCS-MPC; HIL system (Hardware in the loop).

ملخص

تواجه أغلب بلدان العالم في السنوات الأخيرة تحدي عظيم والمتمثل في تحديث البنية الأساسية للشبكة القديمة للحصول على شبكة ذكية جديدة، التي تتميز بميزات خاصة من شأنها تحسين الفعالية الكلية لنظام الطاقة إضافة الى جعله صديق للبيئة مع انبعاثات كربون منخفضة، تحسين جودة الطاقة بحيث تتوافق مع المتطلبات الجديدة وتصبح أكثر موثوقية، مرونة واستدامة. وعلاوة على ذلك، فإن نظم الطاقة المتجددة، التي تعتبر ملائمة للبيئة، قد وظفت على نطاق واسع مما أدى إلى زيادة الموارد المتجددة في شبكة الطاقة. ومن أجل تلبية متطلبات رموز الشبكة مع القدرة على استيعاب المزيد من مصادر الطاقة المتجددة في النظام، فإن جودة الطاقة والموثوقية تجذب الكثير من اهتمام الباحثين في مثل هذه الأنظمة.

للقيام بذلك، نقترح استخدام عاكس معدَّل من خمسة مستويات ذو خلايا على شكل U مع استراتيجية التحكم التنبؤي في النموذج (MPC) لتطبيق فلتر الطاقة النشط أحادي الطور (APF)، والتي يتم تطبيقها للتخلص من التيار التوافقي وتعويض الطاقة التفاعلية عند نقطة التوصيل المشترك (PCC)، والتي تنتج عن الأحمال غير الخطية المحلية المتصلة بالشبكة. يتكون عاكس MPUC من عدة مكثفات للتيار المستمر والتي يجب أن يكون الجهد فيها متوازن. في هذا السياق، تم تصميم نموذج جديد للتحكم التنبؤي (MPC) وتطبيقه لضمان موازنة الجهد الكهربائي للمكثفات، وتوليد جهد كهربائي من خمسة مستويات في مخرج العاكس. بالنسبة لتطبيقات APF، يجب أن يكون المحول قادرًا على توفير الطاقة التفاعلية المطلوبة في نقطة PCC وضمان تصحيح عالي لعامل الطاقة.

ومن ناحية أخرى، تقدم هذه الدراسة محول MPUC5 في نظام الكهروضوئية أحادي الطور، والذي يتسم بعامل طاقة الوحدة. ويعمل النظام المقترح ك APF أحادي الطور قادر على تعويض الطاقة التفاعلية الناتجة عن الأحمال غير الخطية المتصلة بالشبكة، وأيضا يقوم بتغذية الحمل غير الخطي بواسطة الطاقة الكهربائية التي تم إنتاجها، إضافة الى حقن الطاقة الإضافية في الشبكة، حيث تم تصميم خوارزمية FCS-MPC المقترحة لضمان جودة عالية لتيار الشبكة، مع مراعاة مشكلة موازنة جهد المكثفات وتقليل تردد التحويل إلى أدنى حد. علاوة على ذلك، يُوفر هذا الهيكل تحسيناً كبيراً في سلامة وحماية نظام الكهروضوئي مع التخلص من تيار التسرب الشائع في النظام غير المعزول.

لإظهار فعالية الأنظمة المقترحة، تم تطوير نماذج محاكاة مكتملة باستخدام بيئة MATLAB/Simulink^{TM} والتأكد منها عن طريق نظام HIL وتبين النتائج التي تم الحصول عليها الأداء الممتاز لمخططات المراقبة المقترحة.

الكلمات المفتاحية :لشبكة الذكية; تحسين جودة الطاقة ; نظام الكهروضوئية ; عاكس متعدد المستويات MPUC5 ;التحكم التنبؤي في النموذج FCS-MPC; نظام HIL.